

# ENGINEERING EDGE

Accelerate Innovation  
with CFD & Thermal  
Characterization

Exhaust gas

**ThyssenKrupp**  
Designing a Modern  
Submarine  
**Page 10**

**Danfoss Drives GmbH**  
Liquid Cooling the  
ShowerPower®  
Turbulator  
**Page 14**

**TsAGI, Zhukovsky**  
Helicopter Rotor  
Simulation  
**Page 38**

**Mentor  
Graphics**

Mechanical Analysis



# MicReD® Industrial Power Tester 1500A



**An industry-first all-encompassing system for Power Cycling and Thermal Transient Measurements:**

- Industry-proven T3Ster™ technology with laboratory-precision accuracy
- Single operation testing for Continuous Power Cycling
- Real-time Structure Function diagnostics

## **ANNOUNCING – the Next Generation MicReD® Industrial Power Tester 1500A**

- Test up to 12 devices simultaneously
- Power cycling and thermal transient measurements conducted without the need to remove components from the test environment



Watch the video online:  
[www.mentor.com/powertester-1500a](http://www.mentor.com/powertester-1500a)

**Mentor Graphics®**

— Mechanical Analysis





**Mentor Graphics**

— Mechanical Analysis

**Mentor Graphics Corporation**

Pury Hill Business Park,  
The Maltings,  
Towcester, NN12 7TB,  
United Kingdom  
Tel: +44 (0)1327 306000  
email: ee@mentor.com

**Editor:**

Keith Hanna

**Managing Editor:**

Natasha Antunes

**Copy Editor:**

Jane Wade

**Contributors:**

Ian Clark, Ivo Weinhold, James Forsyth, John Murray, John Parry, Kate Boyd, Kelly Cordell-Morris, Mike Croegeart, Polina Subbotina, Robin Bornoff, Sarah Pyle, Tatiana Trebunskikh

**With special thanks to:**

Amkor Technology,  
Danfoss Drives GmbH,  
Discom B.V.,  
Emerson Network Power,  
EnginSoft S.p.A.,  
Flow Design Bureau AS,  
North China Electric Power University,  
ThyssenKrupp Marine Systems,  
TsAGI Zhukovsky, and  
Universitat Politècnica de Catalunya (UPC)

©2015 Mentor Graphics Corporation, all rights reserved. This document contains information that is proprietary to Mentor Graphics Corporation and may be duplicated in whole or in part by the original recipient for internal business purposes only, provided that this entire notice appears in all copies. In accepting this document, the recipient agrees to make every reasonable effort to prevent unauthorized use of this information. All trademarks mentioned in this publication are the trademarks of their respective owners.

# Perspective

Vol. 04, Issue. 01



Greetings readers! The annual Movie Awards season, that culminated in the Hollywood Oscars in February, meant that as always we saw lots of our favorite screenstars in their finery. In watching them, I was reminded of my two colleagues who recently picked up Awards for MAD Products – John Wilson in Las Vegas, received an LED Sapphire Award for our unique T3Ster, TeraLED and FloEFD LED Module lighting design & test suite, and Mike Fletcher in London at the NMI Awards for our 1500A Power Tester power electronics thermal cycling hardware solution in 2014 (page 9).

The teams within our “factory” helped conceive, deploy, promote and deliver these unique new product offerings. I therefore view these Awards as a ringing endorsement of the strategies we have employed in those markets over the last few years and to the efforts of my development colleagues in Budapest and Moscow in particular. Indeed, 2014 was our best ever year for a number of our product lines: the MicReD team’s launch of the Power Tester 1500A/3C meets the needs of the power electronics market such that we have announced this year a new 12 channel version (page 8) to cope with mass IGBT thermal cycling and lifecycle testing demands; and our Flowmaster product line enjoyed its best year and continues to grow its breadth of capabilities and leading edge accuracy.

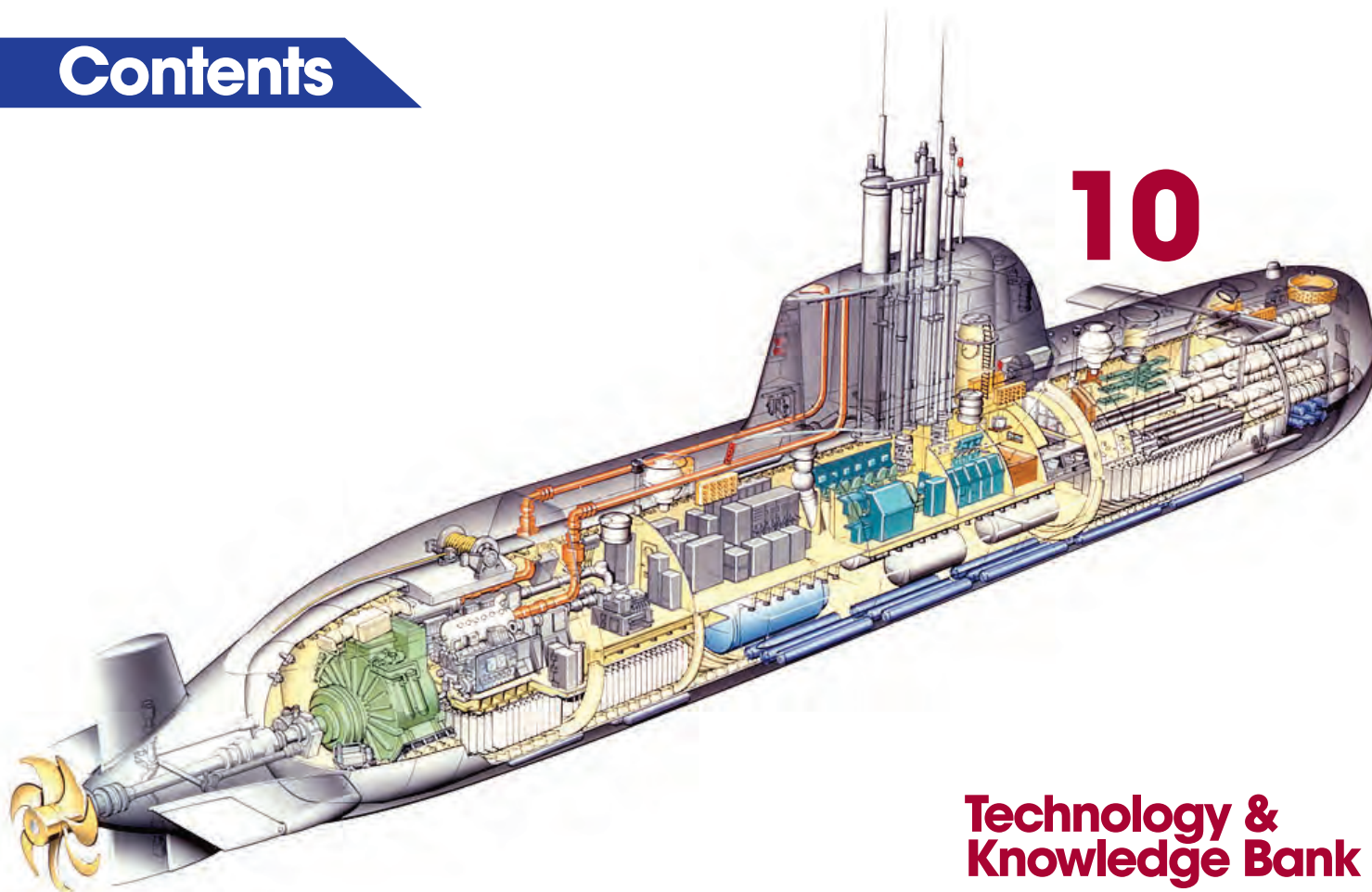
And while we are talking about awards and recognition, the Harvey Rosten Award for Thermal Excellence was recently won by Cameron Nelson, Jesse Galloway, and Philip Fosnot of Amkor Technology (page 44) in this its 20th year of existence. At the SemiTHERM Show, Robin Bornoff and John Parry revealed what we affectionately call “Dolly the Heatsink” – a novel innovative way to couple design space exploration within FloTHERM simulations, and additive manufacturing 3D Printers to organically “grow” an optimal heatsink design for a given electronics cooling scenario. Robin and John have applied for a patent for this interesting invention and if you haven’t already read them, do check out Robin’s popular blog series on our website describing how they came to their invention. This to me feels like a brave new world for electronics cooling, and in particular for FloTHERM, but also for CFD simulation in general because of the coupling of design space exploration, thermal predictions and new manufacturing techniques. I salute my two colleagues for pushing the frontiers of the application of our technology to new and exciting areas.

In this edition of Engineering Edge I have been taken by the article from my Russian colleague Tatiana Trebunskikh in association with a major Russian helicopter manufacturer, TsAGI, on the validation of a rotating helicopter blade inside FloEFD using our new sliding mesh capability. As a former helicopter pilot in my military days, and knowing how notoriously hard the compressible physics is to resolve, this is exciting and extends the code’s capabilities in the aerospace sector. It is great to see such good agreement to experiment. I also encourage you to read the great breadth of customer application stories in this newsletter - Flowmaster is well represented by ALBA in Spain for synchrotron cooling systems, ThyssenKrupp for submarine systems in Germany, and North China Electric Power simulations; Emerson Power in America; and FloEFD usage by Discom B.V. to model automotive exhaust gas systems to prevent hot spots.

Finally, do check out our new product releases – FloTHERM XT V2 has been recently released, as well as the new 12 Channel MicReD Industrial Power Tester 1500A. The interview of Klaus Olesen at Danfoss in Germany illustrates his worldview for IGBT liquid cooling and showcases his world-leading ShowerPower® cooling system simulation in FloEFD. And not to forget my dear friend, Dr. Ivo Weinhold, who draws on his quarter century of experience to outline what he sees as “The Third Wave of CFD” related to the demands of user experience in modern software.

**Roland Feldhinkel, General Manager  
Mechanical Analysis Division, Mentor Graphics**





## Engineering Edge

### 10 ThyssenKrupp Marine Systems

Designing a Modern Submarine

### 13 Discom B.V.

Avoiding Hot Spots in Train Exhaust Systems

### 14 Danfoss Drives GmbH

ShowerPower® Turbulator Design to keep IGBTs Cool

### 18 Emerson Network Power

FloTHERM® Powering Power Supply Development

### 22 ALBA Synchrotron

Synchrotron Light Source Upgrade

### 32 The Third Wave of Commercial CFD

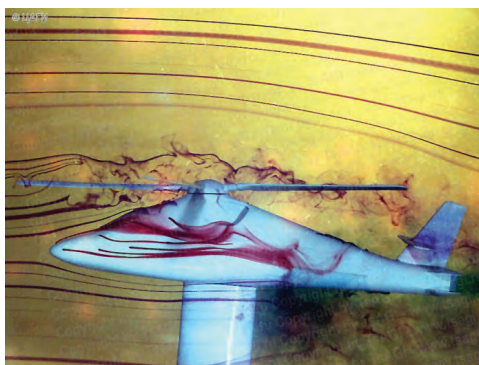
### 35 NCEPU Nuclear Power Station Validation

### 38 TsAGI Zhukovsky

Engineering Techniques for a Helicopter Rotor Simulation

### 44 Harvey Rosten Award Paper

Extracting TIM Properties with Localized Transient Pulses



## News

### 5 Flowmaster goes Mobile with EnginSoft S.p.A

### 6 New Release: FloTHERM® XT V2

### 8 New Release: Power Tester 1500A 12C

### 8 Mentor Customer Support Expansion

### 9 Mentor Awards

# 38

## Technology & Knowledge Bank

### 28 How To Guide:

A Guide to Power Cycling

### 30 Modeling Air Flow & Heat Dissipation in Vehicle ECUs

### 43 How to Grow Your Own Heatsink!

## Regular Features

### 20 Ask the GSS Expert

Model & Solve for an Extrusion Die

### 17 Interview

Klaus Olesen, Danfoss Drives

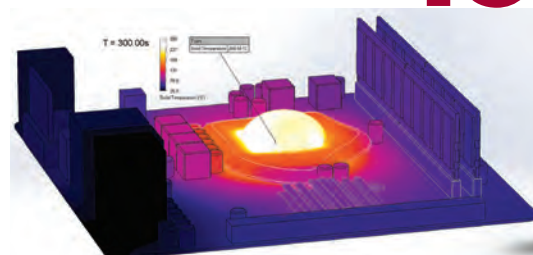
### 46 Geek Hub

Frying an Egg on a CPU!

### 50 Brownian Motion

The random musings of a Fluid Dynamicist

# 46





# Flowmaster goes Mobile at EnginSoft S.p.A

News

**F**lowmaster opened up the possibilities of real time simulation with Version 7.9.1 and the introduction of response surface modeling. Further enhancements in follow up releases have been made to provide a comprehensive means of generating surfaces that accurately represent the performance of a 1D thermo-fluid simulation model. While each surface represents only a single performance characteristic, multiple surfaces can be used together to provide a whole array of results in a detailed meta-model. The obvious advantage of doing this is that the simulation results can be obtained very quickly, because the detailed calculations do not need to be evaluated. Instead, the user defined boundary conditions are used to evaluate the response surfaces, to provide the system performance results. Related to this is the fact the meta-model does not require a great deal of computing power. This truly opens the door for the use on mobile devices such as smart phones and tablets.



## EnginSoft S.p.A

In their Summer 2014 newsletter, Alberto Deponi and Edoardo Di Lorenzo of Enginsoft S.p.A, Italy, showed how to create a smart phone application that could evaluate a predefined meta-model of a cooling system. The example had four user inputs and can provide three system performance results. The inputs can be adjusted using slider bars for quick changes and the user can see the results of the changes on the same screen. This is a relatively simple example of what could be done and with the flexibility of the response surface creation the complexity of the system that can be run on a mobile device is only limited by the number of inputs the user would want to vary.

The question is: Is this something that an engineer would really use in their day-to-day work environment? To answer that just look around you and see how mobile devices are used by many people as a tool to help them. From the package delivery people who have handheld devices to scan and track your packages, which provide you real-time updates on the status of your delivery, to

the sales person who can process your sale without having to go to a computer terminal or cash register. It is quite easy to see how this similar technology can and is being used in the engineering field.

Consider this example, a chemical processing facility uses steam at various locations in the plant for heating the chemicals being manufactured. Since the plant has a limitation on how much steam it can produce, the facility engineer needs to know the impact on the system when he makes changes to the demand on the steam at different locations in the plant. If he has a process that requires heating which is further from the steam source, it will have more pressure drop than processes that are closer, therefore, he has to manage the flow control valves to ensure that he is maintaining a high enough pressure to deliver enough steam to the far process while still providing adequate steam to the other processes. He has three ways he can do this:

- 1. Trial and Error** – keep adjusting the valves manually until he gets the required steam flow and pressure.
- 2. Run a simulation at his desk** – return to the office and pull up his simulation software and run the simulation to determine proper valve positions and then return to the plant and make the adjustments.
- 3. Run a simulation on his mobile device at the plant** – enter the required flow rates on his mobile application and have the proper valve setting within seconds.

The time and cost saving can be significant by simply being able to make an accurate design and act on it quickly. In commodity markets, like the chemical industry, halting production for even an hour can have a considerable effect on margins.

This is just one example and there are many others where this technology can and will be used in the future. With its response surface capabilities, Flowmaster is well positioned to allow its end users to make better decisions faster, by allowing them to put the information they need, in the mobile device they have in the palm of their hand.

# New Release: FloTHERM® XT V2

**F**ollowing on from the successful launch of the FloTHERM XT V1 series, we now have a significant update of the product line to announce for the V2 series. Over the coming months, the FloTHERM XT V2 series will provide crucial updates and innovation in core technology, parametric analysis, EDA synchronization and user experience.

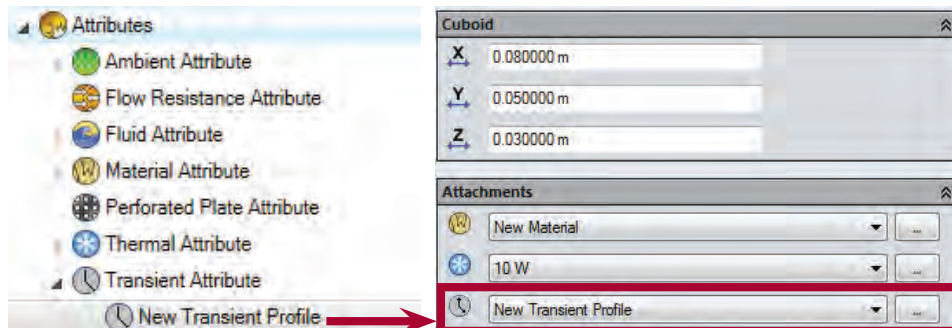
## Core Technology

We are introducing an update to our state-of-the-art solver, along with appropriate UI and data model support for time-varying analyses across all electronics thermal applications. The software has a number of new features in support of transient analysis, including:

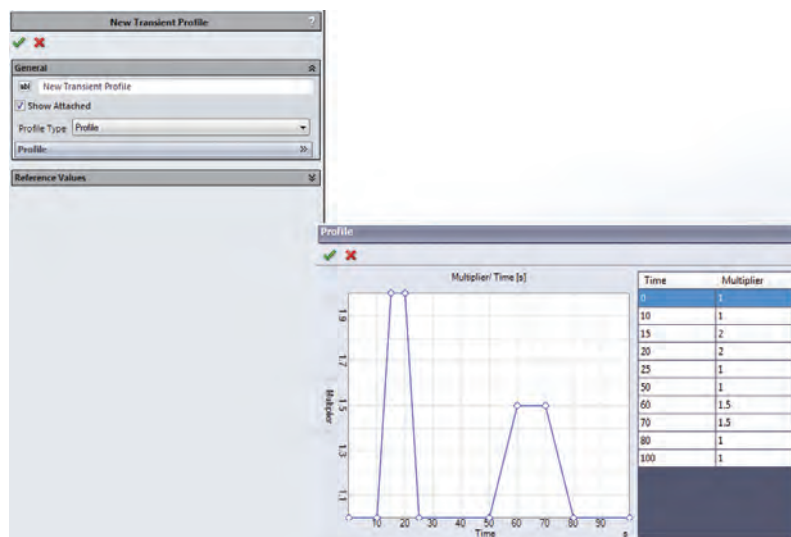
- Both automatic and manual time step definition.
- Post-processing features for both graphical and tabular output have all been appropriately updated.



- Transient attributes attachable to objects.

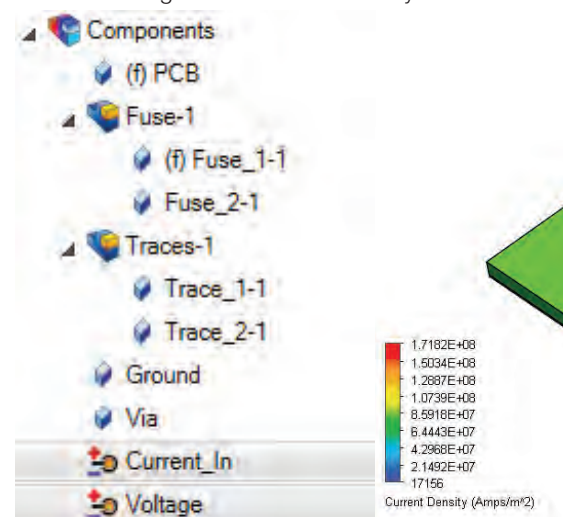


- Created or imported profiles, plus standard function definitions.



The other primary core technology update in the V2 series is general Joule Heating support. This is designed as a complete analysis platform for predicting current density, electric potential and associated Joule Heating effects in complex electronics PCB's and other high power devices and is of particular importance in the automotive and power electronics sectors.

Joule Heating is automatically activated with any valid definition of an electrical circuit on electrically conducting solid objects and after solution, several new data fields are available for post-processing graphically, via the data inspectors and report generation: electrical potential, current density, Joule Heating and electrical resistivity.





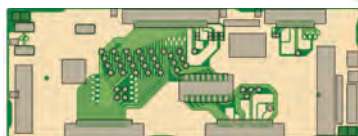
## Parametric Study

The FloTHERM XT V1 series supported the use of configurations for manipulating CAD dimensions and mates. In the V2 series, we are introducing a new integrated environment for defining, solving and analyzing results for parametric variations of geometry, attributes (e.g. material, thermal) and solution parameters.

The new user interface supports the variation of model input variables of any type and comparison between scenarios using goals. The post-processing scene and data inspector views are automatically updated when moving between scenarios and the report generation has been updated to support output of the scenario table.

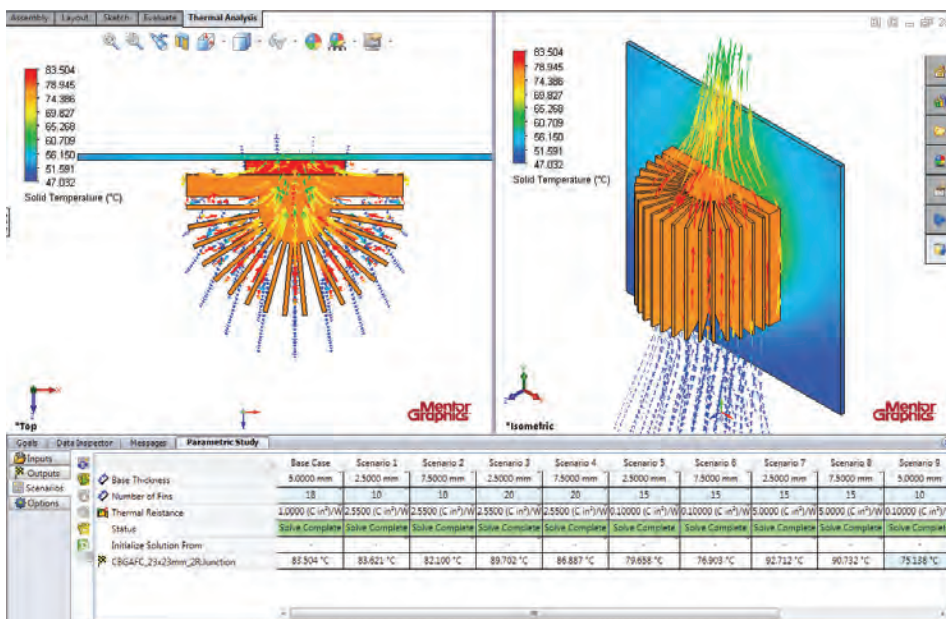
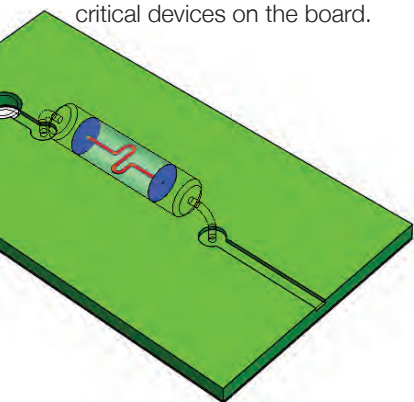
## EDA Synchronisation

FloTHERM XT continues to develop its best-in-class capabilities in interfacing with the EDA world. The new release, is introducing an ODB++ import capability, with full support for the board outline, component layout, layer stack up and metallic distribution on all layers. This means that we can now support data input from non-Mentor Graphics layout tools, thus making it easier for customers to use the tool of their choice and expand use of existing data.



In addition, it is now possible to import a board and component layout and modify the data for position, size, orientation, shape and modeling level prior to transfer to FloTHERM XT.

The V2.2 release will also have a new modeling level option to represent the PCB copper nets and traces in full 3D detail, important for high power applications involving Joule Heating effects or when higher-fidelity solutions are required for critical devices on the board.

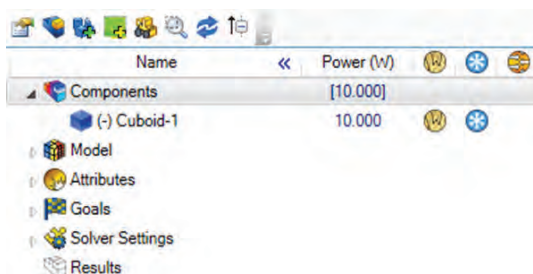


## User Experience

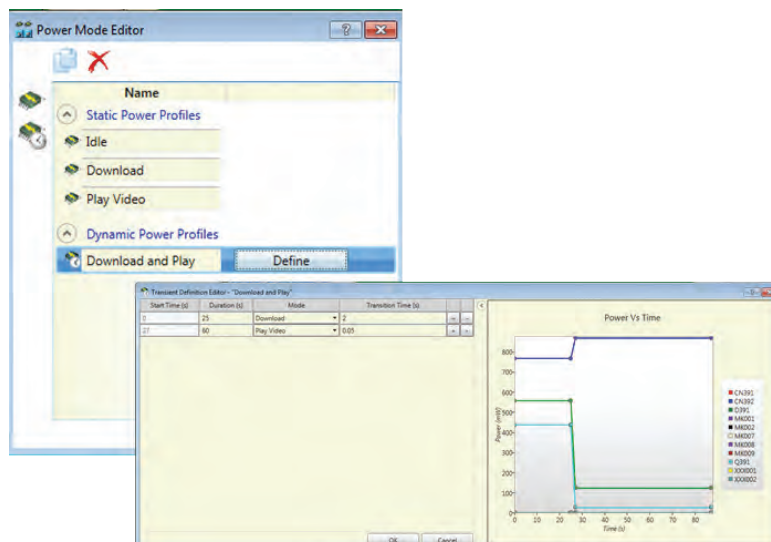
Building on the feedback from our customers using the V1 series, we have also significantly updated the software in a number of areas, including:

- A new Project Tree, with column based informational feedback on powers and attribute attachments;

- Capture Display Area – a new screen grab feature;
- Goals redesign with filtering and column ordering;
- Command-line solve support; and
- Smart Legends providing direct access to change settings via the graphics display area.



- Advanced modeling diagnostics using Check Geometry and Leak Tracking features;
- FloEDA bridge power mode support for steady-state and transient analyses;



The FloTHERM XT V2 series is a very significant update over V1 and provides an unrivalled, broad-based design environment for electronics thermal applications across all sectors. In so doing, it continues to build on our strengths of seamlessly working with MCAD data, synchronization with the EDA world and an evolving user environment based on customer feedback.

# New Release: MicReD® Industrial Power Tester 1500A 12C

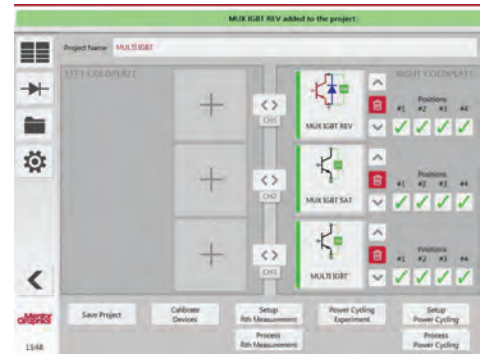
**M**entor Graphics have released the next-generation MicReD® Industrial Power Tester 1500A product for electronics components power cycling and thermal testing for up to 12 devices simultaneously. Based on customer feedback of the three channel Power Tester released in 2014, enhancements have been made to accommodate more device testing for greater productivity and lifecycle performance, including measurements of top and bottom transistors in half-bridge structures simultaneously.

“Advanced thermal management is crucial for the design of power modules and power electronics packages” said Chang-Sheng Chen, manager, at the Industrial Technology Research Institute (ITRI). The new MicReD Power Tester 1500A with 12 channels

can increase the throughput of our power tester by four times, allowing us to finish our projects significantly faster.”

Mentor Graphics remain committed to serving the needs of our customers, particularly automotive and transportation customers, who requested that we expand even further the productivity of the MicReD Industrial Power Tester 1500A.

“Knowing that their electronic components will perform to optimum standards is crucial for their success, so using the MicReD Power Tester gives them added confidence by helping them develop and validate both electronic parts and batches of parts for manufacturing with greater performance reliability.” Roland Feldhinkel, General Manager, Mentor Graphics Mechanical Analysis.



The MicReD Industrial 1500A Power Tester is now available as both a three-channel and 12-channel variant.

## Mentor Graphics Announces Customer Support Expansion

**W**e continue to evolve the CSD organization by expanding our range of Productivity Services, developing our Tiered Support offerings, and accelerating the roll out of On-Demand Training.

Given this context, now is the right time for us to introduce a new identity that communicates the broader services portfolio we provide. Going forward, the Customer Support Division is changing its name to Global Support and Services (GSS).

In parallel we have also been working hard to refresh the look and feel of how we present our Services to customers and partners.

I would also like to assure you that while our organizational name and look and feel are changing, some things will remain constant:

- Our absolute commitment to Customer Service Excellence;
- Our approach to teamwork and customer collaboration;
- The expertise and know-how of our people;
- The trust our customers place in us; and
- The peace of mind we provide to thousands of design engineers around the world.

Shaun Mammen, General Manager GSS





# And the Winner is...

News

## Sapphire Awards

**M**entor Graphics' Mechanical Analysis Division won the first annual LEDs Magazine Sapphire Award in the category of SSL Tools and Test.

With over 100 products nominated across 13 categories, the winners were announced at a gala evening in Las Vegas. Products were benchmarked against a virtual perfect product in each category and then rated on a scale of zero to five Sapphires. Fractional scoring was allowed to help further differentiate products in each category.

According to Maury Wright, Editor in Chief at LEDs Magazine, "for a score in excess of three Sapphires, the judges were asked to

consider to what degree the entry could deliver outstanding performance." The unique combination of T3Ster, TeraLED and FloEFD was given four Sapphires. One of the judges even noted that the suite comprises an "excellent complete temperature analysis and simulation system".

For more information visit: <http://www.ledsmagazine.com/index.html>



John Wilson accepts LEDs Sapphire Award for Mentor Graphics

## NMI Award for Innovation in Power Electronics

**T**he National Microelectronics Institute in the UK comprises a number of internationally renowned company and university members who are innovators in the development of electronic and semi-conductor technology and equipment.

In recognition of their achievement and contribution to industry, the NMI hosted an awards event in November last year where the MicReD Industrial Power Tester 1500A was awarded the NMI Award for Innovation in Power Electronics. Mike Fletcher, Mentor Graphics Senior Account Manager, was on hand to accept the award on behalf of the MicReD team.

The growth of the power electronics industry in recent years can be attributed to an increase in demand for consumer and industrial power electronic systems. From advances in the aviation industry to the

development of electric vehicles and high-speed railways, power electronics-related industries have also benefited from the shift to provide more robust and high reliability products. The Mentor Graphics MicReD Industrial Power Tester 1500A is the world's

first device for power cycling and thermal testing to simulate and measure lifetime performance in electronic components. For more information visit: <http://nmi.org.uk/nmi-annual-awards-winners-announced/>



Mike Fletcher accepting the NMI Award for Innovation in Power Electronics

# Designing a Modern Submarine

The challenges faced by ThyssenKrupp Marine Systems, overcome by Flowmaster®

By T. Zikofsky, ThyssenKrupp Marine Systems

ThyssenKrupp Marine Systems



ThyssenKrupp



Figure 1. HDW Class 212A submarine U34 (Photo Courtesy of ThyssenKrupp Marine Systems)

**E**ven today, building a submarine is still far removed from the design processes we know from the automotive engineering-scene.

Partly on one hand, this is owing to the high number of integrated systems and parts and on the other hand because of the low numbers of boats ordered by a customer.

The combination of these facts and the very steady process in the defense-business

makes it difficult for the engineers to improve systems during an ordered batch. Therefore a well developed 1D CFD tool is needed to acquire all the necessary information for the design process and to ensure the system behavior is defined before the first submarine is commissioned.

Flowmaster provides the functions that help engineers to find the best and most effective solution for pipe design and the needed power consumption of pumps. With this

software you are able to calculate pressure drops, NPSH-values, flow rates, fluid velocities, oscillations etc. and furthermore, it is possible to calculate the heat transfer between solids and fluids (interaction).

This article outlines the challenges engineers are faced with in the design process of one of the most complex machines man can build. It will also provide insight as to how Flowmaster is used in the ThyssenKrupp Marine Systems submarine yard in Kiel, Germany.





## The Conventional Submarine

A modern conventional submarine uses a non-nuclear air independent propulsion system (AIP) based on a diesel fuel cell combination. The tactical advantages of this system are very low heat and acoustic signatures combined with the ability to stay submerged for long periods. In 2013 the German Navy submarine U32 set a new world record by staying fully submerged longer than ever before, during its trip from Germany to the east coast of the USA. The fluid systems of the modern HDW Class 212A and 214 Submarines are integrated with nearly 3000 valves and many kilometers of pipeline. These systems are divided into single sub-systems such as cooling seawater systems, fuel-cell systems, ballast system, freeing and compensating systems, fuel oil system, chilled water system, weapon compensating system, fire-fighting system, etc.

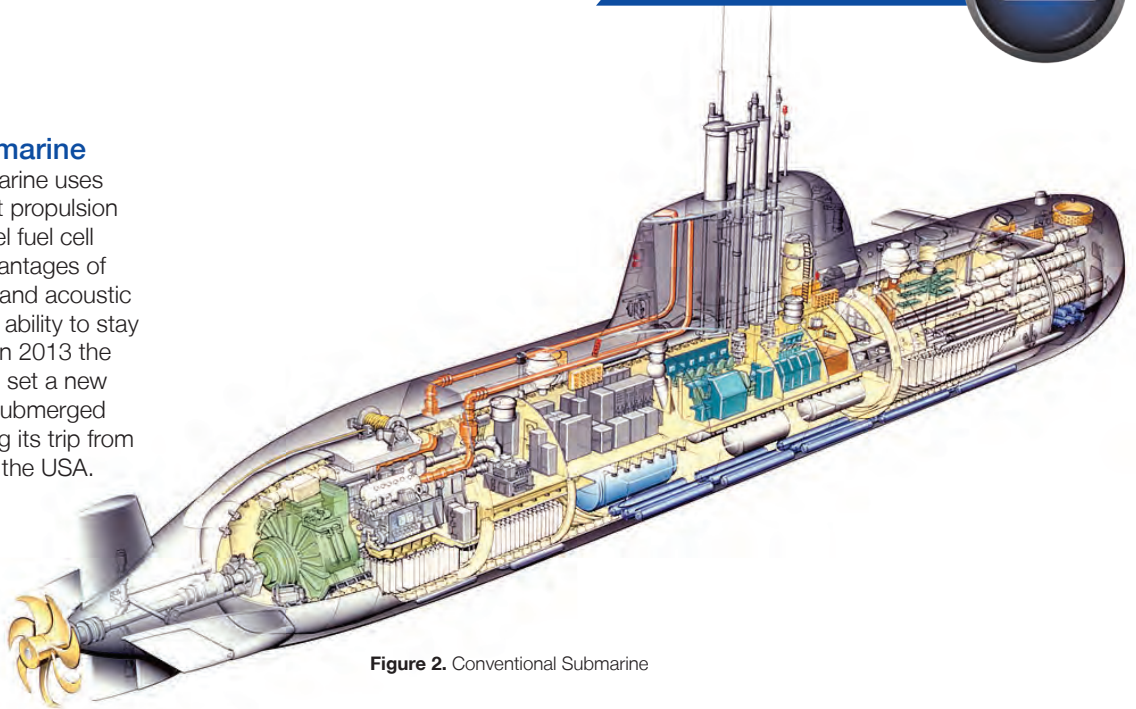


Figure 2. Conventional Submarine

Of course, all systems have to be robust and reliable because the conditions at sea can be rough and sometimes hostile, even without battle scenarios.

## Simulation of Cooling Systems

There are two simulation scenarios in submarine systems: 1. Checking the performance of an existing system and 2. Designing a completely new one. The first way is the easiest because, in most cases, there are normally existing CAD-data or isometric drawings of the pipe routing so that the network can be built very quickly. The second way is more difficult because the final routing of the pipes is not clarified in detail. The engineer has to estimate the future routing and has to calculate possible failures. The timescale of a project makes it necessary to order the pumps a long time before the piping arrangement is finished, so the second way must be used. Building up numeric networks is always a question of time and money. Usually a simple network will be chosen to shorten the time of getting a first solution.

If one needs an exact solution or a lot of additional features, you have to invest much more time in describing the model and of course the time necessary for transient simulations will increase. In general, it is possible to generate a network according to the specification with a detailed scale of 100%.

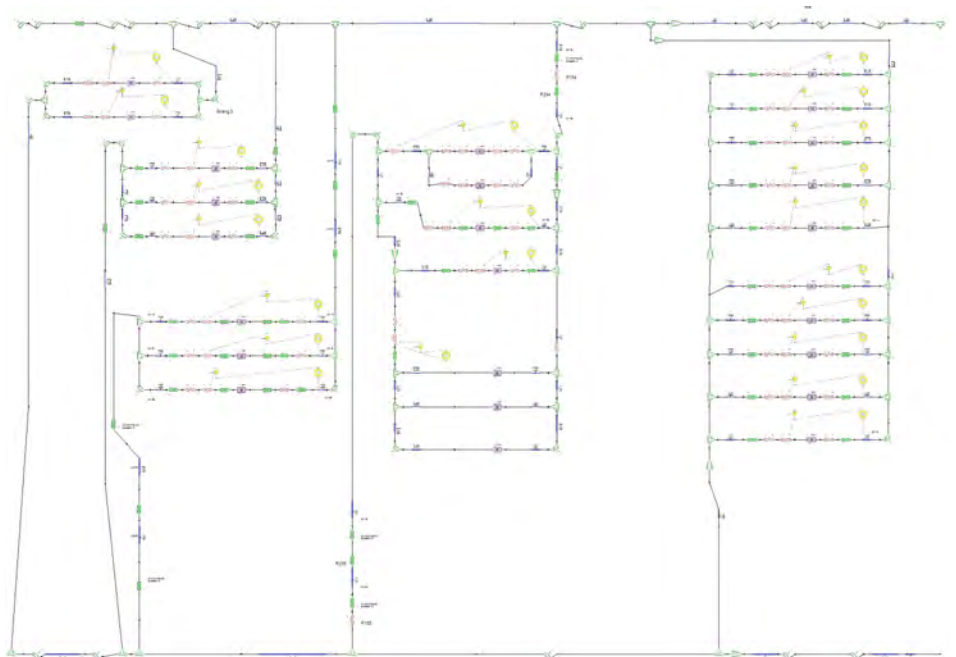


Figure 3. Part of a Network of a Complex Cooling System

At ThyssenKrupp Marine Systems the networks are used for:

- Calculating duty points of pumps;
- Calculating NPSH-values;
- Simulating interferences during changes in rotating speeds of pumps (oscillations);
- Checking the thermo management of the system;
- Gathering all information of valve positions for the technical manual;
- Checking the flow speeds in the pipelines according to mechanical and acoustic boards; and

- Calculating the fill quantity of the pipe system to support the weight calculation of the submarine.
- All before the submarine is to be commissioned, necessary to save time and money.

## System Complexity

Currently ThyssenKrupp Marine Systems simulates systems that use water, seawater, fuel oil, air, ideal gas, oxygen and hydrogen as working fluids. For this, and in order to use the internal pipe standard of different

pipe diameters, materials, pump curves, pressure drops of valves, flaps and filters are saved in Flowmaster. This makes it easier to define a complex network and to set the necessary boundary conditions. In some networks more than 1,100 components are used.

Figure 3 shows a network with a large number of components. It is possible to calculate the required pump dimension and the fluid distribution in the different flow paths with this system. It is also possible to calculate the temperatures in the pipes because of the thermal heat duty in the heat exchangers. A special feature while using a transient solver is changing the opening position of single valves during the running simulation, so that one can see a live reaction of the system.

### Transient Scenarios

In each operating condition of the submarine, the installed cooling pumps have to support a different flow rate. With Flowmaster it is possible to define single operating set-ups for use in parametric studies. Figure 4 shows an example of such a result plot of a transient interference analysis. According to the specification for this cruising condition, pump no. 1 has to provide a constant flow rate although the pumps no. 2, 3 and 4 are starting. It becomes obvious that with the current pipe configuration pump no.1 will not be able to provide the needed flow rate without increasing its rotating speed. With this information the required pump speed of pump no. 1 can be calculated and the best steering and automatic engineering concept for each cruising condition can be found.

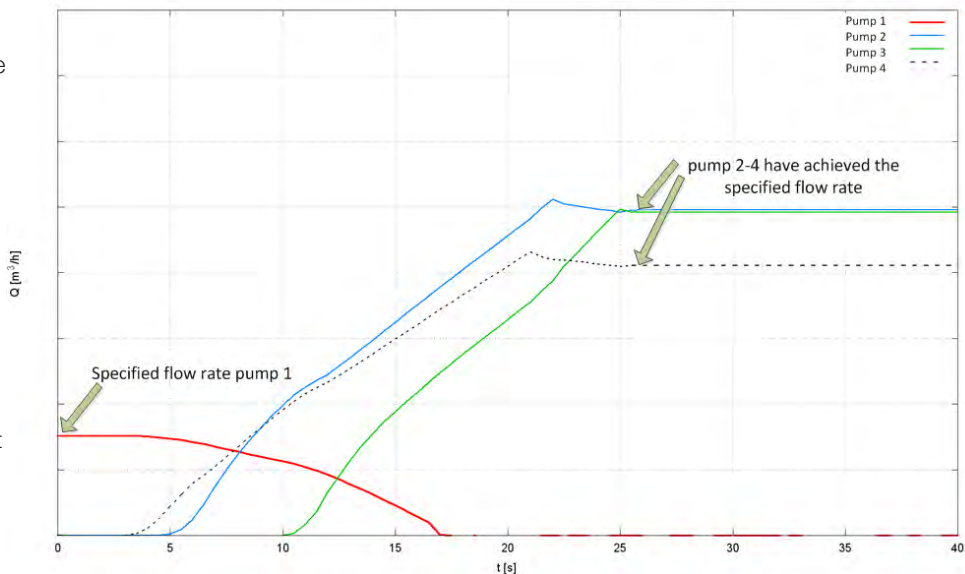


Figure 4. Post Processing Example: Interference Analysis for Complex Pump Systems

Figure 5 shows a network of an exhaust gas system for the diesel generator during submerged cruising condition. Some pipes of the system are flushed with seawater at the exterior wall and some parts are isolated. With this configuration it is possible to calculate the heat exchanges between the pipelines and the sea and also to calculate the temperatures of the exhaust gas in the pipes.

support the submarine crew to find the best system setting by calculating valve positions or pump rotating speeds offline. With the Flowmaster software and the SQL-database a large number of engineers can also work in parallel on a large project, improving efficiency and reducing the design cycle.

### Conclusion

Numerical system simulations in the design process of submarines are a good tool for engineers to find the best solution for a fluid or piping system layout within a minimal amount of time. Flowmaster is the tool of choice for ThyssenKrupp Marine Systems for system analysis. It is also possible to

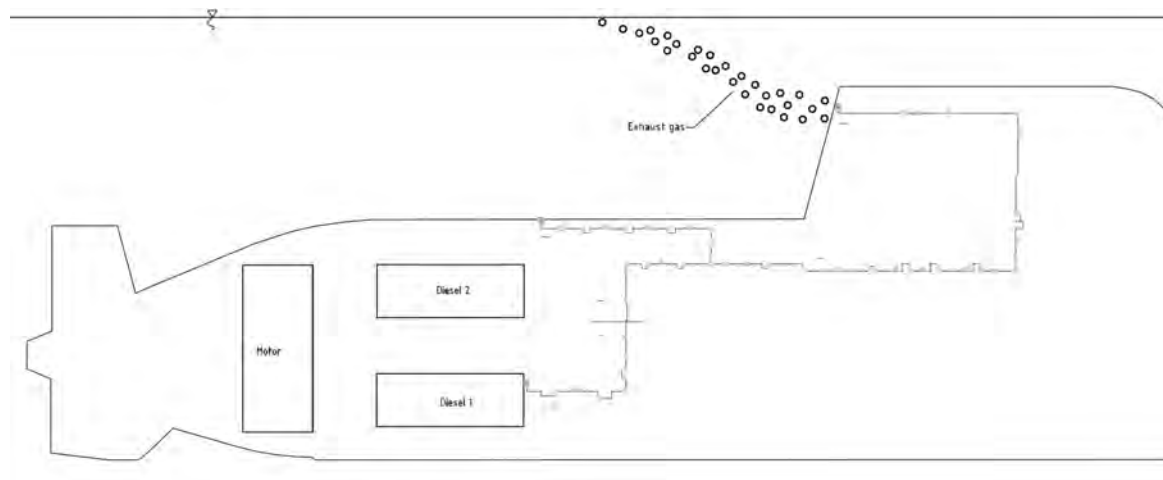


Figure 5. Exhaust Gas System Network during Submerged Cruising Condition





# Avoiding Hot Spots

Discom B.V. use FloEFD™ to ensure Temperatures are kept within Bounds



In their 30 years as designers and suppliers of exhaust gas systems, Discom B.V. have seen the requirements regarding noise and emissions change and tighten considerably. Investment in research and development is therefore critical to creating new designs and ensuring the continued success of the company.

The challenges they face come not just from meeting or exceeding regulatory requirements, but also to ensure that the systems offer high reliability over their design lifetime. These requirements are made more complex due to the need to ensure that the final design can be practically installed and maintained within the often tight spaces set aside for them.

Given these requirements, it's essential that the tools that support the design process are integrated within the overall suite used, and can provide clear and reliable results with the minimum of user intervention. It's for these reasons that FloEFD, operated by HEC on behalf of Discom, can prove so valuable. For instance, when considering the lifetime estimation of thermal loading on an exhaust silencer for a train, the CAD embedded nature of FloEFD allowed for even this complicated geometry to be prepared and discretized with minimum effort. The results from the simulation can then be fed in to the structural finite element package to define the boundary conditions for the resulting simulations.

Underpinning all such work are two key aspects of the FloEFD package: a comprehensive materials library, which allows for the thermal properties of both metals and insulation materials to be accounted for. In addition, an advanced

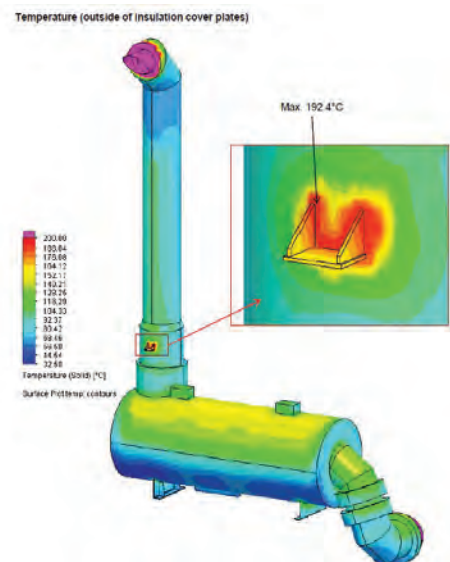


**Figure 1.** Identification of Local 'Hot Spot' in Train Exhaust Systems

radiation model allows for the effects of these materials, their surface finish and even solar radiation to be accounted for. When such detail is applied alongside a detailed CAD model, it is easy to identify and predict individual hot-spots should they occur. Being able to do all this 'upfront' in a virtual environment ensures that the optimum configuration can be derived before any metal has been cut.

**For more information:**  
[www.discom.eu](http://www.discom.eu)



**Figure 2.** Discom B.V. headquarters in The Netherlands

# ShowerPower®

# Turbulator keeps

# IGBTs Cool

FloEFD™ Efficiently Cools IGBT Power Modules

By Klaus Olesen, Thermal Design Specialist,  
Danfoss Drives, Germany



**T**he ShowerPower® liquid cooling heat exchange turbulator (Figure 1) was designed in 2005 by Danfoss GmbH engineers to efficiently cool IGBT power modules. The driver at the time was the fact that every electronic circuit generates heat during normal operation (except perhaps for superconductivity scenarios which are rare in industrial situations).

availability of liquids in certain applications. Liquid cooling outperforms air cooling by producing heat transfer coefficients several orders of magnitude higher, thus enabling much higher power densities and more compact module and inverter solutions. The acceptance of liquid cooling varies from business segment to business segment. The automotive industry for example has been using liquid cooling

for internal combustion engines for more than a century, so the idea of liquid cooling of power electronics in an automotive application is considered a non-issue. In other industries the idea of having fluids flowing through power electronic assemblies often finds resistance and concerns. The term “turbulator” for the ShowerPower is a little misleading: under normal flow conditions, liquid flow in the flow channels

This heat generation is due to conductive and switching losses in active devices as well as ohmic losses in conductor tracks. And since every new generation of power semiconductors becomes smaller than the preceding one, and the market expects smaller and more compact solutions, the demands to be met by the thermal design engineer kept growing. Sufficient cooling of power electronics is therefore crucial for good operational performance. The dominant failure mechanisms in power semiconductor components are related not only to high absolute temperatures but to changes in temperature during cycling; temperature swings produce thermo-mechanically induced stresses and strains in the material interfaces of the components (that have mismatches in coefficients of thermal expansion) which in turn lead to fatigue failures.

Liquid cooling of power electronics has been around for many years, primarily because of the ever-increasing power densities demanded, and due to the

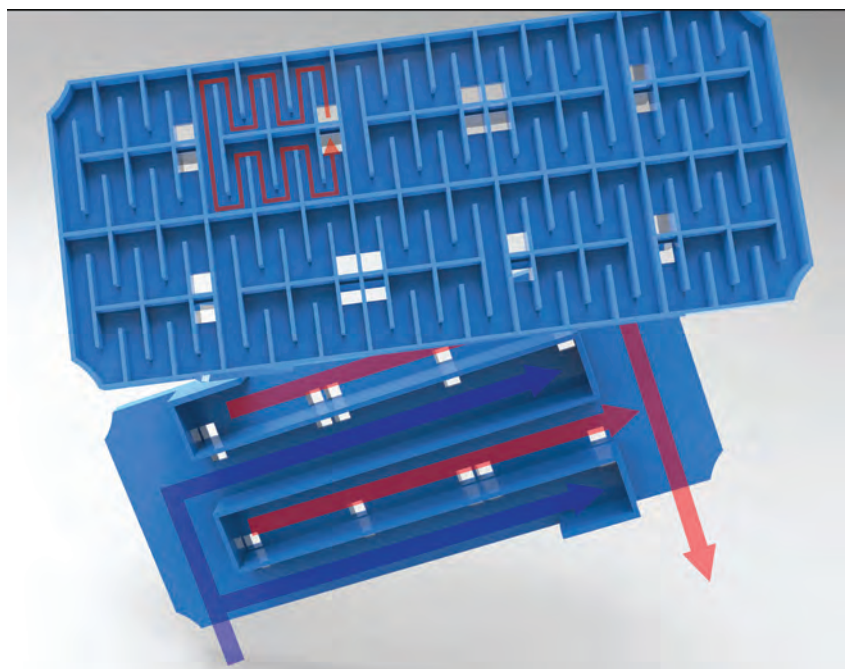


**Figure 1.** The general Danfoss ShowerPower® turbulator concept (cooling liquid in blue; warmed up liquid in red)



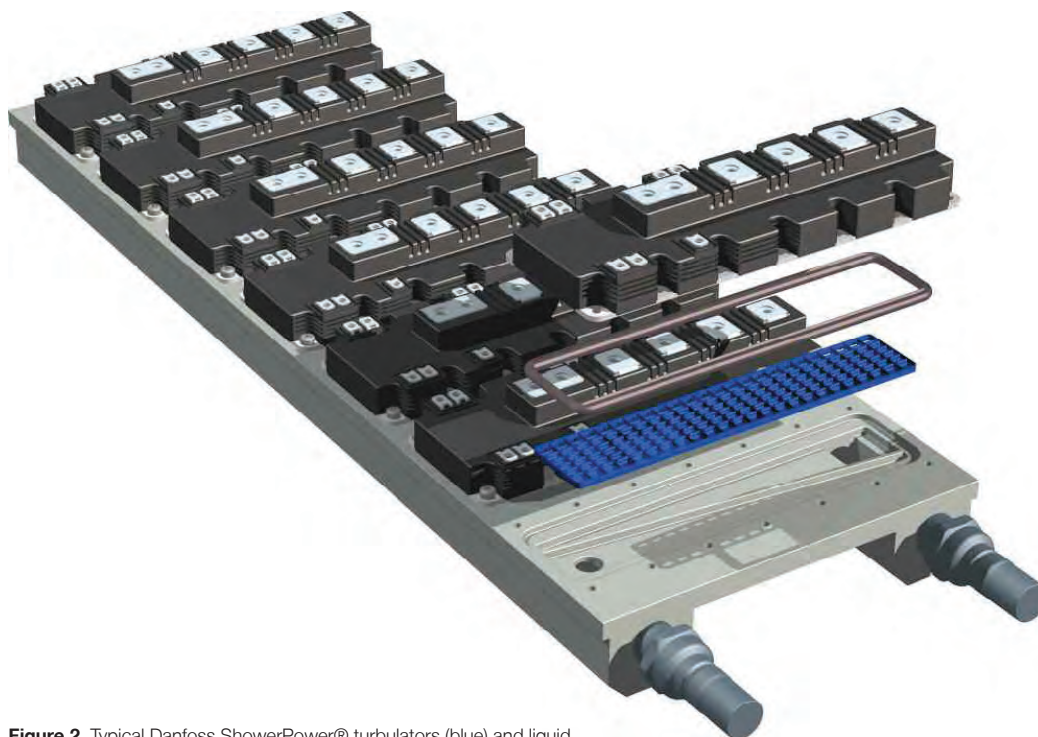


**Figure 2.** Typical Danfoss ShowerPower® turbulators (blue) and liquid cooling base plate for seven P3 power electronics modules in parallel

is laminar; typical Reynolds numbers range around 500 and the transition into the turbulence regime occurs at a Reynolds number around 2,400.

Liquid cooling solutions may be divided into two groups - indirect and direct liquid cooling. Indirect cooling means that the power module is assembled on a closed cooler, e.g. a cold plate. Cold plates may be manufactured by for example gun drilling holes in aluminum plates or by pressed-in copper tubes in aluminum extrusions. When dealing with cold plates it is necessary to apply a layer of TIM (Thermal Interface Material) between the power module and the cold plate. Direct liquid cooling on the other hand means that the coolant is in direct contact with the surface to be cooled. Here the cooling efficiency is improved by increasing the surface area and this is commonly done by various pin fin designs. Direct liquid cooling (Figure 2) eliminates the otherwise required layer of TIM. Because the TIM layer accounts for 30%-50% of the  $R_{th}$ , junction-coolant, this TIM-elimination results in an improved thermal environment for the power module. Since dominant failure mechanisms are temperature-driven, this will lead to higher reliability of the power module.

The ShowerPower cooler assembly in Figure 2 is for a wind turbine application featuring seven P3 IGBT modules, turbulators, sealings and a manifold. The design ensures that all chips in all modules are cooled

equally efficiently. The concept enables tailored cooling if hot spots need extra attention; this is simply done by designing the cooling channels individually. For further information on the principles of ShowerPower please refer to References 1 and 2. The general ShowerPower plastic part (in blue) has several cooling cells in the X and Y directions and needs a manifold structure on the backside of the plastic part; this ensures that each cooling cell receives water at the same temperature. Since the P3 module is relatively long and narrow only one cell is necessary across the module; this makes the plastic part much simpler since the manifold structure on the backside becomes obsolete.

Overall, the ShowerPower concept has several inherent benefits:

1. The ability to homogeneously cool large flat baseplate power modules, and systems of modules, thereby eliminating temperature gradients thus improving life and facilitating paralleling of many power chips;
2. Eliminating the need for TIM - No TIM-related pump-out and dry-out effects;
3. A very low differential pressure drop,
4. Compact, low weight, high degree of design freedom enabling 3D designs; and
5. Low manufacturing costs: metal-to-plastic conversion into simple plastic

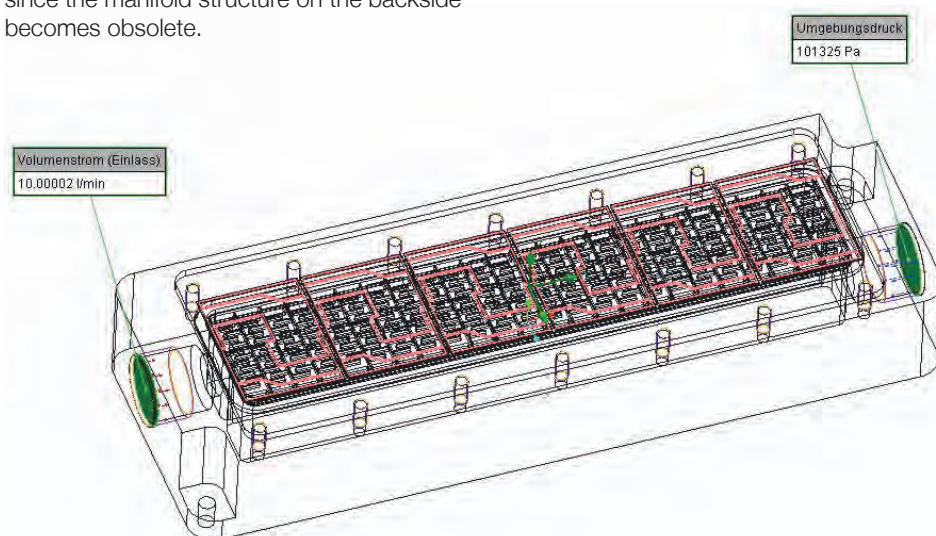


**Figure 3.** Typical Danfoss ShowerPower® liquid cooling CFD simulation of a Power Module geometry inside FloEFD for Creo

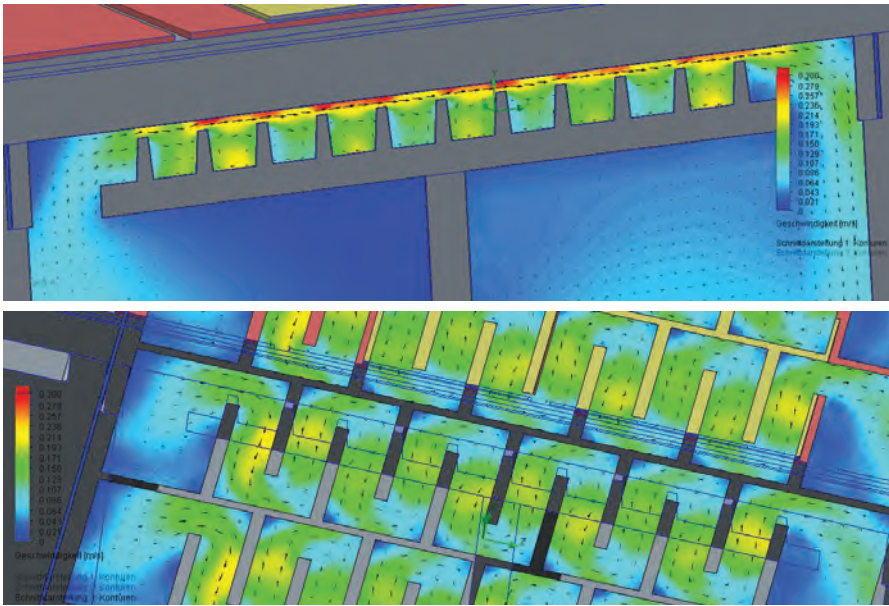


**Figure 4.** Typical Danfoss ShowerPower® liquid cooling CFD simulation of a Power Module geometry showing sectional views of flow vectors and velocity magnitude contours.

parts. Numerous CFD simulations and test measurements have been done over the years on various Danfoss ShowerPower designs to validate the concept and to extend it to niche and custom applications. Engineering simulations, (thermal, fluid, mechanical, stress, vibrational etc.) are a crucial part in any Power Module product development project, the obvious reason being, to reduce the number of time-consuming and costly experimental tests necessary. Computational Fluid Dynamics, CFD, is the best way to simulate a ShowerPower liquid cooling system. CFD will predict fluid flow so that the correct heat transfer rates and pressure drop conditions are found and thus the relevant temperatures, e.g. semiconductor junction temperatures are calculated and maintained.

When designing a liquid cooled system in the FloEFD for Creo CFD package (Figure 3) we consider several issues in order to ensure a reliable solution that is capable of delivering the performance needed over the required lifetime of the system. We also consider other factors such as corrosion, "tightness", sedimentation (including bio growth) and anti-freezing issues for instance. The permutations in the turbulator geometry are quite large:

- Width of channel;
- Depth of channel;
- Height of bypass;
- Amount of channels per meander; and
- Channel cross section area to avoid the risk of blockage.

Figure 4 illustrates such a CFD prediction for a typical ShowerPower application. With FloEFD we can easily create several

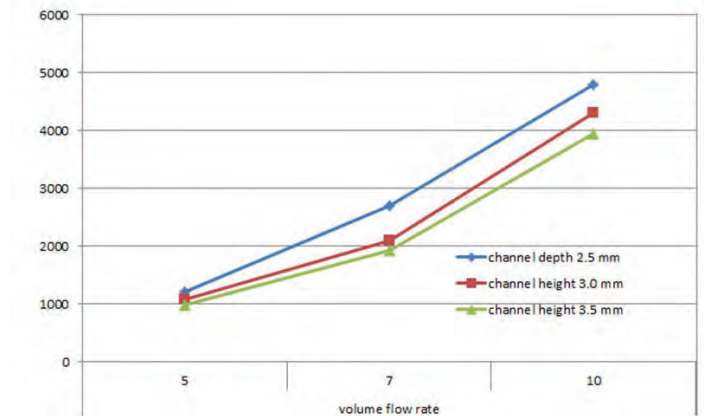


**Figure 5.** FloEFD Pressure drop curves for different volume flow rates in the ShowerPower®

different simulation cases to allow the design engineer to make optimization judgements. Finding the best design out of many CFD cases is supported by effective parametric results comparison in the software. We are able to look at many different channel dimensions for a range of flowrates (Figure 5). FloEFD ultimately gives us predictions of the surface temperatures on the IGBT/ShowerPower system before we iterate to a final prototype and build and

test it (Figure 6).

#### References:

1. K. Olesen et al., "ShowerPower® New Cooling Concept", PCIM Conference Proceedings 2004, Nuremberg.
2. K. Olesen et al., "Designing for reliability, liquid cooled power stack for the wind industry", EWEA Conference Proceedings, Copenhagen, Denmark, 2012.

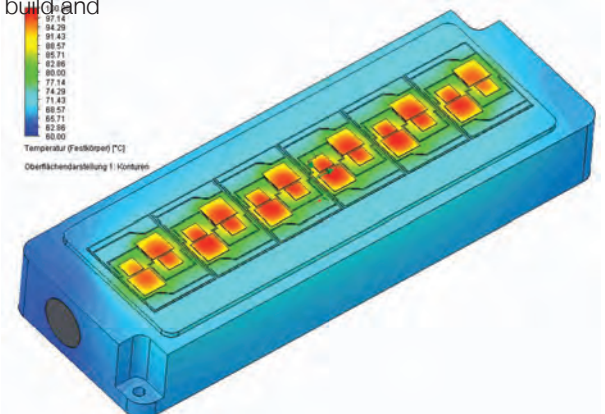


**Figure 6.** CFD temperature surface plot on a Danfoss Power module with an operating ShowerPower®





**Klaus Olesen, Thermal Design Specialist, Danfoss Drives**

**Q. Tell us about Danfoss, and the Drives Division and what you do?**

A. Danfoss is headquartered in Denmark and is a \$5.5Bn company. I work in the Danfoss Silicon Power GmbH, in Flensburg, Germany, a part of the Danfoss Drives division. In late 2014, Danfoss Power Electronics acquired Vacon a Finnish motor drives company. Now Danfoss is the second biggest low-voltage motor drives manufacturer in the world. I am a thermal design specialist, responsible for developing new cooling technologies for our power electronic components and systems. I cover thermal, thermo-mechanical and fluid dynamics simulation tools (FEM, CFD), power electronics reliability and, lifetime assessment, from concept development to feasibility studies. Danfoss Silicon Power aims to be the best choice of power module supplier in the world with our off-the-shelf and customized solutions.

**Q. You have worked for Danfoss for 25 years, what have been the major changes and trends you have experienced?**

A. When I started in 1990, Danfoss was vertically integrated with many factories for supporting processes like chemical treatment, plastic molding etc. This has changed dramatically in the last 10 years as we have become leaner and have focused on our core capabilities while outsourcing supporting processes. In Flensburg, we focus on getting the best thermal designs for our power modules and tailor solutions to customer applications. We find that the market expects a cost reduction each year for control electronics and computers. While chip manufacturers need to have smaller chips, each generation with more current going through them (in a power law relationship). We are constantly challenged to deal with more heat, to manage in a shrinking space! In terms of applications for IGBTs, modern wind turbines are being designed for a lifetime of 15-20 years with the turbines expected to run 24 hours a day, 365 days a year when the wind allows. This corresponds to 150-180,000 hours of service which is 10-20 times the lifetime expectancy

for typical automotive IGBT applications and 3-5 times the expectancy for other industrial applications. To secure sufficient reliability over the expected life of any such critical system calls for an in-depth understanding of the relevant failure mechanisms and mission profiles of the specific application.

**Q. You invented the Danfoss ShowerPower® – the leading IGBT Liquid Cooling equipment for Power Modules. How has IGBT liquid cooling evolved over the last 10 years and what's next?**

A. With greater and greater quantities of heat needing to be removed from IGBTs we recognized some time back that an effective form of liquid cooling was necessary. The ShowerPower invention was our patented response. We used CFD to design this complicated heat exchanger unit that was introduced to the market in 2008. We verified the CFD results against university experimental test data. We custom design and manufacture ShowerPower that attach to IGBT modules to maintain a constant surface temperature for optimal performance. We guarantee thermal and structural reliability of our solutions for long warranty periods without failures of the cooling circuits.

**Q. How has your CFD design process evolved in the last 10 years?**

A. For a typical customer application we may need to do 50 or more CFD simulations to check for good fluid flow and heat transfer in the ShowerPower. Ideally we want to compress our design cycles further each year, whilst dealing with increasingly complex geometries. We chose FloEFD as our CFD design tool because we didn't want to be CAD geometry and meshing jockeys. We wanted a tool that was user friendly, embedded in PTC Creo, our CAD tool, and accurate. I like FloEFD compared to other more complicated CFD tools because I can dip in and out of it all year with minimal effort to pick it up again. It's also robust and easy to mesh our complex geometries inside Creo. Our ShowerPower product is the best compromise between manufactured cost and homogeneous thermal performance with our use of aluminum heatsinks. We were the first to do effective liquid cooling and we intend to maintain our technical advantage.

**Q. What do you see as future megatrends and challenges in your area of Power Electronics?**

A. We are seeing bigger and bigger cities emerging all over the world with larger and larger electrical infrastructures that produce HVAC and power conversion challenges. Even the explosion of elevator and lift technology in tall city skyscrapers puts a

## Interview

challenge on next generation motor drives. Power densities are increasing each year. In the automotive sector with the increase in electrification of vehicles we are seeing demands for power electronics to be embedded in other components like gear boxes. This impacts their performance because of the aggressive environments they need to operate in and reliability is therefore key. I can also foresee whole new geometrical shapes and materials emerging from the 3D printing industry that we will have to deal with and even nanotechnology surface coatings for enhanced heat transfer will become a challenge for us over time.

**Q. Where do you see CFD going in the Power Electronics arena in future?**

A. In terms of computer-aided engineering (CAE) tools generally, I see a trend towards CFD and FEM structural analysis tools merging and offering true concurrent "multiphysics" solutions. Because electrical power losses lead to temperature effects (CFD) impacting structural deformations and crack formation (stress analysis) which in turn impact power thermal and structural changes over the component's lifetime – they're all interlinked. I also foresee the need for more design of experiments in CAE modeling of power electronics - to yield a precise die position in a module or to simulate a particular gate drive switching strategy. We will always need more and more simulations as early as possible in the design cycle. I think engineers in future will therefore need to be multi-talented, and in terms of CFD in particular, there will be an increasing need for early rough simulations to yield data to make faster and faster design judgements.

**Q. The other part of your job is Power Electronics Reliability – how do you see that relative to your thermal expertise?**

A. Yes, I cover lifetime assessment of IGBTs and this is becoming increasingly important as they run hotter and hotter in warmer ambient conditions where reliability is mission critical. We do "Physics of Failure" using a combination of statistical analysis, simulation tools and physical testing. We work closely with local universities at Aalborg and Fraunhofer to develop better techniques. The cycling and drive cycling our products experience obviously has a profound effect on their reliability. A big challenge we face is the change in physical properties of our materials over time during normal operation, due to the power loads they have to sustain and impairments in thermal performance.

# FloTHERM® - Powering Power Supply Development

A case study of Emerson Network Power

By John Parry,  
Electronics Industry Vertical  
Manager, Mentor Graphics



**T**he development of electronic devices has seen a trend towards their miniaturization and an increase in their functionality.

Both of these put high demands on heat dissipation. High MOSFET temperatures can lead to instability, shortened life expectancy, and even lead to the device exploding! High temperatures can also contribute to thermal breakdown in electrolytic capacitors, dramatically shortening their life. While inductors and other magnetic components can withstand high temperatures, peripheral devices can be impacted.

To ensure that the power devices operate effectively within a given temperature range, attention needs to be paid to a product's thermal design. Reliable thermal design can guarantee the life and reliability of the product, and ultimately reduce costs in the long-term.

Emerson Network Power are a \$6.2bn company with about 45,000 employees [1]. Thermal Management is a Center of Expertise that has been strengthened by the acquisitions of Liebert, Hiross, Cooligy and Knurr, to critical cooling issues at room, rack or chip level. Emerson take a holistic approach to thermal design, using FloTHERM from the chip package up to the room in which the equipment sits, to produce the best overall thermal design. This endeavor is greatly assisted by FloTHERM's Cartesian meshing supporting localized mesh regions, allowing multiple length scales to be included within a single model.

At the package level, Emerson aim to create a thermal model that is as close to reality as possible to help evaluate the transient response of their power electronics components with accurate junction temperature prediction – the goal of all thermal design studies.

At the PCB level, emphasis is placed on using the correct material property values, capturing the actual copper distribution in the board. Attention is paid to refining the mesh around large and high power components such as, MOSFETs, to accurately capture temperature gradients in both the air and the solid. Thermal radiation contributes to both heat loss and heat exchange between components, so radiation is also included in the calculation, so the surface emissivity of the components and board must be factored in.

At the modular level, the environment is an important factor to capture in the simulation. In the case of a small sub-rack for example, which is cooled by natural convection, the ambient temperature can be 30°C. With stratification in the ambient air affecting the air flow through the enclosure, the simulation model must be extended to include the local environment. As the scale of the model increases, care is needed to preserve the fidelity of the modeling effort.

Comparison with test data becomes tricky, as it is difficult to control the environment, particularly when testing products cooled by natural convection, as small drafts and other effects can affect the measurements.

Integrating the electronics together at the cabinet level adds a new level of complexity to the simulations, as failures or disturbances in the power network can cause the supply voltage to drop. Under these circumstances, the power electronics must be able to function as normal to avoid an impact on downstream equipment.

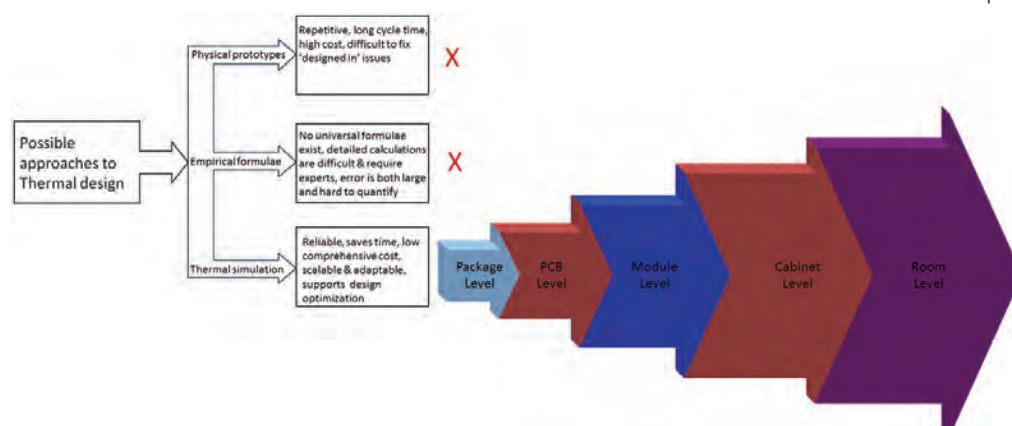
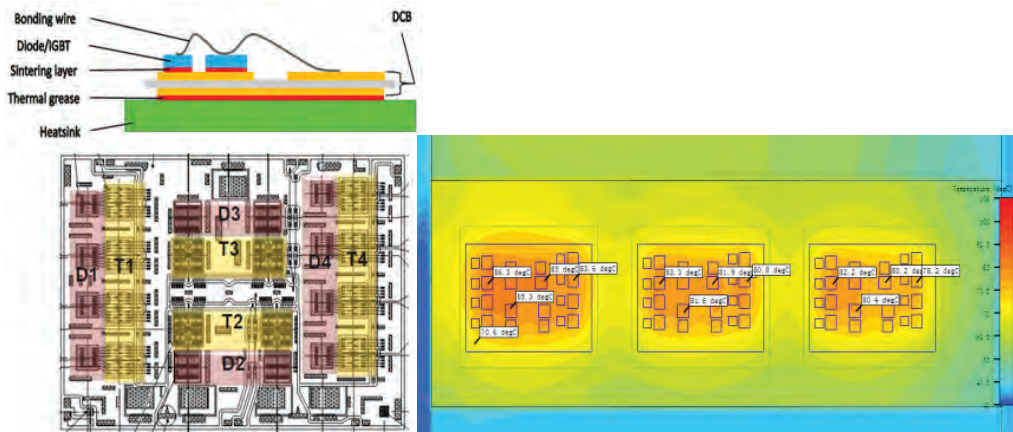


Figure 1. Emerson's exclusive use of thermal simulation at all packaging levels





**Figure 2.** Stackup of Power Module showing die detail, and FloTHERM model

When operating in this manner, the power dissipation within the devices increases, leading to a further rise in temperature within the components in just a few seconds, this must however, remain below the maximum operating temperature for the components.

Emerson Network Power's equipment can be used in multiple configurations and in a variety of environments, so there is considerable scope for equipment-to-equipment thermal interaction at the room level. In some installations, this is prevented by using a room-level cooling strategy, such as cold aisle containment in datacenters.

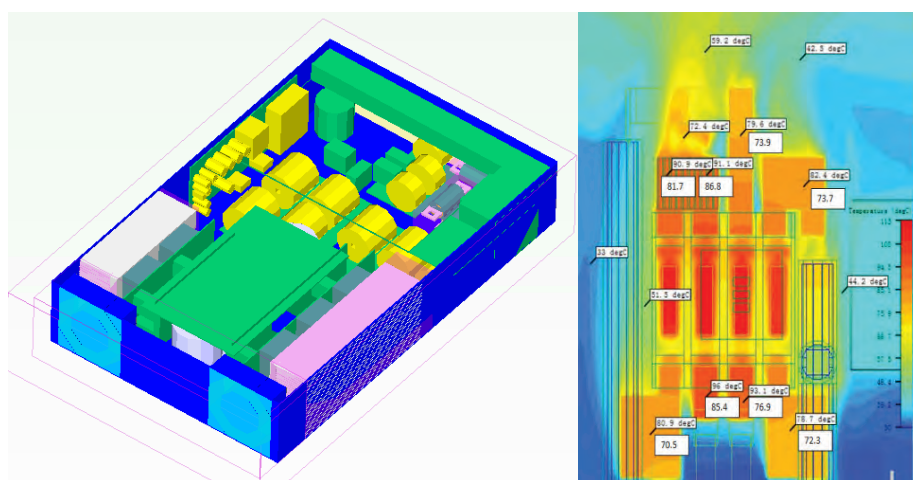


**Figure 4.** Typical Module and Temperatures within a Sub-Rack

To make the most efficient use of FloTHERM, Emerson use Mentor webparts [2] to define models of porous materials, centrifugal blowers, thermoelectric coolers (TECs), fans at high altitude, and complex geometry. In this way thermal simulation is repeatedly used to validate ideas during design and improve knowledge sharing with colleagues and other stakeholders.

Emerson also make extensive use of thermal measurements, including Mentor's Transient Thermal Tester, T3Ster®, to obtain thermal data for components and heatsink thermal resistances, to increase the fidelity of their thermal simulation work – a practice that is becoming increasingly common in best-in-class companies.

## References:

- [1] [www.emersonnetworkpower.com/documentation/en-US/About/Documents/FactSheetEmersonNetworkPowerFY13.pdf](http://www.emersonnetworkpower.com/documentation/en-US/About/Documents/FactSheetEmersonNetworkPowerFY13.pdf)
- [2] [webparts.mentor.com/flotherm/support/webparts.jsp](http://webparts.mentor.com/flotherm/support/webparts.jsp)

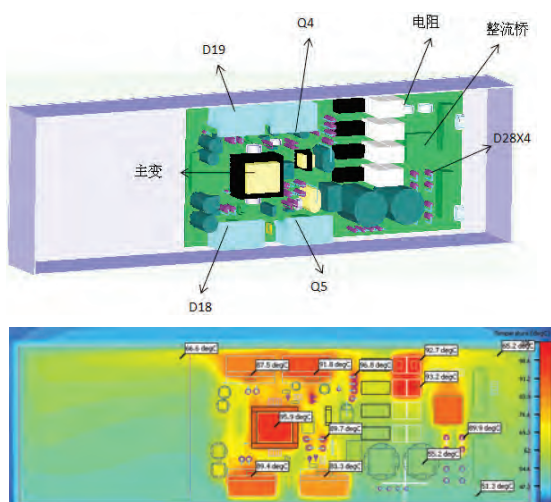


**Figure 3.** PCB and FloTHERM simulation results

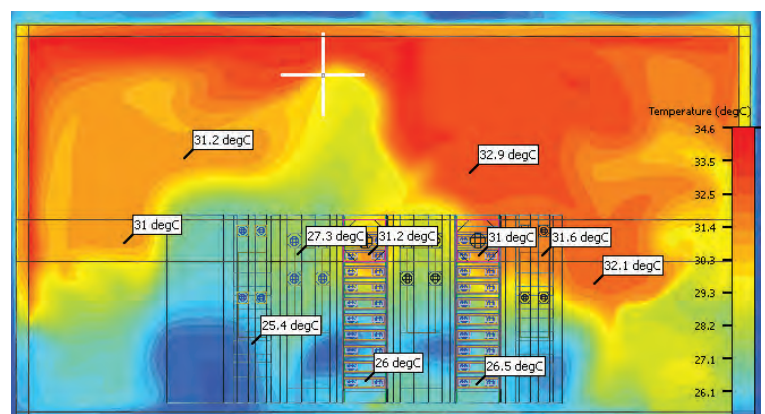


**Figure 5.** Temperature distribution through several racks showing stratification in the room

# Model & Solve for an Extrusion Die

How to use FloEFD™'s Customizable Fluids and Flow Freezing Features to Model Non-Newtonian Fluids



Kate Boyd, Corporate Application Engineer



**N**on-Newtonian fluids are a quirk of nature in which viscosity is dependent on shear rate. This can lead to such wonderful phenomena as running across a pool of corn starch and water and such disappointing phenomena as a glob of ketchup (or mayonnaise) on your fries when you only wanted a dab.

A common example of non-Newtonian fluids in industry can be seen in the manufacture of extrusion molding products, namely plastics and rubbers. Using FloEFD's ability to create customizable fluids and system conditions, one is able to accurately model the appropriate viscous effects of using non-Newtonian fluids.

When creating the new custom fluid, it is important to characterize the dynamic viscosity properly. This can be done either by setting up a data table of points showing dynamic viscosity versus shear rate or as a consistency coefficient and viscosity model (i.e. Herschel-Bulkley, Power-law, etc.). Upper and lower limitations on viscosity can also be added, if appropriate. The new, user-defined non-Newtonian fluid materials are added to the Engineering Database of FloEFD and can be assigned to projects.

Since many extrusion molding machines have thin channels through which the fluid flows, it is important to have a fine enough mesh resolution through these passages. This can be accomplished by setting a Local Initial Mesh in FloEFD and enabling the Narrow Channel Refinement option within the manual settings of the Local Initial Mesh. Typically, it is recommended to have at least four cells spanning the narrow channel or gap in order to accurately resolve the flow (Figure 2).

In the example given here, we're looking at combining two streams of the same non-Newtonian fluid to be passed through a die. This could easily be updated to model the combination or mixing effects of two different non-Newtonian materials by simply changing the fluid assigned to one of the inlet flow conditions.

It should be noted, however, that if one is using two different fluids, it is possible to reach a situation where the pressure drop is near convergence, but one of the materials has not reached the outlet. To address this issue and speed up the simulation time it is necessary to pause the simulation and turn on the "flow freezing" option under the Advanced tab in the Calculation Control

Options. One can specify parameters controlling the procedure of saving the CPU time by freezing (i.e., taking from the previous iteration) values of all flow parameters, with the exception of fluid and solid temperatures and fluid substance concentrations, which converge more slowly than the other flow parameters, so the temperature and concentrations are calculated at each iteration. This option is useful because we have a time-dependent problem with substantial heat transfer and fluid substances propagation.

One also has the option of periodic or permanent flow freezing. In the case of two fluids, it can be difficult to assess how many iterations would be needed to allow the penetrating material to fully propagate through the model, so setting the flow freezing option to permanent may be the better choice.

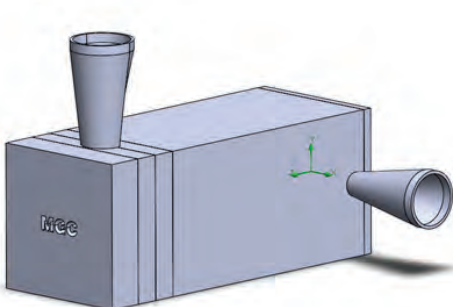


Figure 1. An Extrusion Die Machine

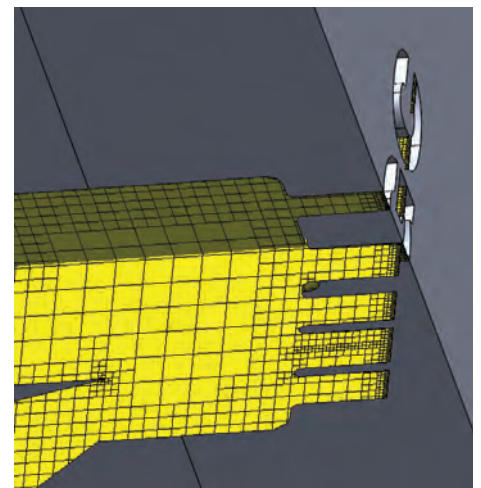
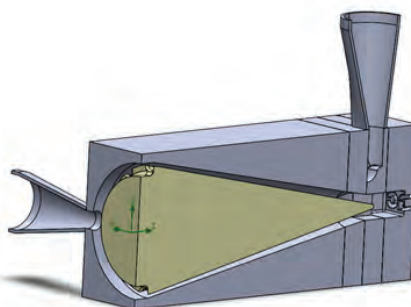
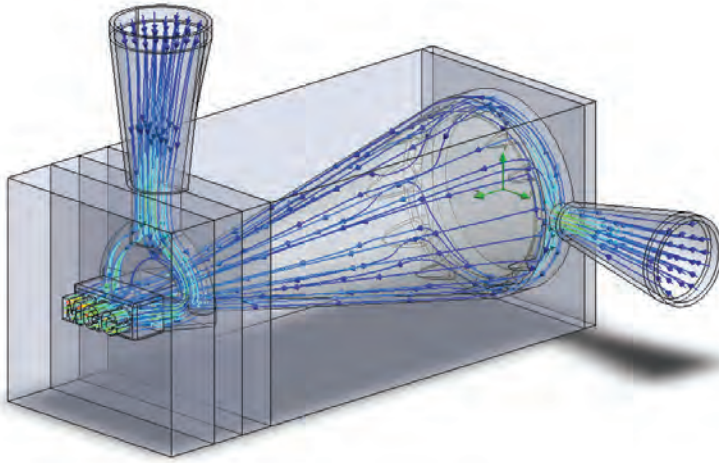


Figure 2. Mesh Resolution Across Small Gaps





**Figure 3.** Flow Trajectories through the Model

Once the penetrating material has reached the outlet of the model, flow freezing can be switched off and the model analysis allowed to continue until convergence of all parameters is reached.

Back to our one fluid model, having created a suitable mesh, defined the non-Newtonian fluid materials as described above and applied the necessary boundary conditions, the analysis is ready to be started. The volume of the fluid cavity is initialized with 100% of the non-Newtonian fluid. The inlet conditions are specified as mass flow boundaries where the material is released independently in two separate inlets. After about 200 iterations, the model is converged.

Looking at our results using the Flow Trajectories function, we can see that the fluid trajectory's results are just as we would prefer (or expect) them to be as visualized through the inlets and the die (Figure 3). However, we notice some areas of higher velocity which require further inspection (Figure 4).

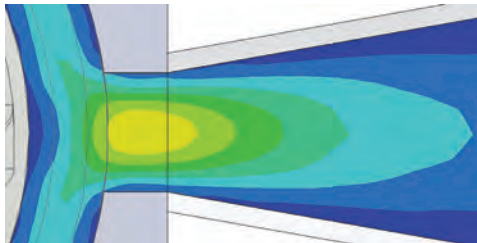


**Figure 5.** Areas of High Velocity needing further inspection

Using the cut plot feature of FloEFD, we inspect the local velocities in the areas of interest. We are interested in areas of high velocity gradient because we don't wish for the consistency of our material change during the extrusion process. Areas of high velocity gradient could be indicative of areas

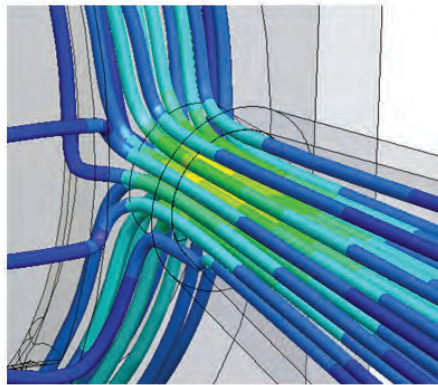
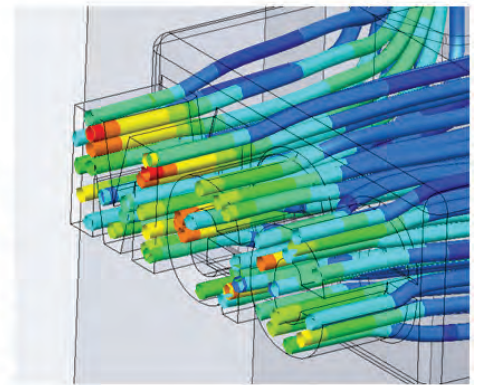


**Figure 4.** Local Velocities around the Rear Fluid Inlet

with a high shear stress and thus run the risk of our materials seizing or becoming too thin.

Figure 5 shows the local velocities around the rear fluid inlet. While there is some gradient, it should be easily remedied with some simple geometry changes.

Figure 6 shows the local velocity magnitude distribution at the outlet cross-section around the die. Here we see much higher gradients through the die which are completely unacceptable. One of the main goals of the design process related to the extruder model is to achieve a more uniform



distribution at the outlet so as to avoid the risks of having areas of high shear stress, as mentioned earlier.

By using the various capabilities of FloEFD, we were able to accurately capture the fluid flow through the extrusion machine and thus reach the conclusion that further refinement or tooling of the machine is needed in order to ensure proper functioning. FloEFD can further be used in the continuation of the project to model design changes or variations, thus continuing to reduce the time and effort required to complete the project.

Email: support\_team@mentor.com

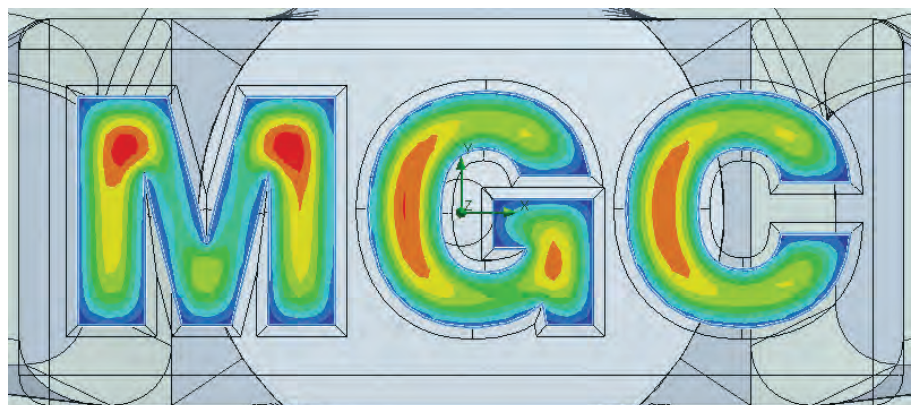


**Figure 6.** Local Velocities at the Outlet Cross-Section



# ALBA Synchrotron Cooling System Evaluation Using Flowmaster®

After five years in operation, the ALBA Synchrotron Light Source realize the first upgrade process of its cooling system.

By Marcos Quispe, ALBA Synchrotron Light Source; Xavier Escaler and Montserrat Prieto, Universitat Politècnica de Catalunya (UPC); and Morten Kjeldsen, Flow Design Bureau AS



Figure 1. Alba 3<sup>rd</sup> Generation Synchrotron Light Facility in Barcelona, Spain

**A** LBA is a 3rd generation Synchrotron Light facility in Barcelona, Spain. Made up of a complex network of electron accelerators that produce synchrotron light, it allows for the visualization of the atomic structure of matter as well as the study of its properties.

The 3 GeV electron beam energy at ALBA is achieved by powerful combinations of a Linear ACcelerator (LINAC) and a low-emittance, full-energy BOOSTER located in the same tunnel as the STORAGE RING. ALBA's 270 meter perimeter has 17 straight

sections all of which are used for the installation of insertion devices. ALBA currently has seven operational state-of-the-art phase-I beamlines, comprising soft and hard X-rays, which are devoted mainly to biosciences, condensed matter (magnetic and electronic properties, nanoscience), and materials science. Additionally, two phase-II beamlines are in construction (infrared microspectroscopy and low-energy ultra-high-resolution angular photoemission for complex materials).

This large scientific infrastructure provides more than 5,000 hours of beam time per

year for the academic and the industrial sector, serving over 1,000 researchers every year.

ALBA is a facility committed to scientific excellence and to improving the well-being and progress of society as a whole.

After five years in operation, the ALBA Synchrotron Light Source has realized the first upgrade process of its cooling system. The main objective of the project was to enhance the hydraulic plant and its control system. Specifically, this enhancement is expected to significantly improve the



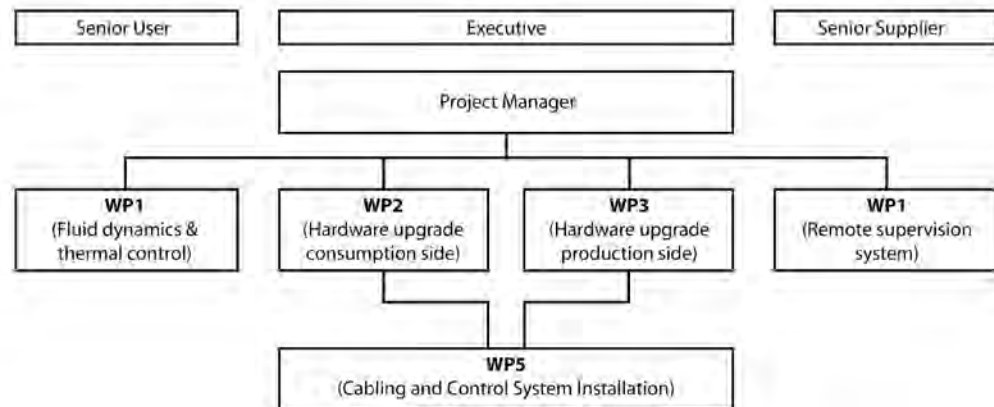


**Figure 1.** Organization of work packages for the project "ALBA Cooling System Upgrade".

facility's reliability by providing more protection against single point failure, its stability as a result of more robust in-front-of-load variations and/or external perturbations, and tolerability in fail mode to ensure maximum service readiness. To embark on this objective a Project Manager structure was defined and all the activities were grouped in the following five work packages (WP) as detailed in Figure 1. This article will focus on Work Package 1 (WP1) which set out to better understand the cooling system from a fluid dynamics control point of view.

## The ALBA Cooling System

The ALBA cooling system is outlined on the left of Figure 2 and comprises two main parts: production and consumption. For the purposes of this article, the focus will be mainly on the consumption side which is composed of four rings that require refrigeration. They are named Experimental Area (EA), Service Area (SA), Storage Ring (SR), and Booster (BO) as indicated on the right of Figure 2. Both the Storage and the Service Area rings operate with a pair of twin-pumps mounted in parallel and the rest

with a single pump. The deionized water is heated through all the rings and is collected in a common return line. Another pump (P11) takes the heated water from the return and feeds heat exchangers that cool it. The cooled water is brought to a large volume accumulator from which a suction line takes water again to the rings' pumps. In order to regulate the water temperature, a series of controlled mixing valves allow for the combination of the cooled and heated water to take place, prior to being pumped to the rings. Moreover, a pressure maintenance system with a compressor is mounted at the exit line of the heat exchangers before the accumulator. Finally, a pipe line connecting the accumulator with the common return line enables the compensation for the lack or excess of flow to the cooling loop when the total flow rate changes in the rings' loops.

## The Rings Model

As can be seen in Figure 2, each ring (EA, BO, SR and EA) consists of two concentric ring-shaped pipelines (inlet and return flow) that refrigerate a specific number of sub-systems. At the same time, most of these

sub-systems are made up of additional sub-networks that supply the cooled deionised water to final consumptions.

Currently, Experimental Area Ring feeds nine sub-systems, seven of which correspond to Beam Lines (each Beam Line has various components to refrigerate) and the rest are provisional by-passes. The Booster Ring has 104 sub-systems. One of them is a Radiofrequency Cavity (RF) that refrigerates 14 components by the means of a manifold. The remaining 103 sub-systems are single electromagnets which are present in eight variations. With regards to the Storage Ring's sub-systems, 21 are different types of electromagnets (8 to 17 magnets are fed by each sub-system), ten are Front Ends (each one cools one to five consumptions), and three correspond to RFs Cavities. In relation to the Service Area Ring's sub-systems, nine supply cold water to Power Supplies, one feeds the LINAC and some Power Supplies and the last four sub-systems are connected to RFs Plants.

The rings' models have been built up from the available components in Flowmaster

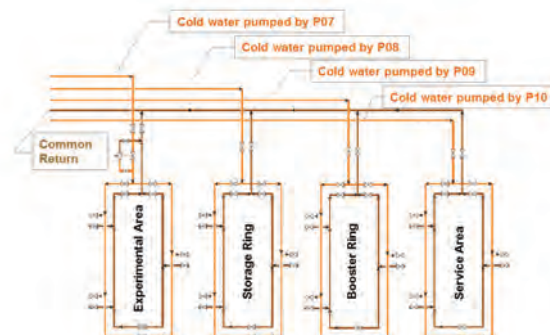
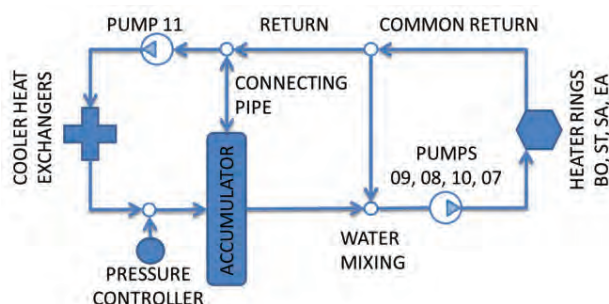


**Figure 2.** Outline of the cooling system (left) and of the consumption side (right)

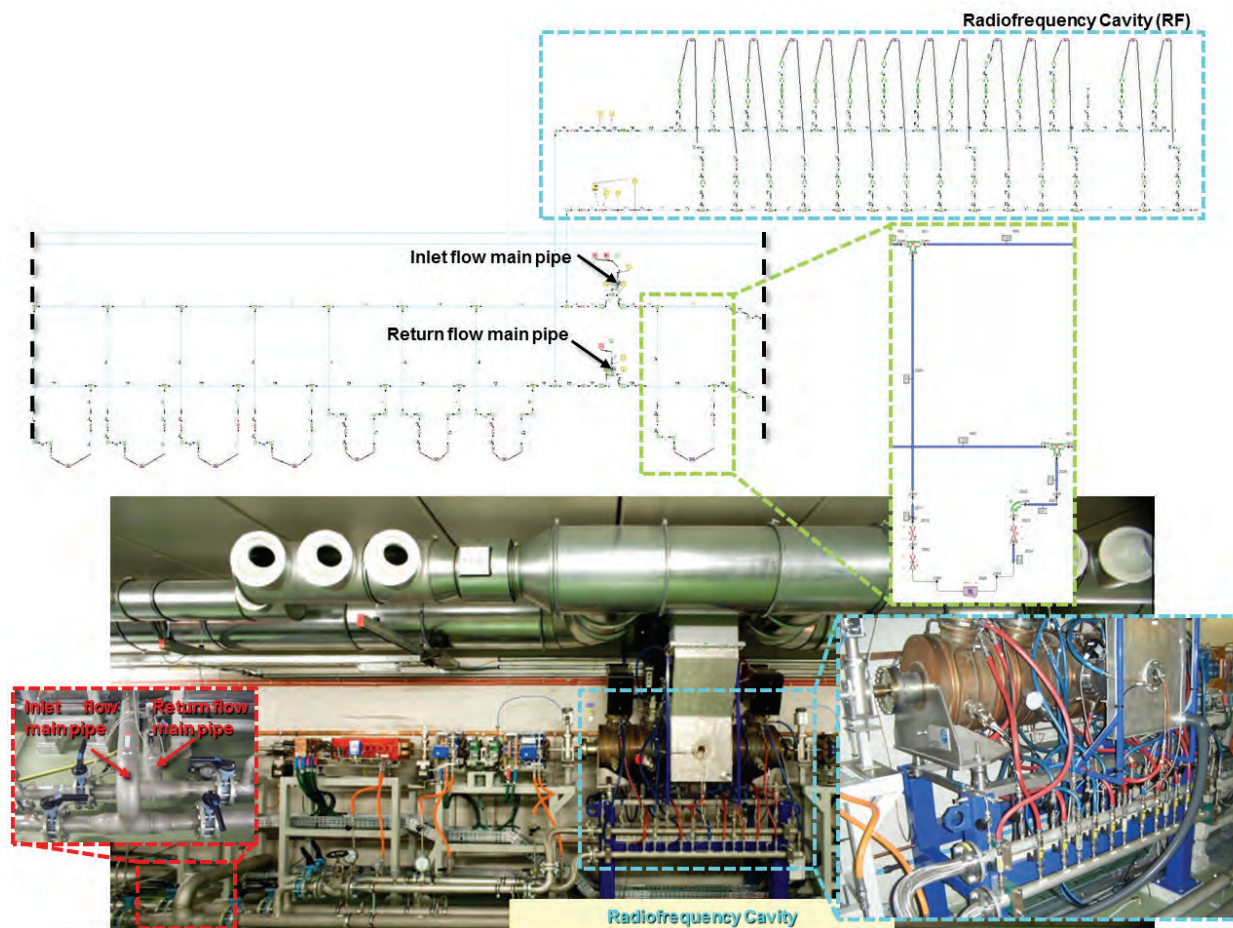


**Figure 3.** Comparison between a section of the Booster Ring (bottom) and its modeling (top)

software. The properties of each component have been selected based on the information provided by the corresponding manufacturer in the form of construction planes, technical documentation and so on. The lack of reliable information has been overcome with visual inspections and measurements in-situ. However, for the current study such level of detail has not been achieved on each ring due to their dense and complex structure as well as owing to the lack of time. As a result, the selected rings' sub-systems to model with detail, according to the needs of the ALBA

Synchrotron, are as follows.

The completely modeled sub-system of the Experimental Area Ring is one Beam Line (BL). Nevertheless, the by-pass piping networks for two future BLs have also been modeled, and the remainder ignored. The different consumptions of these BLs have been simplified with a unique heat exchanger.

When considering the Booster Ring's sub-systems, all have been modeled down to the last detail. For instance, the top of Figure

3 shows the modeling of the two main pipes of the Booster Ring and nine of its sub-systems (eight electromagnets and the RF Cavity); with bottom of Figure 3 depicting this section. Another example is the model of the RF Cavity which is shown in Figure 4 where we can see the configuration of the manifold which supplies water to 14 local consumptions.

In contrast, the Storage Ring's fully modeled sub-systems are only four: one is the secondary distributor at sector 15 (which is grouping 16 electromagnets) and the other three are RFs cavities. Again, the geometry of the pipelines of the rest of the sub-systems has not been considered. In addition, the combination from one to five consumptions of each Front End has been modeled with a single heat exchanger. Despite this, a characterized heat exchanger element models each one of the various consumptions fed by the rest of the simplified sub-systems.

The Service Area Ring's are two detailed sub-systems: the RF Plant at sector 14 (see

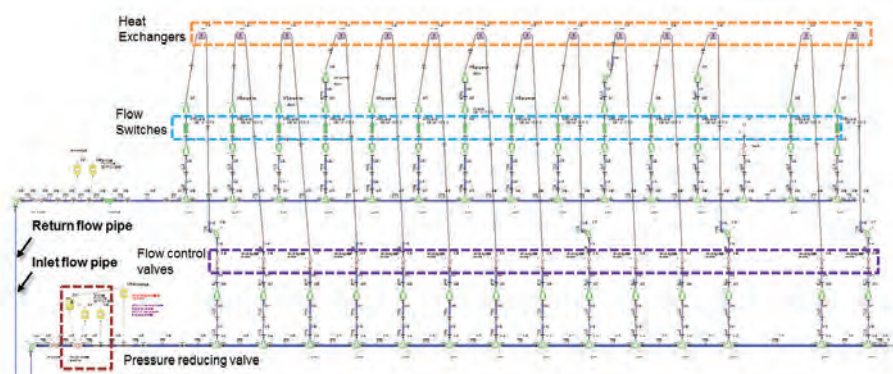


**Figure 4.** Schematic of the Radiofrequency Cavity of the Booster Ring





blue highlighted zoom of Figure 5) and the sub-system that combines the LINAC and some Power Supplies. A duly characterized heat exchanger element models each one of the different consumptions of these two sub-systems. Once again, the geometry of the other two RFs' manifold and of the pipelines of the rest of the sub-systems has not been modeled. A heat exchanger emulates not only the two simplified RFs' components but also the combination of Racks refrigerated by each one of the rest of the sub-systems (see green highlighted zoom of Figure 5). The contrast between the detailed and simplified sub-systems can be observed in Figure 5. Furthermore, Figure 6 demonstrates how meticulous the modeling of one RF's consumption is.

## Improving Pipe Velocity Distribution

Originally, the four rings had the same flow distribution: (i) the inlet flow was equally distributed to the left and right branch through a T-junction, by opening the two exit valves so that they tend to converge towards the opposite 180° ring location; (ii) for the return flow, the directions were reversed and two flows tend to converge towards the main outlet pipe. This original flow distribution is indicated as "180° circulation" on the left of Figure 7. This configuration causes the reduction of the flow velocities, as the two inlet flows approach and a zero velocity point should be ideally achieved in some undefined location which is dependent on the local consumption distributions. Consequently, there is a risk of air accumulation in a zone that might be close to some critical

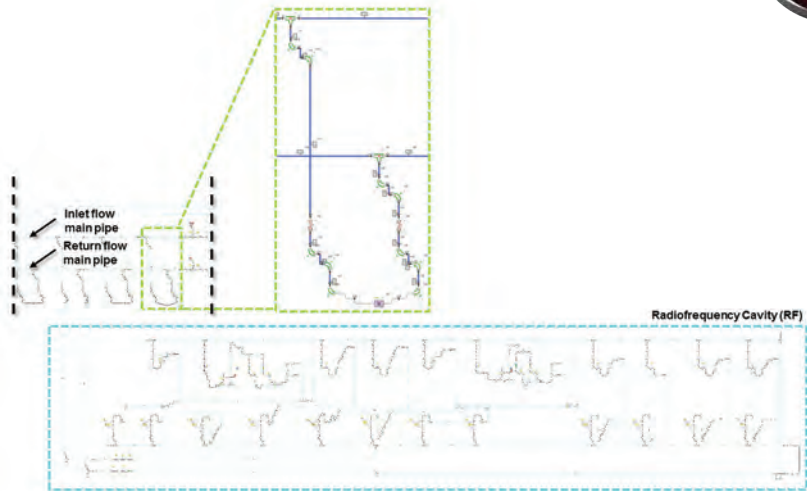


Figure 5. Schematic of a section of the Service Area ring model

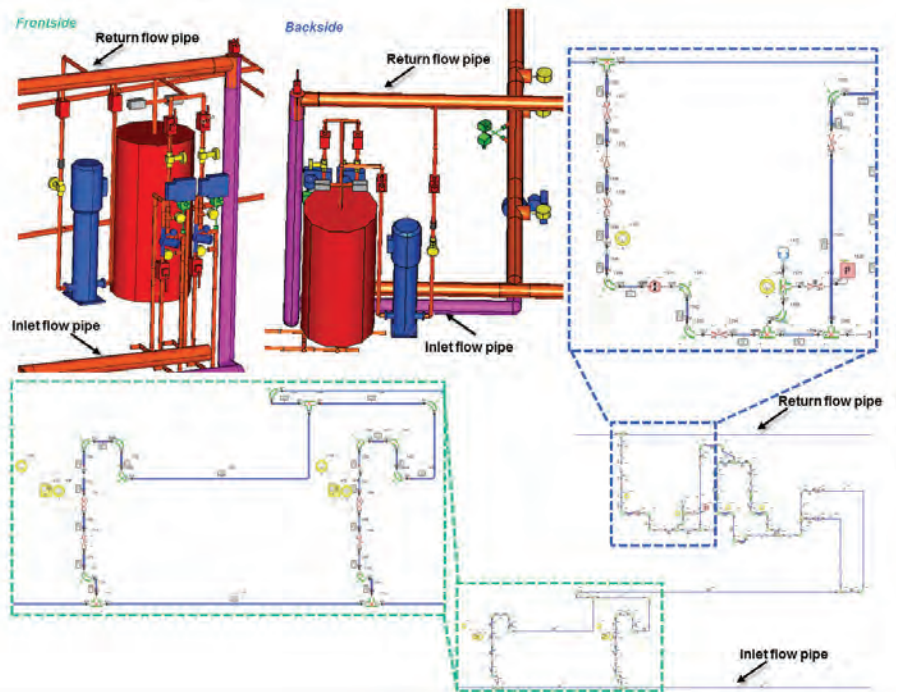


Figure 6. Comparison between the real appearance (CAD pictures) and Flowmaster modeling of one RF's consumption

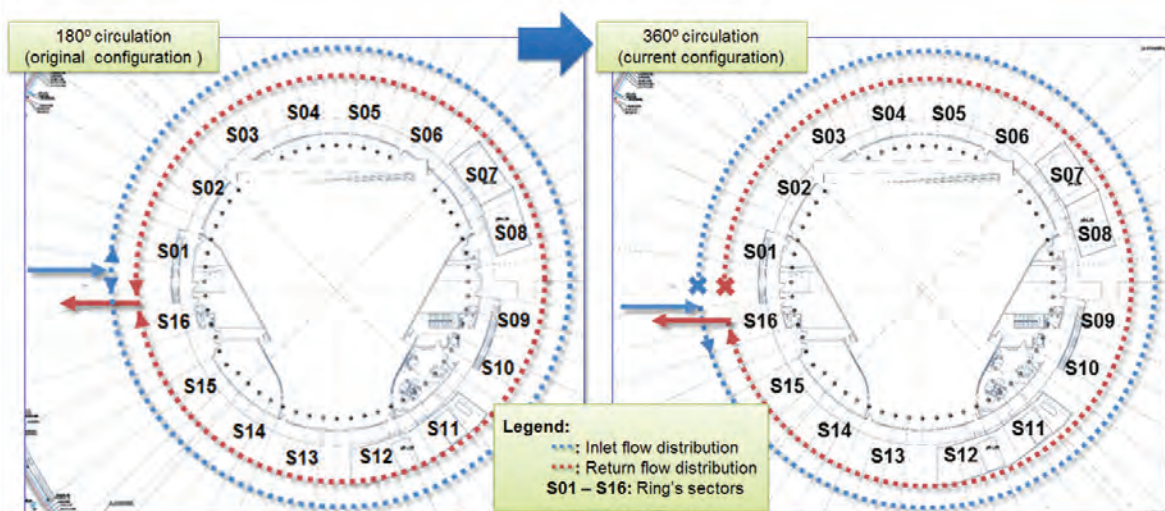


Figure 7. Schematic of the 180° original flow distribution (left) and of the 360° current flow distribution (right) at Experimental Area ring.

sub-system. In order to improve the flow velocity distribution along the rings, it was considered to change the position of the valves by closing one valve of the T-junction exit branches and to force a 360° circulation as indicated on the right of Figure 7. According to the opening or closing of T-junction exit valves, it is possible to distinguish a total of five flow distributions in each ring (one of 180° and four of 360° circulations) as observed in Table 1.

In summary, the Flowmaster software has been used to simulate all the possible configurations with the aim of establishing the existence of an optimal flow distribution that minimizes the locations with the lowest velocities.

### Accuracy of the Model

A preliminary validation of the Flowmaster model has been carried out with the production side comprising the pumping units. For that, the simulated results have been compared with the real hydraulic

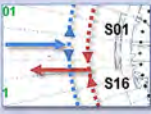


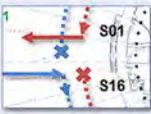

FLOW DISTRIBUTION			Opening of the S16 exit valve	Opening of the S01 exit valve
180° Circulation		Inlet flow	100%	100%
		Outlet flow	100%	100%
360° Right Circulation		Inlet flow	100%	0%
		Outlet flow	100%	0%
360° Left Circulation		Inlet flow	0%	100%
		Outlet flow	0%	100%
360° Right - Left Circulation		Inlet flow	100%	0%
		Outlet flow	0%	100%
360° Left - Right Circulation		Inlet flow	0%	100%
		Outlet flow	100%	0%

Table 1. Studied Flow Distributions

Pump Group	Q <sub>CELLS</sub> [m³/h]	Q <sub>SIM</sub> [m³/h]	% dev.	n <sub>CELLS</sub> [min⁻¹]	n <sub>SIM</sub> [min⁻¹]	% dev.	Pimp <sub>CELLS</sub> [bar]	Pimp <sub>SIM</sub> [bar]	% dev.
P09 (BO)	28.60	28.60	0.0	2600	2550	-2.0	10.20	10.22	0.2
P08 (SR)	271.00	271.10	0.0	2582	2458	-5.0	10.20	10.17	-0.3
P10 (SA)	200.00	200.10	0.1	2737	2793	2.0	10.00	10.17	1.7
P07 (EA)	16.20	16.20	0.0	2516	2355	-6.8	7.50	7.09	-5.8

Table 2. Comparative Analysis between the Real Measurements and the Flowmaster Simulated Results.

variables like flow rates (Q), pump rotating speeds (n) and pump delivery pressures (Pimp). Table 2 shows the comparative studies for a real working point of the cooling system. For the overall variables of the hydraulic system, the maximum average deviation equals – 6.8% corresponding to pump rotating speeds. The deviation for the main flow rate at the rings is less than 0.1%.

Regarding the rings and their previously described sub-systems, they obviously require a fixed flowrate to cool their consumptions. In order to evaluate the accuracy of the modeled rings, the simulated results (flow rate in each one of the sub-systems) have been compared with the on-site measured ones as indicated in Table 3 in terms of averaged deviations. It must be noted that some local sub-systems were presenting larger deviation values. It can be observed that the maximum average deviation for the simulated flow rates in three of the rings is about 6.5% corresponding to the Service Area.

Nevertheless, the Booster Ring shows a larger deviation that can be explained by the fact that the measured data is not reliable due to a detected calibration problem of its flowmeter. As a result, the 23.7% deviation does not represent the actual goodness of the Booster Ring's model. It must be noted that this flowmeter issue does not take place in the other three rings.

### The Optimal Flow Configurations

The presence of air in pipelines may cause instabilities of the water flow. To avoid air problems in pipelines it is widely accepted that minimum flow velocities are required above 0.5 m/s.

In this work the five possible flow distribution in the main pipe rings has been modeled (as is detailed in Table 1). The simulations results show the map of the water flow velocities and allow quantification of the zones where the velocities are lower than 0.5 m/s. Then the recommended 360° flow distribution is the one that minimizes the lower map with velocities respect to the case 180° circulation. Table 4 indicates which one of the four possible 360° flow distributions is the optimal for each ring and the percent of improvement for both the inlet and return flow distributions through the main ring pipes.

RING	Average flow rate deviation [%]
Experimental Area	3.60
Booster	-23.74
Storage	-3.19
Service Area	-6.48

Table 3. Average Flow Rate Deviation of Simulated Value to Measured Value in Each Ring.





RING	Optimal flow distribution	Inlet flow improvement [%]	Return flow improvement [%]
<b>Experimental Area</b>	360° Right Circulation	60	58
<b>Booster</b>	360° Right - Left Circulation	60	40
<b>Storage</b>	360° Left - Right Circulation	33	33
<b>Service Area</b>	360° Left Circulation	43	43

**Table 4.** Optimal Flow Distribution for Each Ring and Percent of Improvement

The values shown in Table 4 are calculated with the following expression:

$$\text{Improvement} = \frac{100 |N_{\text{opt}} - N_{180}|}{N_{180}}$$

Where  $N_{\text{opt}}$  and  $N_{180}$  are the number of pipes with flow velocities lower than 0.5 m/s in the optimal and in the 180° configurations, respectively.

Figure 8 illustrates the evolution of the flow velocity along the EA ring's inlet flow main pipe caused by the 180° and 360° circulations. Whereas almost all of the EA ring's sectors have velocities lower than 0.5 m/s (shown in red) when the flow distribution is 180°, the 360° current

circulation restricts these undesirable velocities to less than a half of the EA ring. However, there is obviously a zero velocity point next to the closed valve (indicated by the blue cross) but the good point is that it is located relatively far from any sub-system. Therefore, it is clearly observed the fact that the flow distribution change from 180° to 360° entails a significant velocity rise in most of the pipe sectors.

## Conclusions

Thanks to Flowmaster 1D Thermo-fluid simulation software, ALBA Synchrotron has been able to improve the fluid dynamic behavior of the cooling system consumption rings.

Actually, each ring has been modeled with a high level of detail of its local consumptions. The accuracy of the model has been validated with real operation data. The resultant models have allowed for the study of the rings' original flow distribution as well as all the alternative possible circulations. As a result, for each ring it has been identified that the 360° flow distribution make it possible to increase those deficient velocities that take place in the original configuration (180° circulation). The suggested 360° circulations have reduced these undesirable velocities by around 49% on average. Consequently, the cooling system's reliability has been significantly increased.

**For more information:**  
[www.cells.es/en](http://www.cells.es/en)

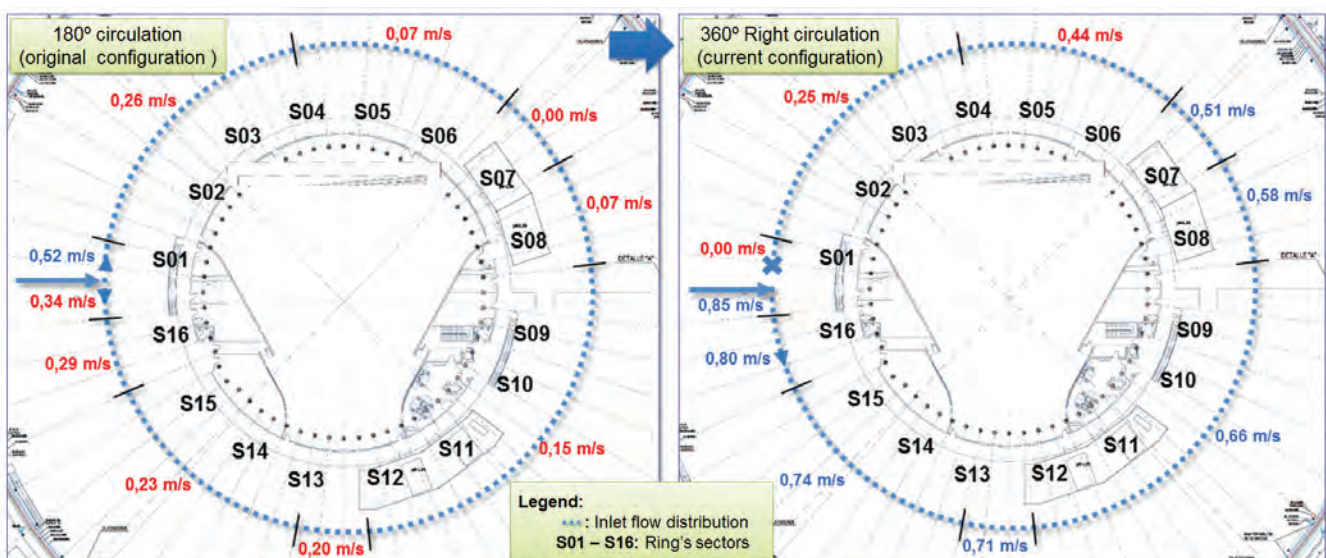


**Figure 8.** Velocity along the Experimental Area ring's inlet flow main pipe due to the 180° circulation (left) and to 360° current circulation (right).

# How To...

## Guide to Understanding Power Cycling

By Mathew Clark, Field Application Engineer, Mentor Graphics



**S**ince the release of MicReD® Power Tester 1500A there is a need for greater knowledge and awareness of Power Cycling.

### For Starters

Power Cycling is used to exert thermo-mechanical stress on different materials. Thanks to thermodynamics, we know that a material can expand and contract at different temperatures according to this equation:

$$\alpha_v = \left( \frac{1}{V} \right) \left( \frac{dV}{dT} \right)$$

What this shows is that materials can change size when a temperature change occurs. What does this mean for testing? Well, as we have more than one material in our components and packages, we have what is called a thermal coefficient mismatch. This means that different materials expand or contract at different rates. This creates strain, and when strained enough, the interface or the materials themselves break.

In addition to this some materials age quicker, corrode or stop functioning. In terms of semiconductors the possibilities

are endless. Of course all of these effects need to be induced and tested with several methods, before a component is verified and shipped. However, the environment and operational condition of the component may determine which failure occurs first.

### Other Issues

Environmental and operational conditions not only bring forth new technology, requirements and conclusions. Ultimately, what everyone is concerned about, is the longevity of their device. Will it last two million cycles? What will the cause be for earlier failure? Is there a difference between

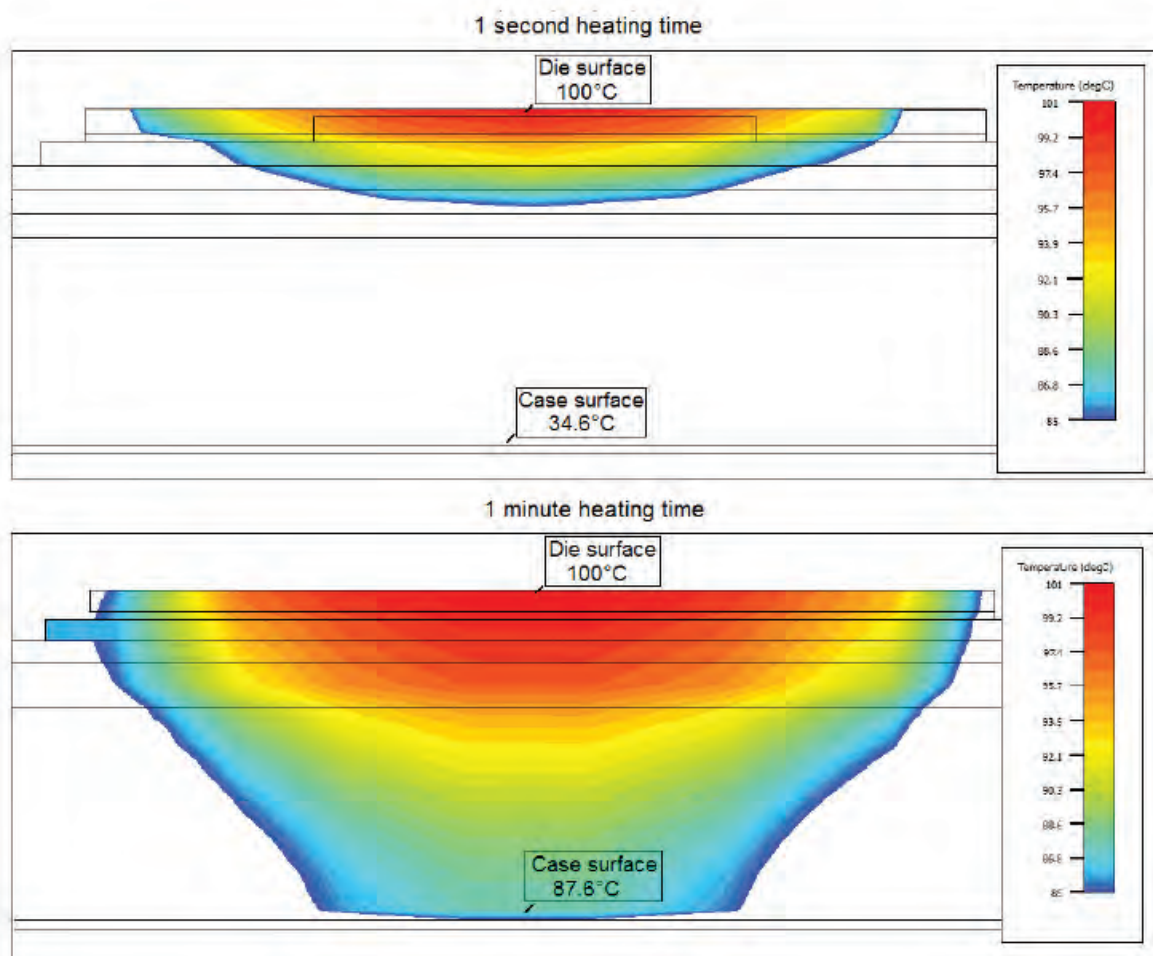


Figure 1. Heat-spreading behavior after 1 seconds (top) and 60 seconds (bottom)



complete failure and accepted failure? For clarification of what these questions entail let us use an electric car as an example. Not only does the automotive industry have some of the toughest reliability standards in the consumer space, but the industry also tends to buy, not fabricate, components. This means that much of the information is provided and then compared.

Going one step further, we want to create our own electric car, and need to purchase IGBTs for our electric motor. Now, aside from all the electric criteria, we would prefer it if the IGBT does not get very hot, performs all functions and has a long life time. Given that we are not in Utopia, we will need to get data from different manufacturers and compare their statements.

one second, might affect it differently than if it's cycled for one minute.

Additionally, different cycling methodologies can be driven to quantify different failure modes. By keeping the change in junction temperature constant over the cycle period, therefore reducing the power as the die attach ages, the system experiences less stress over the entire life span. The other option is to keep the input current constant and not compensating for the degradation.

The effects are relatively straight forward and not all are shown here. In a quick test we can already demonstrate how constant current (blue) differs to constant power (red) and constant temperature change (green). Though the results vary, there is a clear trend and a possibility to “optimize” results.

The reason this is important has several explanations:

1. If you are receiving the IGBTs, make sure you understand the test procedure
2.  $\Delta T$  seems like a useful solution, although cars driven slower to manage the power levels might not suit everyone.
3. Be sure that the testing method applies to your application – wind turbines might need to withstand a hurricane, while a car has to deal with a novice driver that doesn't know the difference between 'R' and '1<sup>st</sup>', or believes that a side walk is shared space.

Cycle Time	Short periods - mostly affecting the die attach and wire bonds	Long Periods - Potentially aging other layers of the device
Heating Parameter	Constant Current - Brute Force Method	Constant Tj - Adjusting Power level to compensate for increased thermal resistance
Test Setup	In-situ - Considering your own heat sink and materials	Component - Thermal path from device can be optimized to keep it cooler

Figure 2. Summary of testing parameters to age high power electronics

## Thermal Resistance

Thermal resistance is a measurable unit in Kelvin per Watt (K/W) – if a device has 2K/W, the temperature will increase by two degrees for every Watt power. Unfortunately the thermal resistance may increase as the device ages. If the device gets too hot, it ages, as it ages it will deteriorate and in so doing it will then become hotter. This then reduces the longevity of the components.

## Cycling Conditions

Another important factor is the conditions at which the device is cycled and stands in direct correlation with the thermal resistance. Turning the device on and off for

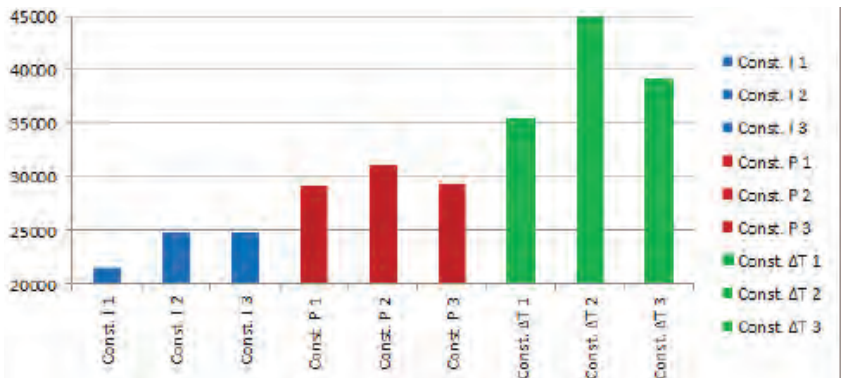


Figure 3. Chart showing the aging of IGBTs after the use of different control strategies. Constant Current (Blue), Constant Power (Red) and Constant change in Junction Temperature (Green)

# Thermal Simulation to Model Airflow and Heat Dissipation for Vehicle ECUs

By Kelly Cordell-Morris, QA/Test Engineer, Mentor Graphics

**E**lectronic control units (ECUs) are a vital part of vehicle operation, controlling engine functions - fuel injection, ignition timing, and idle speed control. The ECU is part of a feedback loop in which data from sensors around the engine is monitored and used to optimize the control outputs. The ECU must be highly reliable in a harsh environment. Components can be exposed to extreme temperatures, and the push for minimal footprint designs increases the thermal issues. It must take into consideration environmental implications and maintenance-free operation, as well as suitability for high volume manufacturing.

Historically, automotive electronics have been cooled via convection by ambient air. Within the engine bay, ambient air temperatures vary significantly. Often, the ECU is tucked away leaving convection around it compromised. Electronics modules in vehicles, and in particular, modules mounted out-of-cab, are often sealed to prevent moisture ingress. Preventing external air flow from circulating around the electronics directly, making

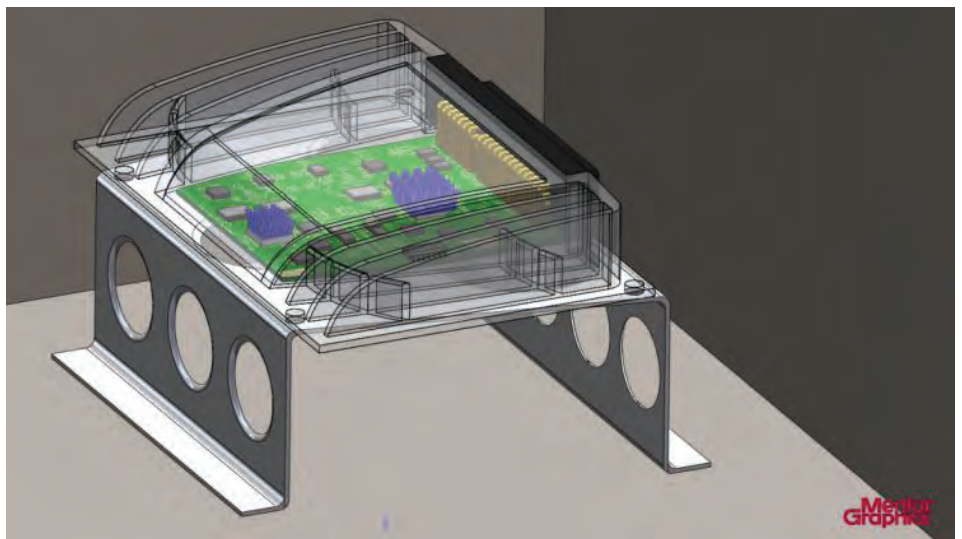


Figure 1. The ECU with the PCB

forced convection impossible.

Convection cannot be relied on as a heat transfer mechanism in these situations. Conduction, normally to the vehicle structural body, becomes the dominant means by which to cool components. With a conduction-influenced design, the materials used in the ECU are an important part of thermal considerations. In this case, we are comparing materials used in the

mounting brackets and their effects on the ECU's internal component average temperatures.

## Modeling the ECU as Mounted in a Vehicle

In the FloTHERM XT model, the ECU was mounted to a metal bracket, mounted to the vehicle chassis (Figure 1). Two thin walls were located close to two sides of the ECU to block airflow around the unit. Total heat dissipation in the unit was 19.8 W (Joules per second).

We modeled two internal ICs as two-resistor (2R) representations to obtain a prediction of junction temperature. Each one dissipated 4.5 W. Pin heatsinks were also mounted on these 2R components. The remaining 24 IC representations were simple conducting cuboids with typical effective conductivity properties applied depending on the type of IC represented. These dissipated between 0.1 to 1 W each. The results give an indication of case temperature (Figure 2).

## Results for Unmodified Mild Steel and Aluminum Brackets

With walls on two sides, there was, as expected a compromised airflow, and hotter

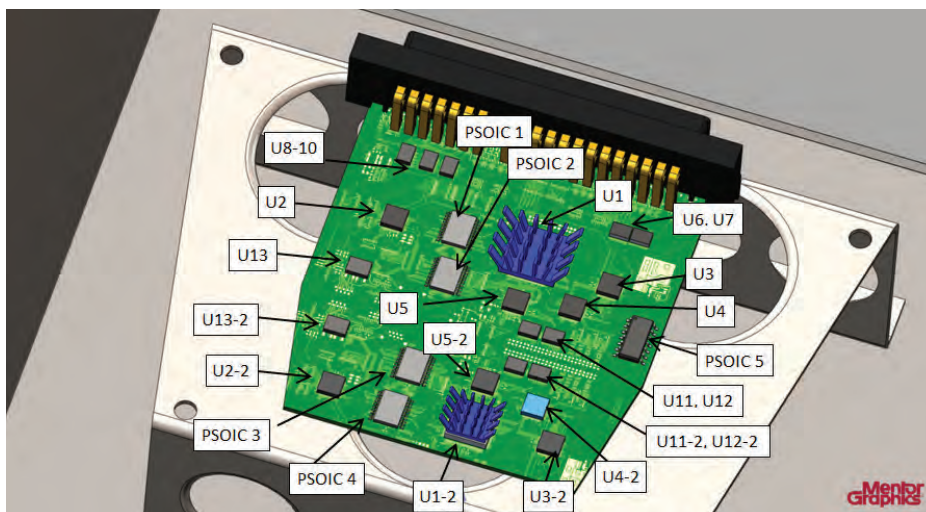
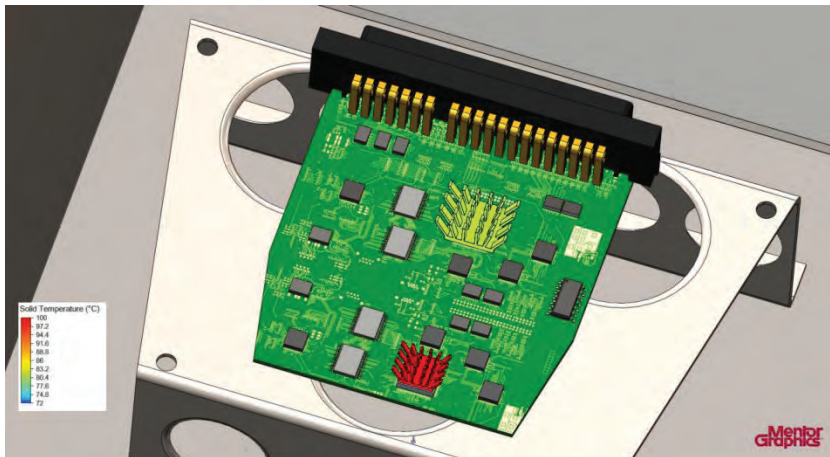


Figure 2. Labeled ICs on the PCB inside the ECU





**Figure 3.** Heatsink surface temperatures for aluminum bracket in FloTHERM XT

enclosure when made of mild steel. Plus a higher airflow velocity resulting from energy lost via convection.

A change of material provided an average improvement of 8°C. PSOIC3 located over a hole in the bracket recorded the smallest change, with convection playing a large part in heat transfer making this IC less sensitive to changes in the material. However, U1 would be more sensitive to change given its location. Including a heatsink gave an alternative heat transfer path to conduction (Figure 3). In conclusion, holes may help airflow; however, on occasion solid mounts may be preferable to maximize conduction when convection is virtually zero.

### Results with Solid Bracket

A new configuration for the bracket where the holes were suppressed was created for both models. Another configuration for each model with the heatsinks removed was also solved to determine just how necessary heatsinks may be to the final design (Figures 4-6).

With a fully solid mounting bracket IC temperatures were generally reduced by around 4°C. Clearly, conduction was more efficient with the new design despite

convection being compromised by the removal of the bracket cut-outs. Changing the bracket material to aluminum reduced temperatures by a further 7-8°C on average. We observed the greatest temperature drop on PSOIC 1, which may be because of its location close to U1. With lower temperatures on the 2R model and thus lower temperatures for the surrounding PCB, more efficient heat loss from PSOIC 1 to the PCB can be achieved.

### Results with No Heatsink

We saw little gain in temperature for the majority of the components. U1 and U1-2 junction temperatures were raised 1.7°C and 1.5°C, respectively, when the heatsinks were removed in the mild steel bracket model. The rise was slightly less when the bracket was aluminum. The greatest change for the 2R models was in case temperature as would be expected with the removal of a heatsink. For the other components on the PCB, PSOICs 1 and 2 were the only ones significantly affected. This is probably because of their proximity to U1, and PSOIC 1 was the most affected because it is closest. Assuming that the small increase in temperature for these few

components is allowable, the addition of heatsinks would appear superfluous. Again, using aluminum for the mounting bracket reduced component temperatures by 7-8°C on average.

### Conclusion

In cases where airflow around the ECU is compromised, material changes can have significant effects to be considered for the thermal design. Using a more thermally conductive material such as aluminum is a simple change that results in a robust and fairly inexpensive design.

Where convection, either forced or natural,

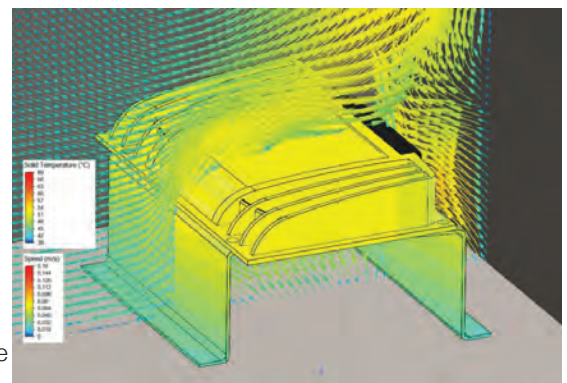


**Figure 5.** Surface temperatures and air flow vectors for enclosure and aluminum solid mounting bracket with no heatsinks

is compromised or impossible, then a simple mounting bracket design can be more effective than a design intended to increase airflow around the ECU casing. This has the added benefit of making manufacturing simpler and thus less costly. As has been shown in this case, heatsinks in a closed system may not be that effective and add unnecessary cost to the final design. Thermal simulation software provides a quick and easy way to test material and thermal changes early on in the design process.

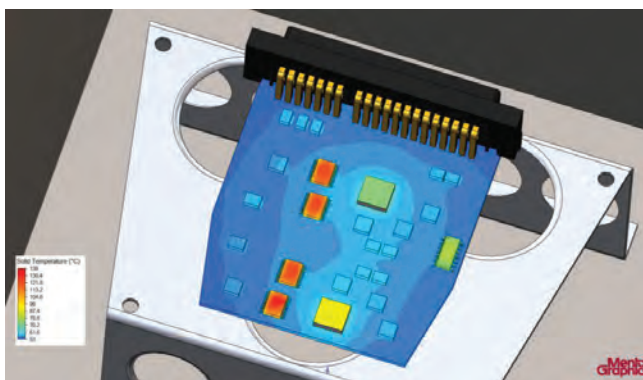


**Figure 4.** IC and PCB surface temperatures for aluminum solid mounting bracket (heatsinks not shown)

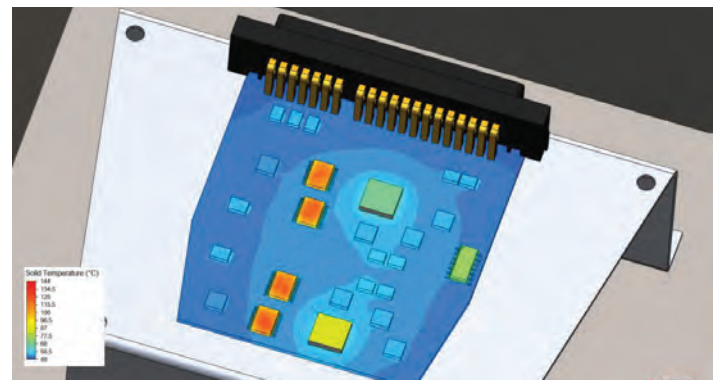


**Figure 6.** IC and PCB surface temperatures for aluminum solid bracket with no heatsinks



# The Three Waves of Commercial CFD

By Ivo Weinhold, User Experience Manager  
and John Parry, Mentor Graphics

**I**n recent years, many papers have been published on the history of flow simulation. Many early CFD pioneers like Brian Spalding, David Tatchell, Ferit Boysan and Michael Engelman have talked or written about their memories. This pool of historical facts, technical information and personal impressions give a remarkably consistent description of the way engineering simulation software evolved from academic research codes towards the modern CFD products we know today. Developed and supported on an industrial scale by multinational software companies.

Closely linked to the performance of available computing hardware, this development was, particularly in the early stages, driven primarily by research and development projects for aerospace and defense, but latterly also increasingly by interest from civilian industry. Looking back, three major phases of the development of CFD software for industrial applications can now be recognized:

- The First Wave: The beginnings of commercial CFD software in the 70s and 80s.
- The Second Wave: In the 90s, CFD enters the research and development departments of large industrial enterprises.
- The Third Wave: After the millennium, CFD becomes an indispensable part of the product development process.

## The First Wave: The beginnings of commercial CFD software

Since 1958 the codes of the CFD software engineers in the first phase had its roots in the work of the Fluid Dynamics Group T-3 at the Los Alamos National Laboratory (USA), and the research activities under Prof. D. B. Spalding at Imperial College London in the 1960s and 1970s.

In the late 1960s, Concentration, Heat and Momentum (CHAM) Ltd., founded by Spalding, and initially located at Imperial College London, dealt with consulting work. The era of commercial CFD software began in 1974, when CHAM Ltd moved to its own offices in New Malden near London. Initially, the development of customized CFD codes was central to the business activities of CHAM. That became too time-consuming and inefficient, so CHAM decided to develop a general-purpose CFD package for in-house consultancy work, and released this as a commercial product, PHOENICS, in 1981. This may well be regarded as the birth of the CFD software industry (see CHAM Ltd, 2008). Others quickly followed suit. For instance, Fluid Dynamics International (USA) followed in 1982 with FIDAP, a FEM-based CFD package, and in 1983 Create Inc (USA) released the finite-volume CFD code, Fluent. Computational Dynamics/ADAPCO (UK/USA), co-founded by Prof. David Gosman, another professor at Imperial College London, released StarCD in 1989.

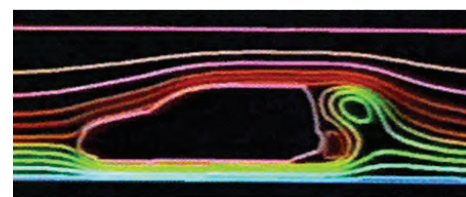


**Figure 1.** Fluid flow simulation in the 1980s, taken from Hanna & Parry (2011)

The basic technologies behind most of the CFD packages of this era had been created by former employees or guest scientists of the two aforementioned research institutions in London and Los Alamos, or were based on their scientific publications. But there were also other developments of CFD technology: in the 1980s alternative approaches for CFD simulation emerged as part of the military and civilian aviation and space program of the former Soviet Union, largely unnoticed by the Western scientific community due to the political situation. Their technical tasks for CFD simulations were similar to those in the West, but the available computing resource for their solution was much more limited. Conversely, because of the high political priority of these research programs, very extensive experimental data for numerous fluid flow and heat transfer phenomena, especially in the near-wall area, were generated. This situation led to the development of alternative CFD methods, which, building on known methods for



## The Second Wave: CFD enters the Research and Development Departments of the Industry

Using technology typical of the first phase, Floerics Ltd., founded in 1988 by David Tatchell and Harvey Rosten in Kingston-upon-Thames (UK), played a pioneering role in marketing CFD software developed exclusively for industrial applications with its software package FloTHERM, first released in 1989. Both founders worked for CHAM Ltd in senior positions before leaving to found Floerics, with the aim of “providing good science to industry” (Tatchell, 2009). FloTHERM was a first paradigm shift in the CFD industry, away from the focus on complex CFD technology, towards the solution of engineering tasks in industry as the central goal. This also meant that from then on engineers working in product development, and not scientists, were the main target users of this type of CFD software. The available CFD technology, computer hardware and operating systems imposed certain limits on such an innovative approach. Therefore Floerics concentrated initially on only two application areas: electronics cooling (with FloTHERM) and built environment HVAC (with FloVENT). The requirements of engineering-oriented CFD software for these application areas were relatively clearly defined and, more important, also just feasible.

This concept opened up completely new market opportunities, because for the first time engineers in product development without special knowledge of numerical methods and without extensive CFD

experience were empowered to employ CFD simulations as a development tool. The solution of a technical engineering task became the center of attention, while the underlying CFD technology was more or less just a means to an end.

Obviously, other CFD providers also recognized the beginning of this paradigm shift and especially the new business opportunities associated with it, responding to this trend with their own product offerings. Overall, huge investments from all CFD software vendors in better user interfaces, robust solvers and reliable physical models could be observed, with the clear objective of entrenching CFD into the research and development departments of large industrial enterprises and thereby attracting a new generation of CFD users.

After establishing CFD as a successful tool for the functional design, verification and optimization of product designs, features, processes and physical effects in large industrial companies in the early 2000s, the reputation of this technology amongst engineers improved significantly. As a result, the demand for CFD simulations showed strong growth, especially in medium-sized and small companies keen to reduce the costs associated with physical prototypes. Another important aspect was the need to integrate CFD simulation into the regular product development process, as these companies usually had as yet no

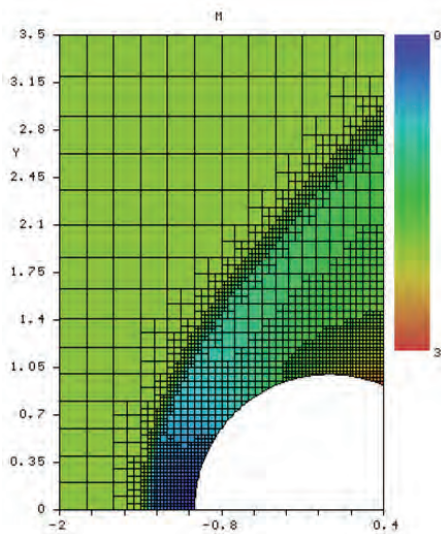


Figure 2. Result plot of Aeroshape-3D (Parry et al., 2012)

Cartesian grids as published in the scientific publications in the West, were based on a combination of numerical, analytical, and empirical data. This innovative approach yielded high-quality simulation results in virtually, arbitrarily complex computational domains while maintaining the low resource requirements and the effectiveness of methods using Cartesian grids. With the gradual economic liberalization in the Soviet Union in the late 1980s, several teams of scientists have commercialized this CFD technology and, since the early 1990s, sold their products and services in Europe and Asia. The best known products of this kind were Aeroshape-3D by Prof. V. N. Gavrilouk and team (Petrova, 1998 & Alyamovskiy, 2008) and FlowVision by Dr. A. A. Aksenov and team (Aksenov et al., 2003).

From the beginning of the 1990s, the conditions for CFD software and simulations changed quite rapidly. Computer hardware, mathematical methods and physical models all experienced huge performance gains. Numerical methods such as unstructured Finite Volume methods, multi-grid methods, sliding mesh, etc., suitable for complex geometry and optimized for HPC, became commercially available as well as more reliable, more flexible and more broadly applicable physical models. CFD technology became much more feasible, and for the first time, quite realistic model sizes, for real industrial applications were possible. These new capabilities heralded a new phase in the usage of commercial CFD software - entry into the research and development departments of industry across the board.

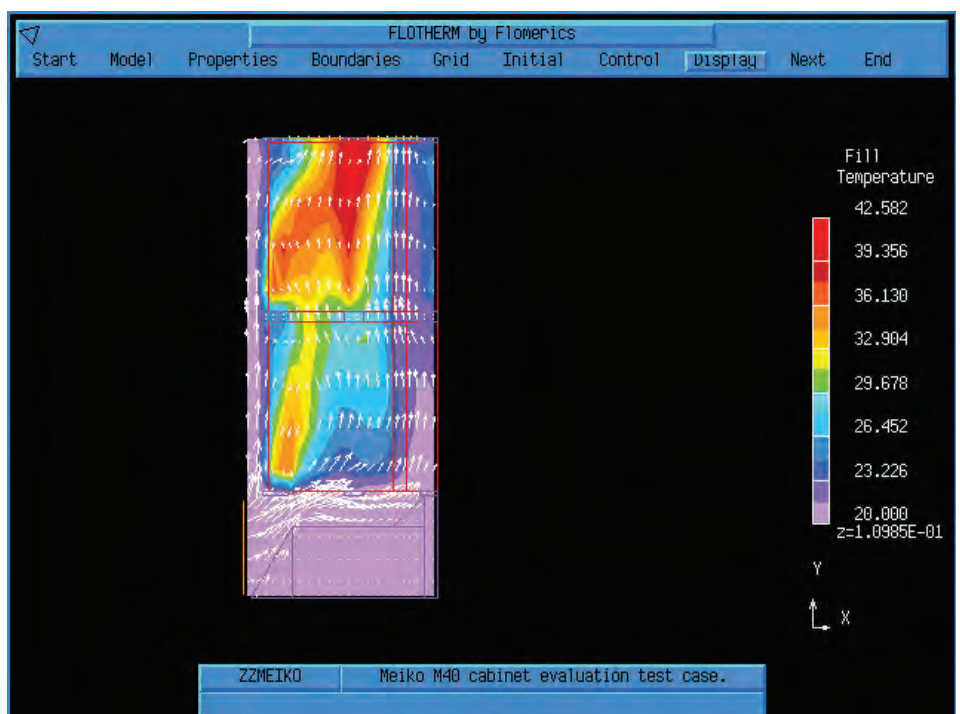


Figure 3. Early version of FloTHERM (Hanna & Parry, 2011)

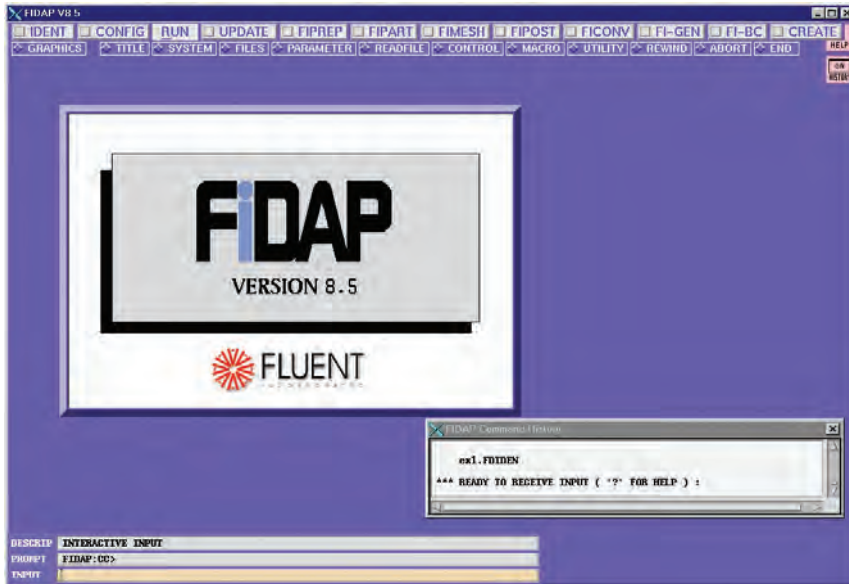


Figure 4. FIDAP User Interface in the late 1990s (University of Delaware, 2007) URL

dedicated simulation departments. This meant that qualified engineers from product development or design groups would perform the simulation themselves. The efficiency with which simulation projects were conducted had to be increased, so CFD results would be available sufficiently in sync with the product design cycles, for the results to help guide proposals for design improvements. In this context the handling of industry-level geometry played a key role. At that time this was already being provided as 3D CAD data which should, of course, be used with as little simplification and modification effort as possible to be useable by the subsequent and preferably fully-automated mesh generation step. The CFD software market responded to these demands with new and improved products – and a third wave of CFD software for industrial product design began and continues to this day.

### The Third Wave – CFD Becomes an Essential Element of the Product Design Process

The major CAD and Product Lifecycle Management (PLM) vendors play a key role in this third phase. Since the 1990s, they have been successfully introducing the concept of PLM, which encompasses CAE. As a result, customers have put pressure on commercial CFD software vendors to conform to this concept and to take steps to integrate their products into the major PLM systems. In the 2000s, virtually all CFD software providers upgraded their systems with, at the least, CAD import interfaces. Some have developed bi-directional links with major CAD/PLM systems, and a few have even embedded their CFD technology directly into the 3D CAD systems themselves. New CFD techniques to support these requirements were also developed, partly from scratch, and partly as enhancements of existing technology.

The company NIKA GmbH, founded in 1999 as a German-Russian joint venture, was a typical example of a new commercial CFD software vendor emerging at the start of this third wave. NIKA exclusively developed, based on the above mentioned Aeroshape-3D technology, CAD embedded CFD software, which is now offered as FloEFD for several major 3D CAD systems.

The current third wave has allowed newcomers from other areas the opportunity to enter the CFD market, refreshing it with new technologies. But all have one thing in common: The industrial user, with his or her need for easy-to-use, task-oriented, automated, reliable, efficient and readily-available CFD software as an indispensable tool for digital prototyping is the focus. The result of changing development processes and, as a consequence, the changing role of the simulation engineer. Aspects like process integration, reliability, modeling safety, and reproducibility are becoming the center of attention, and influence purchasing decisions for CFD software. The further development of CFD software based around

these requirements will bring exciting new technologies and products to market. A new fourth wave may be expected to follow soon...watch this space.

### References:

- Aksenov, A. A., Kharchenko, S. A., Konshin, V. N., Pokhilko, V. I. (2003), FlowVision software: numerical simulation of industrial CFD applications on parallel computer systems. In Parallel Computational Fluid Dynamics 2003: Advanced Numerical Methods, Software and Applications, Elsevier, 2004, pp. 401-408
- Alyamovskiy, A. A. (2008), SolidWorks 2007/2008. Компьютерное моделирование в инженерной практике, bhv-St. Petersburg, 2008, pp. 467-468
- CHAM Ltd (2008), Earlier versions of PHOENICS: -81 to -1.6 A brief history. Available: [http://www.cham.co.uk/phoenics/d\\_polis/d\\_chron/earlyver.htm](http://www.cham.co.uk/phoenics/d_polis/d_chron/earlyver.htm)
- Hanna, K., Parry, J. (2011), Back to the Future: Trends in Commercial CFD, NAFEMS World Congress, Boston (Paper and Presentation Slides)
- Parry, J., Kharitonovich, A., Weinhold, I. (2012), FloEFD – History, Technology & Latest Developments, Mentor Graphics, 2012
- Petrowa, J. (1998), GUS - Informationstechnologien im CeBIT-Spiegel: Partner gesucht. ComputerWeekly, Volume 8, 1998. [http://scripts.online.ru/it/press/cwm/08\\_98/gus.htm](http://scripts.online.ru/it/press/cwm/08_98/gus.htm)
- Tatchell, David (2009), David Tatchell's Blog, Mentor Graphics, 2009. Available: <http://blogs.mentor.com/daviddtatchell/>
- University of Delaware (2007), FIDAP/ GAMBIT. [www.udel.edu/topics/software/special/statmath/fidap/](http://www.udel.edu/topics/software/special/statmath/fidap/)

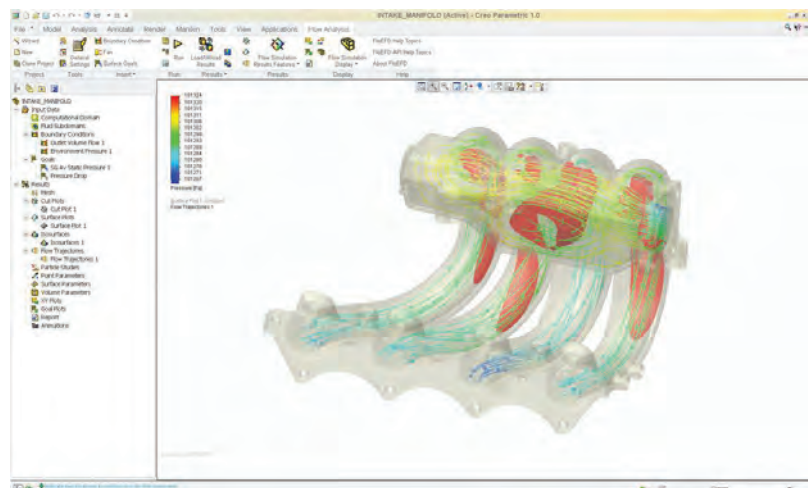


Figure 5. FloEFD for Creo by Mentor Graphics





# Nuclear Power Station

## Thermal-Hydraulic

## Safety

Institute of Nuclear Thermal-Hydraulic Safety and Standardization, NCEPU Validates Feedwater System with Flowmaster

By Liang Liu, Ph.D Student, Department of Nuclear Science and Engineer, North China Electric Power University

**S**afety and reliability are the most important considerations in the operation of nuclear power stations. Many factors such as centrifugal pump start up, valve adjustment, bubble collapse can cause rapid changes of velocity and pressure, resulting in water hammer which can cause severe damage to the piping system including rupture. Conversely, low pressure can lead to tube collapse, and damage to valves and other components.

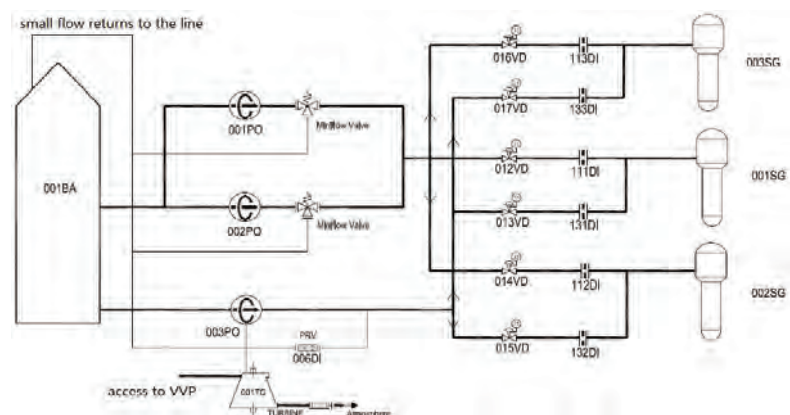


Figure 1. Flow of Auxiliary Feedwater System

Auxiliary feedwater system is designed to provide water for steam generators in three scenarios:

- Normal starting or shutdown of nuclear power station;
- Work as the backup system when the main feedwater system fails; and

- Perform its required functions during or after a natural disaster such as an earthquake.

Its safety function is to prevent damage to the reactor core and get rid of the heat buildup in the reactor core until the residual heat removal system is put back

into operation after a failure. The inability of this system to operate properly when the primary systems fail can be catastrophic as was evident at the Fukushima Nuclear Power Plant in Japan when it was hit by a massive earthquake and Tsunami.

During the design of the auxiliary feedwater system for the Daya Bay second generation nuclear power station, the Institute of Nuclear Thermal Safety and Standardization at the North China Electric Power University turned to Flowmaster to evaluate different operational scenarios to minimize the risk of water hammer occurring in the feedwater system.

A feedwater system is designed with two operational flow paths. The primary path is a steam driven pump that is powered by bypass steam from the main steam system. The auxiliary flow path consists of two electrically driven pumps that are

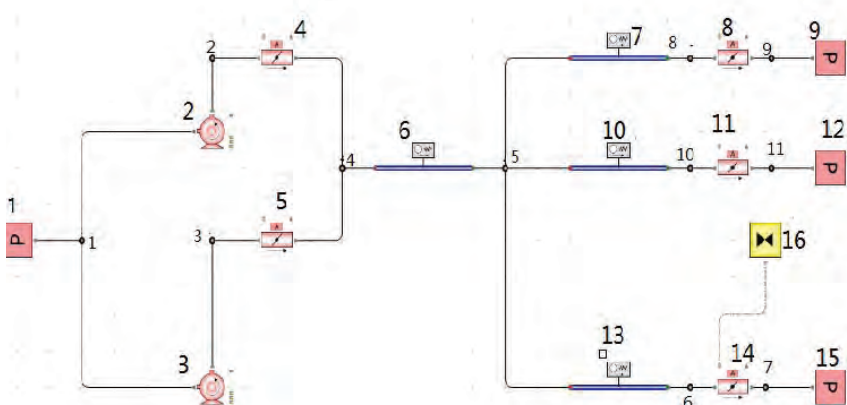


Figure 2. The Simplified Model of Rapid Closure of Valve14

Time (s)	Valve opening
0	1
0.5	0.8
1	0.66
1.5	0.22
2	0
11	0

Figure 3. Parameters of Valve Controller 16

configured in parallel. Each flow path has its own piping system to supply the water to the steam generators. Each piping system has independent control valves and orifices that are used to properly maintain the correct flow rate to each steam generator. Flow paths of auxiliary feedwater system are shown in Figure 1.

The scenarios that they wanted to evaluate were when the main supply of feed water fails, and when the auxiliary system is operational, therefore the primary system is not included in the Flowmaster model as shown in figure 2. The specific case that they wanted to investigate was if there was a line failure feeding one of the steam generators. In Figure 2 the steam generator that fails is represented by the pressure source no. 15. What the designers wanted to know is: what is the best control strategy for closing valve no. 14 to prevent water hammer from occurring in the rest of the system?

- Three different control strategies were simulated:
1. Rapid valve closure;
  2. Slow valve closure; and
  3. Rapid valve closure with an accumulator added just upstream from the control valve.

For the rapid closure case, the control valve is closed completely in two seconds with the closure timing shown in Figure 3. The simulation results for pipe no. 10 just upstream of the valve show significant water hammer effects being created by the rapid valve closure. Figure 4 shows peak pressures near 89.5 bar with a 5 bar change in 0.2 seconds. Figure 5 shows a similar effect on the flow rates as well. The second scenario they tested was a slow valve opening with the valve taking 10 seconds to close completely. The control strategy is shown in Figure 6.

By examining the results for the same pipe it can be seen that the water hammer has been eliminated in the system. With a maximum pressure of 86.75 bar and only a little more than 0.5 bar overall pressure fluctuation: Figure 7. The flow rate also changes in a much smoother manner as

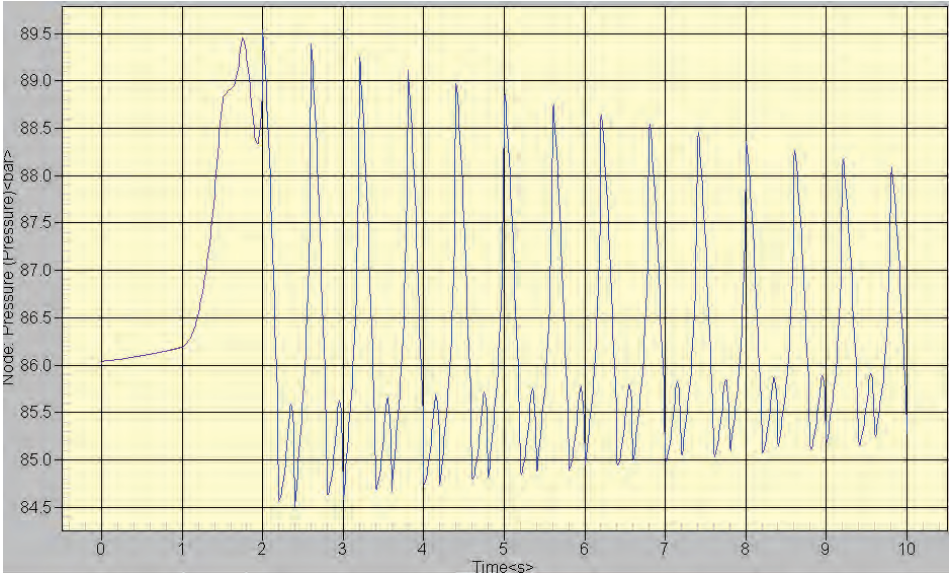


Figure 4. Pressure–Time Curve of Pipe 10 in the Case of Rapid Closure of Valve14

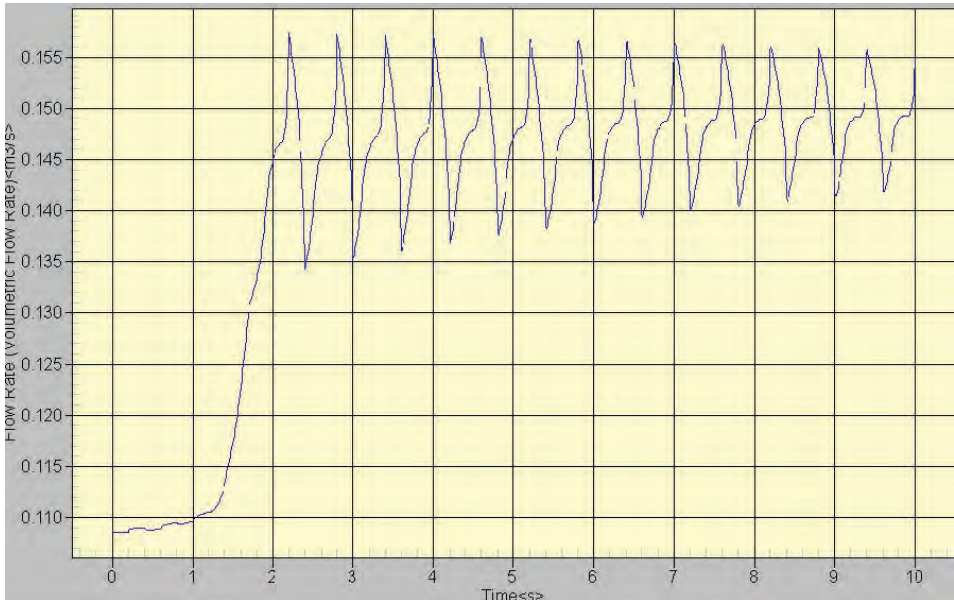


Figure 5. Flow Rate-Time Curve of Pipe 10 in the Case of Rapid Closure of Valve14

Time (s)	Valve opening
0	1
2	0.5
4	0.22
10	0
11	0

Figure 6. Parameters of Valve Controller 16

well with only a small oscillation occurring when the valve first begins to close this is shown if Figure 8.

The final scenario simulated was the rapid closure of the valve but with an accumulator installed just upstream of the valve.

This variation of the model can be seen in Figure 9 with component no. 17

representing the added accumulator. The results of this case are shown in Figures 10 and 11.

These results are very similar to scenario two with the slow valve closure. The pressure curves are nearly identical. The flow rate curves are also very close with a slightly smoother change in the flow rate with the accumulator.

### Conclusions:

By using the transient analysis module of Flowmaster for the studies of transient operation of auxiliary feedwater system of Daya Bay Second-Generation Nuclear Power Station, North China Electric Power University were able to compare the results



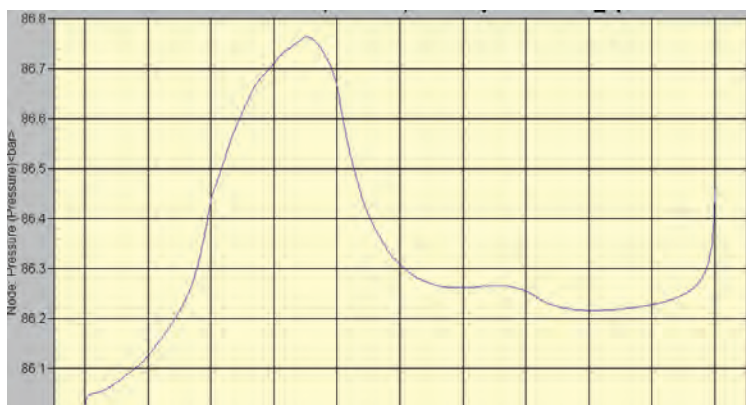


**Figure 7.** Pressure-Time Curve of Pipe 10 in the Case of Slow Closure of Valve14

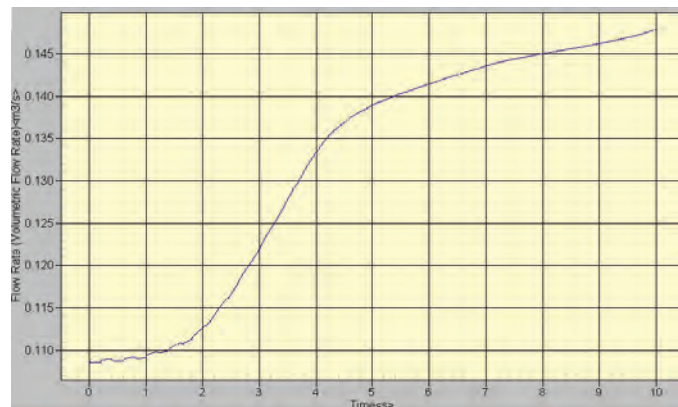


**Figure 8.** Flow Rate-Time Curve of Pipe 10 in the Case of Slow Closure of Valve14

of the different configurations and make the following conclusions.

Using a slow valve closure strategy the designers can mitigate the water hammer effects and prevent the possibility of pipe failure due to instantaneous pressure spikes. Compared to the case of slow closure of valve 14, it may be better able to mitigate flow fluctuation and maintain the stability of the system by the addition of an accumulator upstream of the valve 14. This system's configuration makes it susceptible to water hammer effects when the water flow changes suddenly. In the case of rapid closure of valve 14, the pressure will change suddenly and dramatically, therefore the addition of the accumulator is the most reliable option for mitigating the surge effects and eliminates the dependence on valve closure speed to manage the system performance. The trade-off is cost.

Since the failure scenario tested could occur in any of the three flow paths it would require the addition of an accumulator in each of the branches to properly eliminate the issue. That being said, this allows for a much quicker valve closure which will help preserve the volume of water the system

has available for use, which could be critical in maintaining the integrity of the plant in an emergency situation.

Whichever choice is made the designers know that they have proven options in Flowmaster that can protect their auxiliary

feedwater system from the damaging effects of water hammer.

## Reference:

Luo, Feng, et al (2012). Flowmaster in the Application of Auxiliary Feedwater System's Transient Operation, Power and Energy Engineering Conference (APPEEC), 2012 Asia-Pacific, Shanghai China

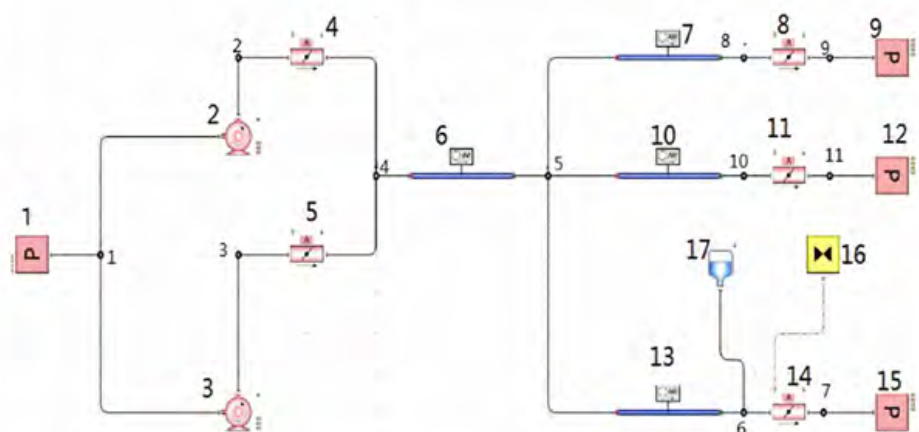


**Figure 9.** The Simplified Model of an Addition Accumulator Located Upstream of the Rapidly Closing Valve14

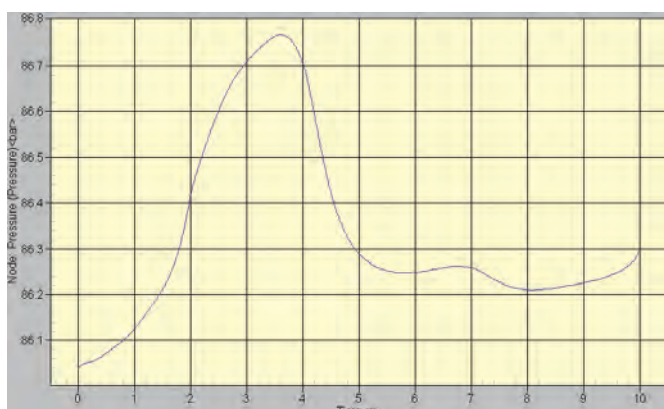


**Figure 10.** Pressure-Time Curve of Pipe 10 in the Case of an Addition Accumulator Located Upstream of the Rapidly Closing Valve14

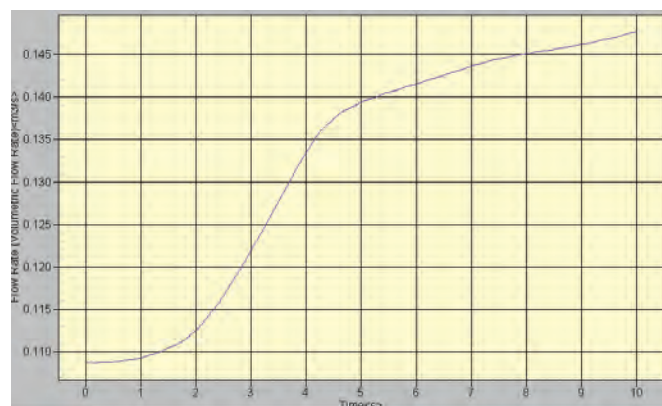


**Figure 11.** Flow Rate-Time Curve of Pipe 10 in the Case of an Addition Accumulator Located Upstream of the Rapidly Closing Valve14

# Engineering Techniques for a Helicopter Rotor Simulation

By P.N. Subbotina, T.V. Trebunskikh, Mentor Graphics;  
B.S. Kritsky, Sc.D., M.S. Makhnev, R.M. Mirgazov, Ph.D.,  
TsAGI, Zhukovsky

**T**he Central Aerohydrodynamic Institute named after N.E. Zhukovsky (TsAGI) was founded on December 1<sup>st</sup>, 1918 under the initiative and leadership of N.E. Zhukovsky, the father of Russian Aviation. It was the first scientific institution to combine basic studies, applied research, structural design, pilot production and testing.

During its distinguished history TsAGI has developed new aerodynamic configurations, aircraft stability/controllability criteria and strength requirements. It was a pioneer in the theory of flutter, along with many other theories, applications and experimental studies [1].

Today TsAGI is one of the largest scientific research centers in the world. Over the last few years, it has established contacts with a majority of research and development centers and aircraft manufacturers in Europe, the United States and Asia and has participated in a large number of joint research programs including the development of next-generation aircraft.

One of the main areas of TsAGI activity is investigating new configurations of helicopters in general, and helicopter rotors in particular. The new sliding technology of rotation brings FloEFD™ into the world of challenging problems in aerodynamics such

as the modeling of a helicopter rotor. This has allowed the validation of the single blade rotor model in cooperation with TsAGI. This technology became available in the latest release of FloEFD V14.0 which provides extended capabilities for simulations of rotating equipment such as pumps, fans, and blowers. With its new sliding technology the software extends the boundaries of simulating turbo-machinery equipment to the cases where fluid quantity is highly non-uniform around a rotating part.

The FloEFD code validation is performed against the experimental data obtained by L.S. Pavlov in 1979 [2] and the numerical data obtained by a traditional CFD code and by the TsAGI specialized software product [3,4].

The model rotor consists of one rectangular, untwisted NACA0012 rigid blade mounted on a hub containing a drive shaft with a balance weight (Figure 3). The model rotor is defined by the geometrical parameters given in Table 1.

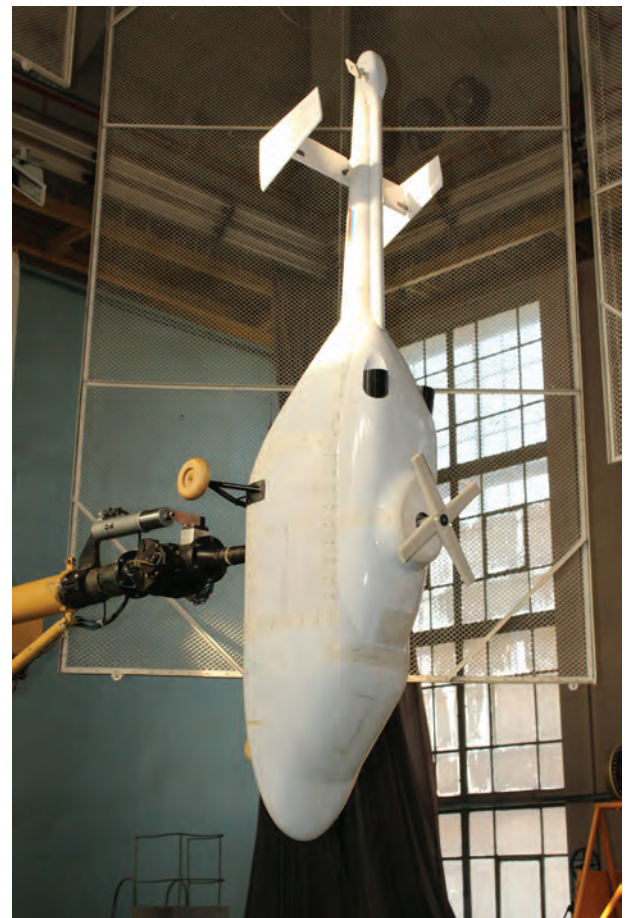


Figure 1. Light Helicopter model tests in wind tunnel T-105.





Pressure distributions have been measured at 10 cross-sections of the blade

$$\bar{r} = \frac{r}{R} = 0.2; 0.3; 0.4; 0.5; 0.6; 0.7; 0.8; 0.9; 0.95; 0.99$$

In the simulation the following forward velocities were considered: hover mode ( $V_\infty = 0$ ) and horizontal flight ( $V_\infty = 11.5$  m/s).

The ambient temperature is 15°C at an atmospheric pressure of 101325 Pa. The blade rotates with an angular velocity of 36.5 rad/s. All presented parameters as well as experimental data were taken from the T-105 wind tunnel experiments of L.S. Pavlov [2].

The mesh settings within FloEFD were set to a uniform mesh with a high mesh density in the vicinity of the rotor and extended to the boundaries of the Computational Domain. Two local meshes, one around the rotor and one on the blade surface, were applied to resolve the tip of the leading edge of the blade. This resulted in an initial mesh of about 2,700,000 cells (Figure 4) and was meshed in about five minutes. The mesh with the traditional CFD (ANSYS Fluent) was made of tetrahedral cells and resulted in a mesh of about 8,500,000 cells.

The FloEFD calculations were performed as transient (unsteady) analysis in three stages with different time steps decreasing from

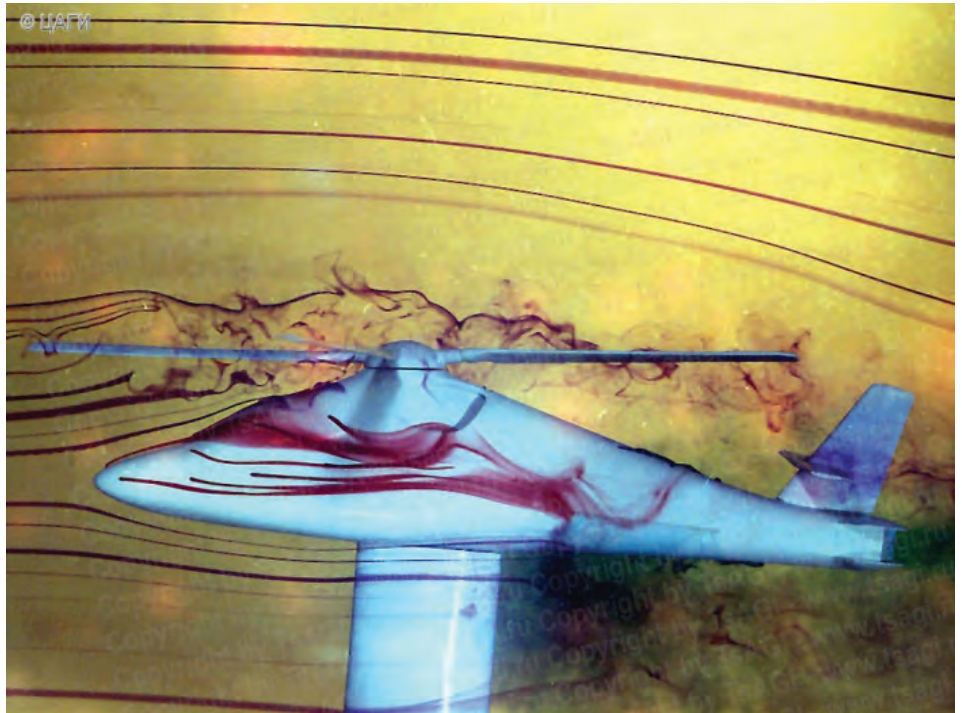


Figure 2. Helicopter model flow tests in the hydro tunnel

Table 1.

Geometrical and Air Flow Parameters:	
Rotor radius	$R = 1.2$ m
Chord length	$c = 0.15$ m
Rotor collective pitch angle	$\varphi = 8^\circ$
Angular velocity of rotation	$\omega = 36.5$ rad/s

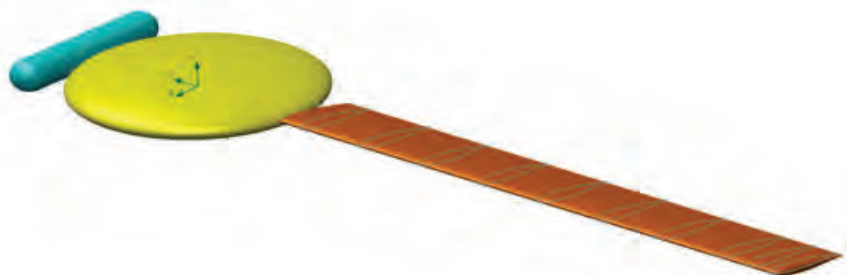
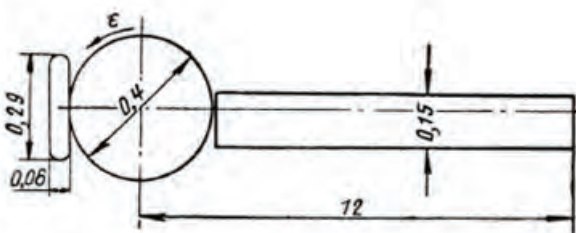
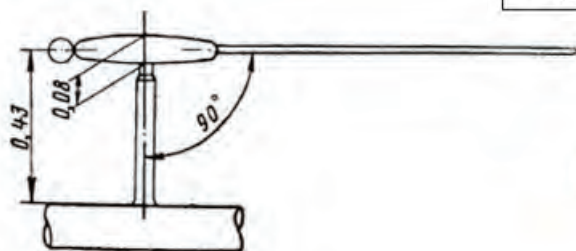
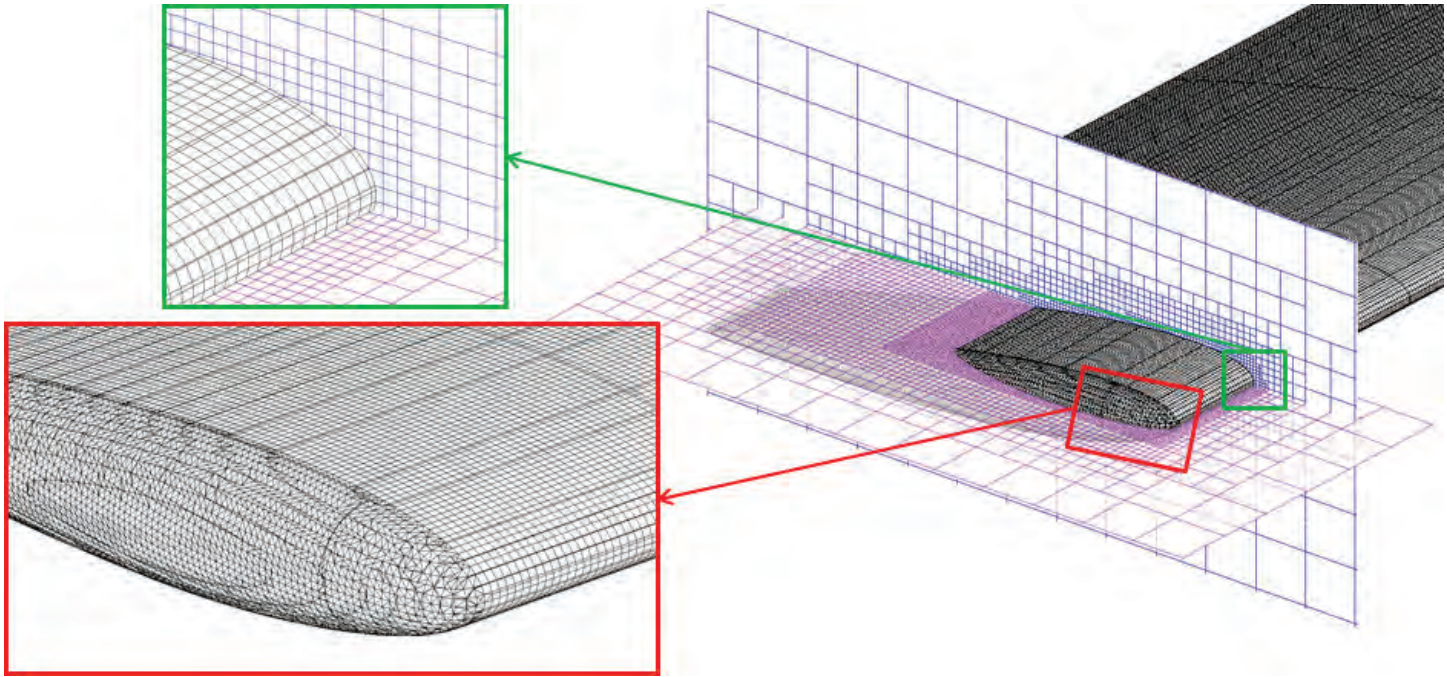


Figure 3. Rotor Blade Model





**Figure 4.** FloEFD mesh with local refinement on the rotor blade surface

the azimuth angle of 9° per one iteration to the azimuth angle of 1° per one iteration for the last revolution on which the presented results were obtained. It has taken about 36 hours to simulate each case on Intel Xeon 2.7 GHz, 8 CPU, 32 Gb RAM and about 30 minutes to specify the project.

The calculations by using ANSYS Fluent were performed on the cluster of 24 computers with Intel Xeon 2.8 GHz, 12 CPU, 100 Gb RAM (the total number of CPU was 288). It has taken about 48 hours to simulate each case and about seven days to specify the project and the calculation mesh.

Also the simulation was performed by using the TsAGI specialized software RC-VTOL based on a nonlinear vortex theory (S.M. Belotserkovsky's school) [3,4]. The calculations were performed on Intel 3 GHz, 4 CPU, 8 Gb RAM and took about 20 minutes per each case.

The wake vortex structures calculated by FloEFD (left) and RC-VTOL (right) are demonstrated in Figure 6. Predicted pressure coefficient ( $C_p$ ) distributions at the cross-section  $r = r = 0.8$  also show good correlation with ones predicted by the traditional CFD tool and the experimental data (Figure 7).

Figure 8 shows the blade section normal force coefficient along the blade radius predicted by FloEFD and RC-VTOL and

the experimental data. It can be seen that there is again good agreement between experiment and simulations.

This study demonstrates that all software tools have successfully validated the problem of predicting the helicopter rotor blade characteristics. RC-VTOL is the least resource-demanding software, but it cannot provide the pressure distributions on the

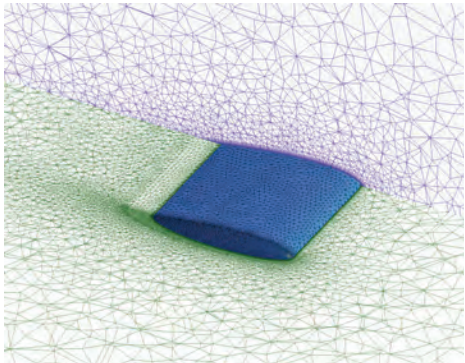


**Figure 5.** Traditional tetrahedral CFD mesh with local refinement on the rotor blade surface (ANSYS Fluent mesh topology)

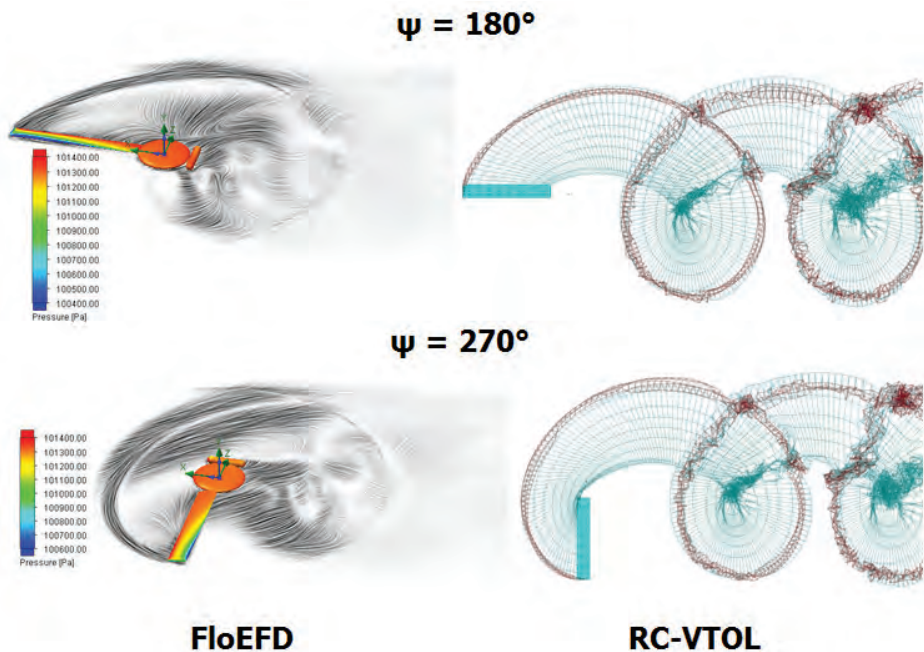


**Figure 6.** The wake vortex structure and the pressure distribution on the blade at the forward velocity of 11.5 m/s and the azimuth angles of 180° and 270°





surfaces. It is worth noting that FloEFD is less demanding of computer resources than the traditional CFD approach: it takes about 30 minutes to prepare a project for calculation including the mesh creation; the calculation mesh required to obtain the acceptable results was three times less than one for the traditional CFD tool.

## References:

- [1] [www.tsagi.ru](http://www.tsagi.ru)
- [2] Pavlov, L.S. Pressure distribution in rectangular wing (blade) sections during curvilinear motion in an incompressible medium. Uchenie Zapiski TsAGI (Scientific Notes of TsAGI), vol. 10, no. 2, 1979, pp. 104-108 (in Russian).
- [3] Belotserkovsky, S.M., Loktev, B.E., Nisht M.I. Computed-aided investigation of aerodynamic and aeroelastic characteristics of helicopter rotor. Mashinostroenie, Moscow, 1992 (in Russian).
- [4] Kritsky, B.S. Mathematical model of rotorcraft aerodynamics. Trudy TsAGI (Works of TsAGI), no.2655, 2002, pp. 50-56 (in Russian).

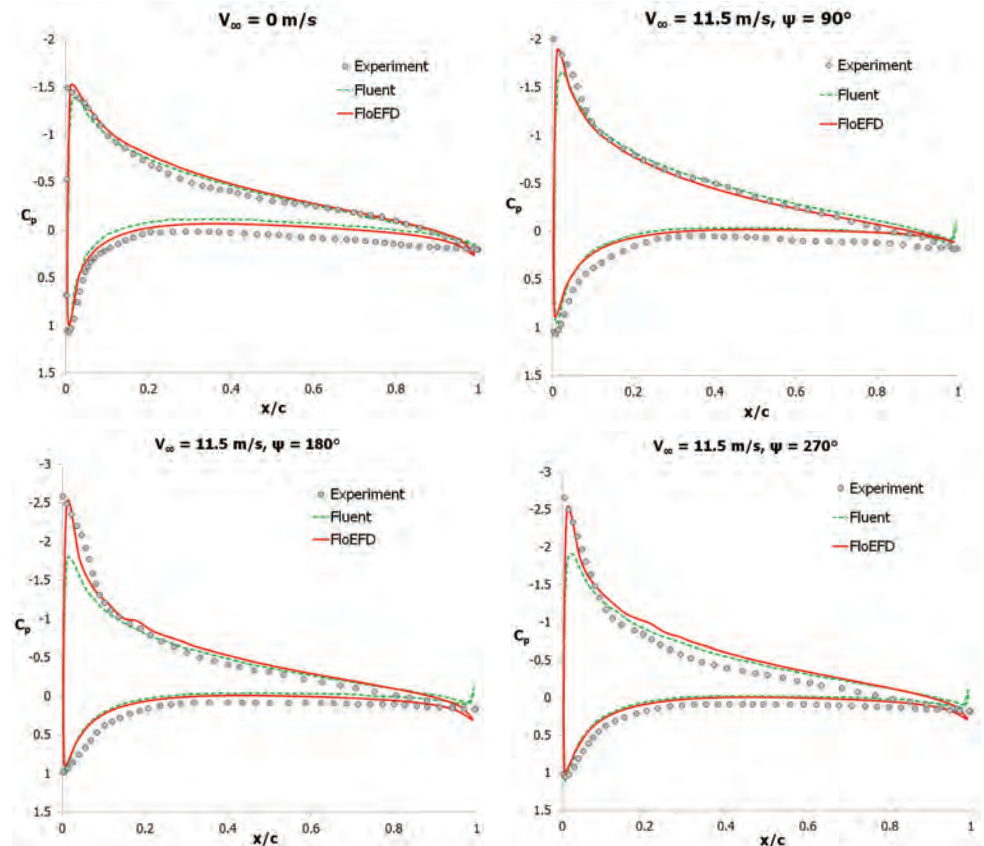


Figure 7. Pressure coefficient  $C_p$  distributions at cross-section  $\bar{r} = 0.8$

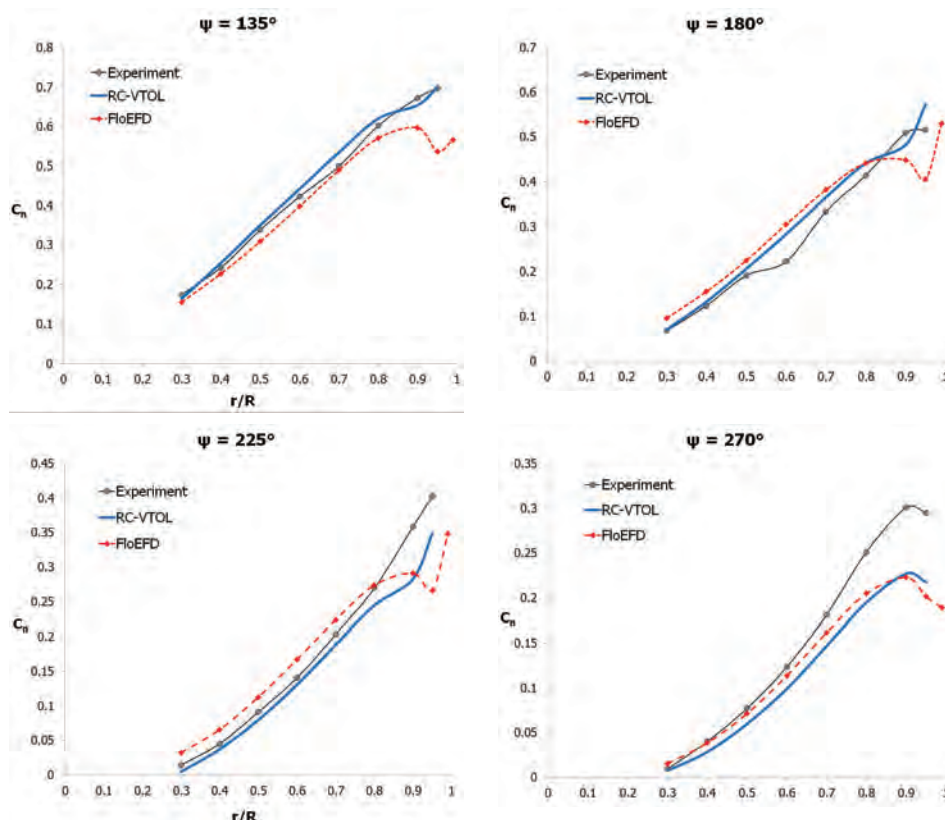


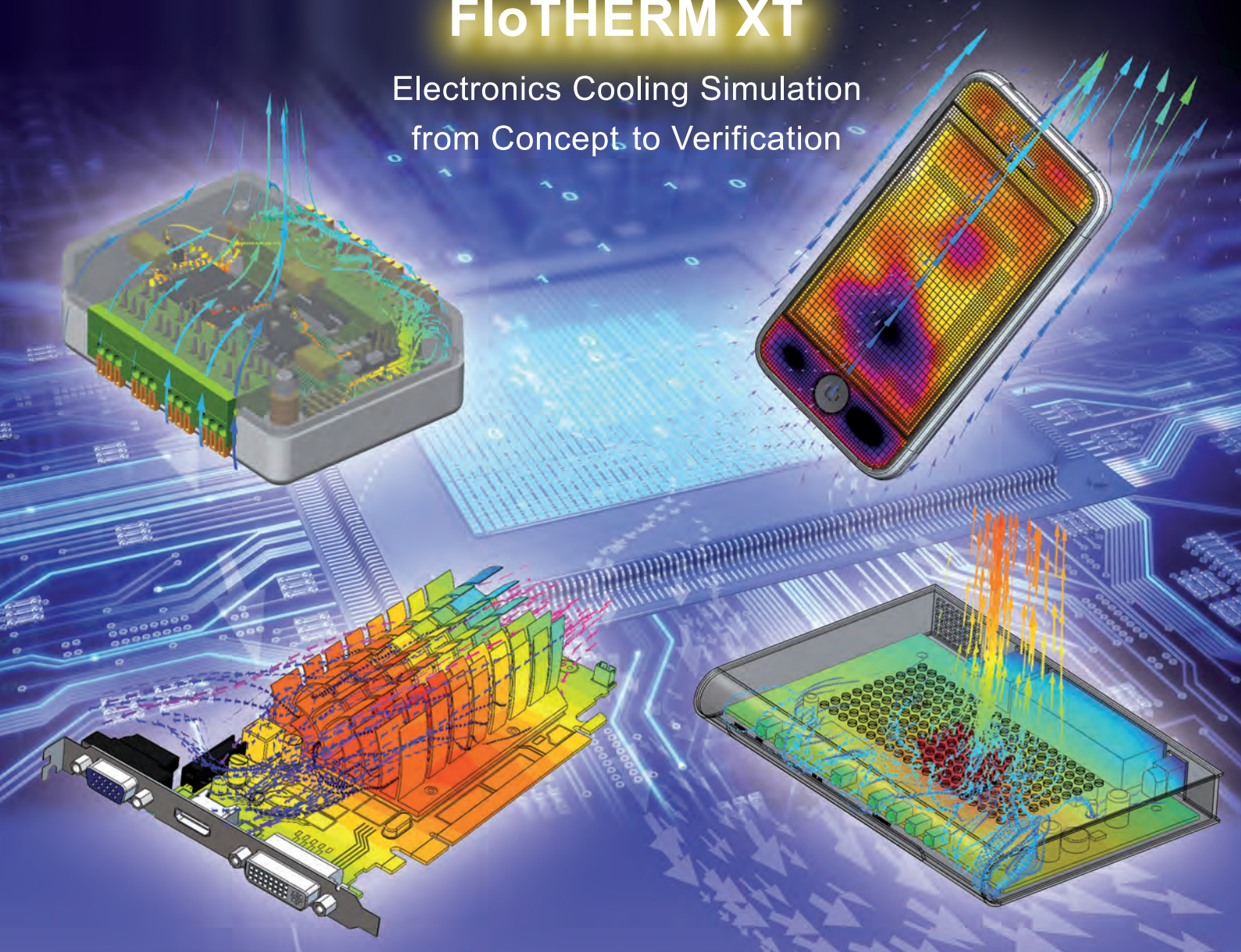
Figure 8. The blade section normal force coefficient distributions at the forward velocity of 11.5 m/s



# Electronics Design Just Got Interesting

## FloTHERM XT

Electronics Cooling Simulation  
from Concept to Verification



FloTHERM XT, the industry's first integrated MCAD – EDA electronics cooling simulation solution, to optimize designs from the early concept stage through to the verification and prototyping stages faster than ever before:

- Electronics cooling simulation solution for **large, complex electronics system design**
- CAD-centric interface and geometry engine as well as direct interfaces to MCAD and EDA software offer **immediate productivity** and short learning curve
- Full geometric and non-geometric SmartParts and Libraries enable **fast/accurate model creation**

Learn how FloTHERM XT can help design better electronics faster – download Step Change in Electronics Thermal Design: Incorporating EDA & MDA Design Flows

[www.mentor.com/mechanical](http://www.mentor.com/mechanical)



# How to Grow Your own Heatsink!

**E**stablished heatsink manufacturing processes such as extrusion and casting, impose constraints on the methods used to design the heatsink. These affect both allowable geometry topologies and absolute sizes. The advent of 3D printing (additive manufacture) may remove many of these constraints, forcing us to reconsider the approach taken during design.

Drs. Robin Bornoff and John Parry at Mentor Graphics have developed a new, patented approach to heatsink design where the geometry topology is not defined a priori, but allowed to develop as part of an additive design process involving a number of sequential simulations.

At its heart, the additive design methodology involves inspection of the performance of a minimal initial design, a determination of where that design should be minimally modified, the modification made, the performance re-evaluated and the process repeated until a design criterion is met.

When applied to heatsink design the process starts by considering the thermal performance of a thin section of heatsink base placed on a heat source, a key from which the heatsink geometry may evolve. This initial geometry is simulated in a cooling environment and the maximum fluid apparent surface temperature location identified. It is then postulated that an improvement in the thermal performance of the heatsink can be achieved by increasing the surface area at the point of highest temperature. To achieve this, a small additional piece of heatsink material geometry is added to the heatsink, on that face, and the slightly modified heatsink geometry re-simulated in FloTHERM.

In this case the thermal performance is taken as the thermal resistance of the heatsink derived from the temperature of the heatsink base at the center of the heat source, the power dissipation and the ambient cooling temperature.

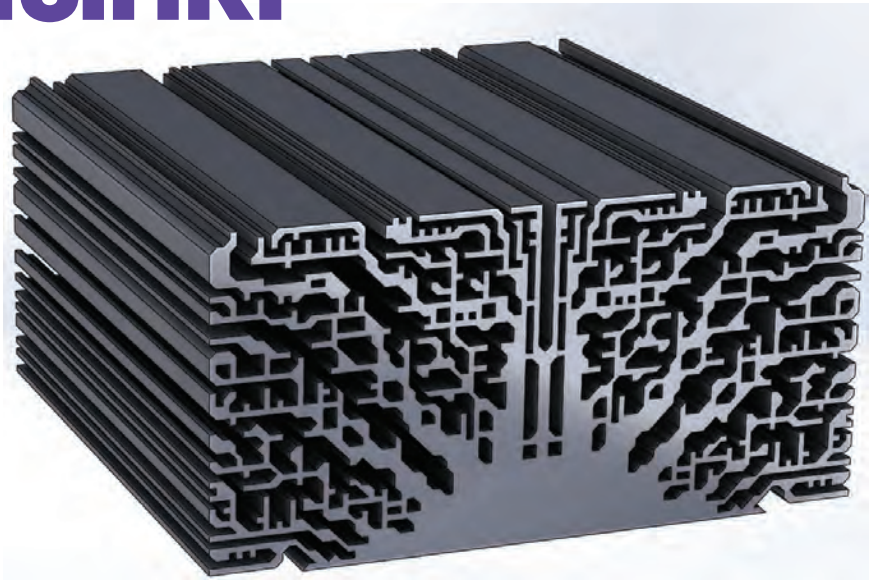


Figure 1. Final Heatsink at the End of Growth Process

If the thermal performance is seen to improve with the addition of the heatsink geometry then the 'evaluate and add geometry' process is repeated. If the thermal performance worsens then the additional piece of geometry is removed and that location marked so that the

same geometry addition may not occur subsequently. Instead, the location with the next highest surface temperature is noted and the process repeated.

The process ends when either the addition of any geometry will cause the heatsink to 'grow' beyond its design bounds or that the addition of any geometry anywhere will cause a decrease in thermal performance.

The resulting thermal performance is within 5% of that of a parametrically optimized defined base/fin type. There is further scope to improve the thermal performance by identifying other topologies that may evolve based on more refined thermal conditions that control the evolution of the geometry, such as Mentor's BottleNeck number, and the inventors plan further work in that area. In addition, extending the application to consider the growth of the heatsink in three dimensions (as opposed to an extruded two dimensions) may lead to both further improvements in thermal performance and open up this technology to new and exciting application areas.

## Reference:

Robin Bornoff, John Parry (2015) "An Additive Design Heatsink Geometry Topology Identification and Optimisation Algorithm", Proceedings of SEMI-THERM Conference, San Jose, March 2015.

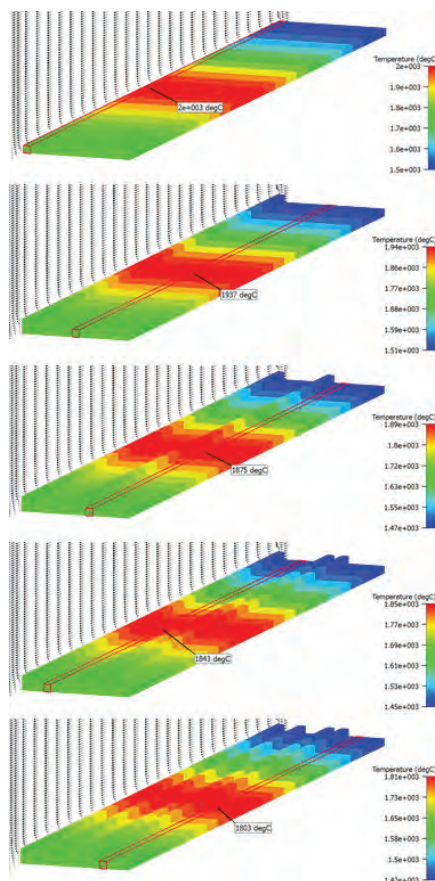


Figure 2. First Five Steps of the Additive Design Process

# Extracting TIM Properties with Localized Transient Pulses

By Cameron Nelson, Jesse Galloway, and Phillip Fosnot, Amkor Technology



Harvey Rosten Award Winners

**A**n inside look at the paper that won the 2014 Harvey Rosten Award for Excellence [1], focusing on the transient experimental and numerical work. The steady state work and uncertainty analysis that form part of the paper are not discussed here.

Thermal engineers require accurate package-level resistance estimates to design optimized cooling systems. Although Theta-JC is a commonly quoted metric to define the junction to case resistance, it does not accurately predict package performance for a range of heatsink and thermal interface material (TIM) conditions.

In high power applications, the majority of the heat flows from the active surface of the die to a heat spreader. The thermal resistance between the die and heat spreader must be characterized before an accurate system thermal analysis can be performed. Four main factors affect a TIM's thermal resistance - its bond line thickness (BLT); bulk thermal conductivity; contact resistance; and voiding propensity. TIMs not only need a low thermal resistance, but must also meet assembly and long-

term reliability requirements. The thermal performance limits of Flip Chip Ball Grid Array (FCBGA) packages are being pushed to practical limits in applications such as telecom and more recently in the tablet space. As a consequence, more precise thermal resistance measurements are required to support high power design targets.

Thermal resistance is known to decrease with an increase in lid clamping pressure. Due to the difference in coefficient of thermal expansion between the silicon die and substrate material, FCBGA packages warp into a "frown face" configuration. The BLT is at a minimum at the die center and increases towards the corners of the die. The thermal resistance of a TIM is not uniform, depending on the BLT, the presence of voids, and any loss of TIM adhesion. In order to quantify the thermal performance of TIMs, a reliable experimental method must be used to measure its actual thermal resistance in assembled packages. Accurate thermal resistance data must be acquired using either thermal test vehicles (TTVs) or functional die within actual FCBGA packages.

Theta-JC is one of the more commonly reported resistances for high power packages. It accounts for the resistance to heat flow between the die and the lid. Measuring Theta-JC in electronic packages is a particularly difficult problem to resolve due to the many factors affecting its measurement. An often-cited reference for Theta-JC measurements can be found in MIL-TD-883. This standard provides a general description for measuring Theta-JC in functional packages.

Transient testing methods are more attractive because they remove some of the uncertainties associated with making steady-state measurements. For example, the case temperature is not needed. When short transient power pulses are considered, the numerical model complexity need only consider regions close to the die. A simplified transient analysis for a FCBGA package was conducted. It compared the temperature response at the junction for a one-dimensional heat flow condition, to a more general three-dimensional case, where heat may also flow into the substrate and mother board.

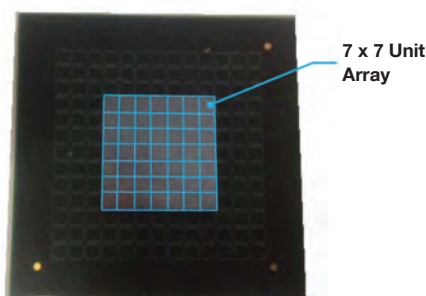


**Figure 1.** FCBGA thermal test vehicle with lid removed. Outline of cell array overlaid on image

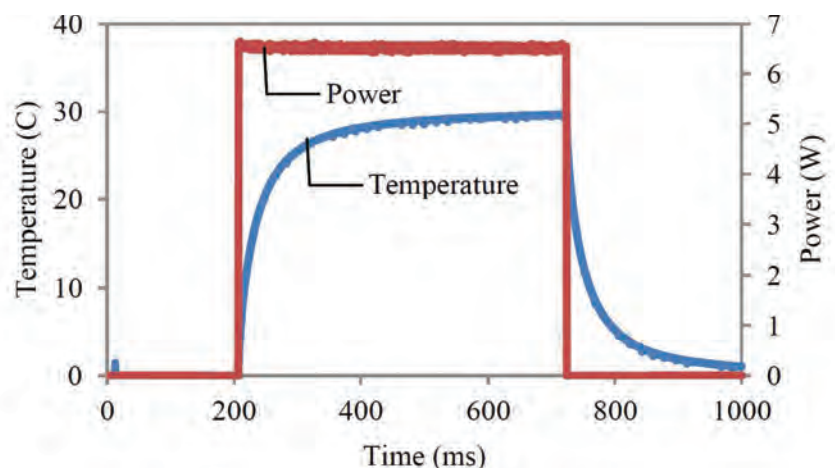


**Figure 2.** Power pulse and change in temperature response for a typical cell test.



18.2	15.7	15.7	16.5	15.8	15.7	18.7
15.4	12.8	12.6	13.0	12.5	12.2	14.3
14.7	12.0	12.4	12.0	12.2	12.6	14.7
14.8	11.8	11.6	11.5	11.0	11.3	13.3
13.5	11.6	11.3	12.0	11.4	12.2	14.7
14.7	16.0	12.8	12.4	12.5	12.1	12.4
19.1	15.2	15.4	15.8	16.1	15.7	18.9

**Figure 3.** Change in temperature for Gel TIM at time = 100ms

In the study, the thermal test vehicle (TTV), consisted of a 17.8mm x 17.8mm die, 45mm x 45mm body with a 1mm thick copper lid FCBGA mounted to the motherboard. The thermal test die is constructed as a 7x7 array of resistive heater cells. Each cell has dimensions of 2.54mm x 2.54mm and has two individual 1.9mm x 0.9mm heaters. A temperature sensing diode is located in the center of each cell. Power to each heater can be supplied individually or can be supplied to all cells simultaneously.

Three different TIMs are considered; an adhesive, a gel, and indium. The TIMs are selected to provide a wide range of resistance to allow for comparison between

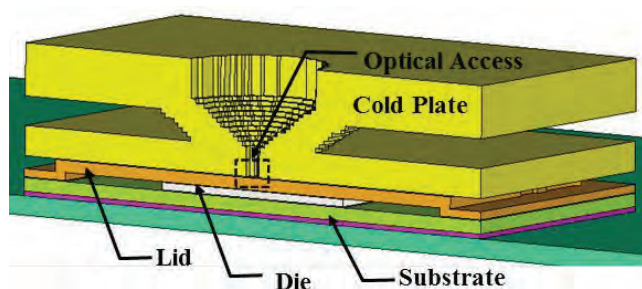


**Figure 4.** The TIM I layer is divided into 49 volumes corresponding to die cell boundaries

the steady-state and transient methods. The transient method applies a discrete power step to each cell's heater, one at a time with a ramp and settling time less than 0.1 ms. Each cell receives about 6W during a transient test. A high-power pulse is needed to produce a sizeable temperature response. A large rise in temperature allows for better resolution and increased range of differences among cells.

A conduction model is used to estimate the TIM I resistance with input from experimental measured case and die temperatures along with heater power data. The model includes much of the experimental system details, see figure 4,

such as the package design, cold-plate design and location where case temperature is measured. The model includes heat flux applied at the same location as the actual TTV. The modeling process begins by assuming a uniform TIM I resistance at all locations. To extract the TIM I resistance, the FEA model adjusts numerical values for the TIM I resistance until the simulated die temperatures match the experimentally measured die temperatures.

Separate transient temperature rise versus time curves, are available for each cell. The shape of the predicted temperature rise versus time is compared to the experimental data at discrete points. After making adjustments to the resistances and re-running the analysis, the transient simulation temperature response closely matches the experimental response after three to four iterations.

A map of the extracted thermal resistances is shown in Figure 5. Lower resistances are predicted in the center of the die and higher thermal resistances along the edges and in the corners.

This is as expected as the BLT will be thicker in the corners and along the die edges as the die pulls away from the lid giving rise to higher resistances in these regions. A comparison of the transient extracted thermal resistance for the three different TIMs is shown in Figure 6.

Transient simulation is inherently more complex and computationally demanding compared to steady-state simulation. The grid size and time step size must be adjusted to ensure that the solution

is not dependent on the selected grid size and time step.

At times less than 10ms, the temperature rise is less than 5°C. Assuming a  $\pm 0.1^\circ\text{C}$  junction temperature error gives an uncertainty of 4%. At 50ms, the junction temperature is approximately  $10^\circ\text{C}$ , thus reducing the uncertainty in temperature measurement to 2%. At later times the

18.5	17.6	17.7	21.1	20.1	18.1	20.3
16.6	10.7	13.1	12.3	12.2	11.4	16.6
16.0	12.8	11.2	10.5	11.1	11.8	15.6
16.1	12.1	11.1	10.0	10.5	11.3	15.9
13.8	11.1	10.3	9.6	9.6	11.3	15.1
15.1	17.1	10.2	12.6	11.5	11.4	10.8
22.5	20.1	19.9	23.9	23.4	21.7	23.2

**Figure 5.** Extracted TIM resistance map gel TIM, in units of  $(^\circ\text{C}/\text{W})/\text{mm}^2$

heat wave propagates through the underfill layer and into the substrate as well as into the lid. Additional layers now must be considered while conducting the uncertainty calculation.

The transient method simplifies experimental testing and corresponding numerical simulations. Models for transient analyses do not require the detailed geometry and are therefore more easily developed. TIM extraction methods using the transient measurements together with simulations are approximately 20% more accurate, with 9%, uncertainty compared with the 30% for the steady-state method. The TIM resistance maps generated provide a detailed understanding of the combined effect of bulk thermal conductivity, voiding, and BLT.

## Reference:

[1] Extracting TIM Properties With Localized Transient Pulses. Cameron Nelson, Jesse Galloway, and Phillip Fosnot, Amkor Technology. 30th SEMI-THERM Symposium Proceedings, March 2015.

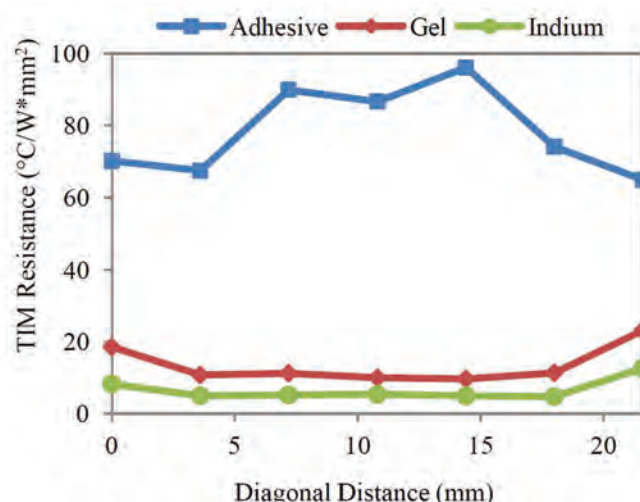


**Figure 6.** TIM resistance across the die diagonal extracted from transient experimental data

# Geek Hub



Our team are passionate about all things CFD and love sharing their findings.

In this issue, Student Intern, James Forsyth demonstrates FloTHERM® XT's capabilities solving complex models. This time...Frying an Egg on a CPU!

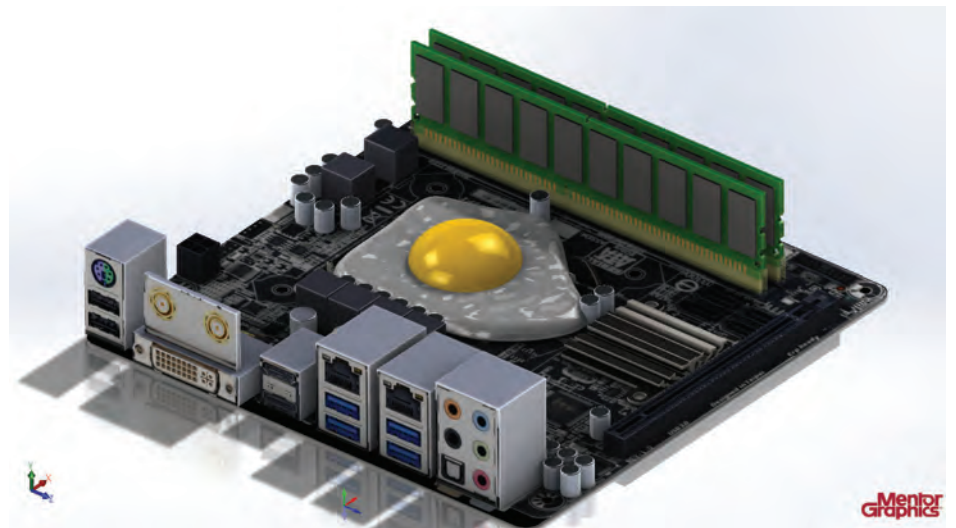


Figure 1. Model of an egg frying on a CPU in FloTHERM XT

**S**olving complex thermal models with CFD requires a lot of processing power and a CPU under full load generates a fair amount of heat. But can you cook an egg on it? Search online and you can find videos of people attempting to cook on their processors, but how effective as a cooling solution is this? Before you throw away your conventional heatsink and fan, in favor of a multifunctional omelette, we'll investigate what CFD in FloTHERM XT can predict about the fate of your PC if you do so.

## Model

As a student intern at Mentor Graphics, I get the opportunity to create and play with interesting and unusual thermal models made in the software. For this concept, I started by creating a very basic project comprising two cuboids and a cylinder to model a motherboard, processor and egg. Then I did some research – standard dimensions for motherboards, CPU thermal design power (TDP), thermal data for eggs.

Using this very simple model, I was able to test things rapidly, get a rough feel for the range of temperatures and evaluate how feasible the concept was to model.

I then created a more detailed model, starting by importing a board using FloEDA Bridge, a tool in FloTHERM XT that allows 3D CAD geometry to be produced from an intuitive 2D EDA environment. Using a topographical image of a representative mITX motherboard and a selection of known dimensions, I was able to accurately scale the image as a texture onto the board. This allowed the footprints of the board components to be positioned accurately against the image.

An excessively detailed board is not necessary for this model as we are only interested in the CPU temperature. To do this, the model needs to include the major sources of heat and any geometry that may alter the flow of air around critical components. The geometry around the CPU, such as the CPU socket, needs to be much more detailed as this has a significant



effect on heat transfer by conduction. The CPU itself is modeled with accurate geometry and a two-Resistor network assembly thermal model, based on an Intel® Core™ i3-4130 as a representative mid-range desktop processor. Typical maximum  $T_{junc}$  and  $T_{case}$  are 90°C and 72°C.[1] The geometry far from the CPU, such as

be converted to the change in chemical enthalpy of the egg as it cooks.[2]

So the question is: how significant is this lost 'cooking energy' to our model? Well, after some research and calculations, not very. The specific enthalpy to denature the egg proteins during cooking is around

2.7 J/g for egg white and around 1.0 J/g egg yolk,[3,4] so for an average 50 g egg, the total energy required is only around 80J. This energy would contribute to a total drop in CPU temperature of approximately 6 °C, but this removal of heat can only happen once per egg. Compare this to the 54 W TDP[1] of the CPU under heavy load; after a few minutes of egg cooking, the heat dissipated is of the order of 10 kJ and the protein denaturation can only mitigate a negligible fraction of this.

The majority of the heat supplied ends up, well, heating the egg. The egg's high water content gives it physical properties similar to water – slightly higher densities of 1130 kg/m<sup>3</sup> for the yolk and 1133 kg/m<sup>3</sup> for the white; specific heat capacities of 3.55-3.60 J/(kg K) for the yolk (increasing with temperature) and 2.55-2.75 J/(kg K) for the white; thermal conductivities of 0.550-0.558 W/(m K) for the yolk and 0.389-0.407 W/(m K) for the white (decreasing with temperature). The actual values used in the model were based on a moving average of reported experimental data.[5].

Another factor not considered in the model is water in the egg heating up to steam which rises, carrying away heat, though this is in small enough quantities compared to the flow of surrounding air that it can be ignored for now.

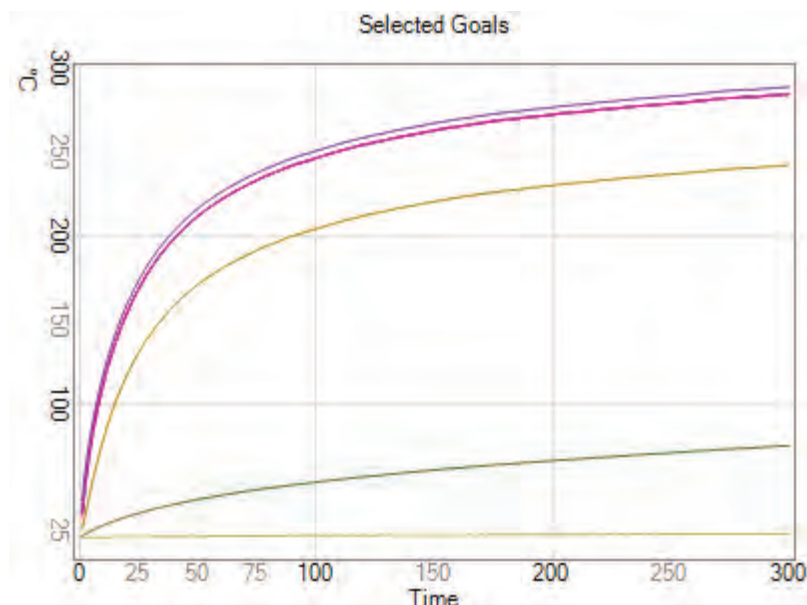


Figure 2. Temperature against time for egg cooled CPU

the I/O ports, can be modeled as simple cuboids that will present an obstacle to air flow on that edge of the board. Additional detail would just prolong the solver computation time with diminutive improvement in accuracy.

## Limitations

One consideration is that the egg cannot quite be simplified to a material with thermal properties dependent on temperature, which FloTHERM XT is easily capable of modeling. For instance, apply heat to a block of aluminum and that energy will all eventually be transferred to the ambient air as it cools. Do the same to an egg and not all of the energy will be transferred to the ambient; cooking an egg is an endothermic process and a proportion of the energy will

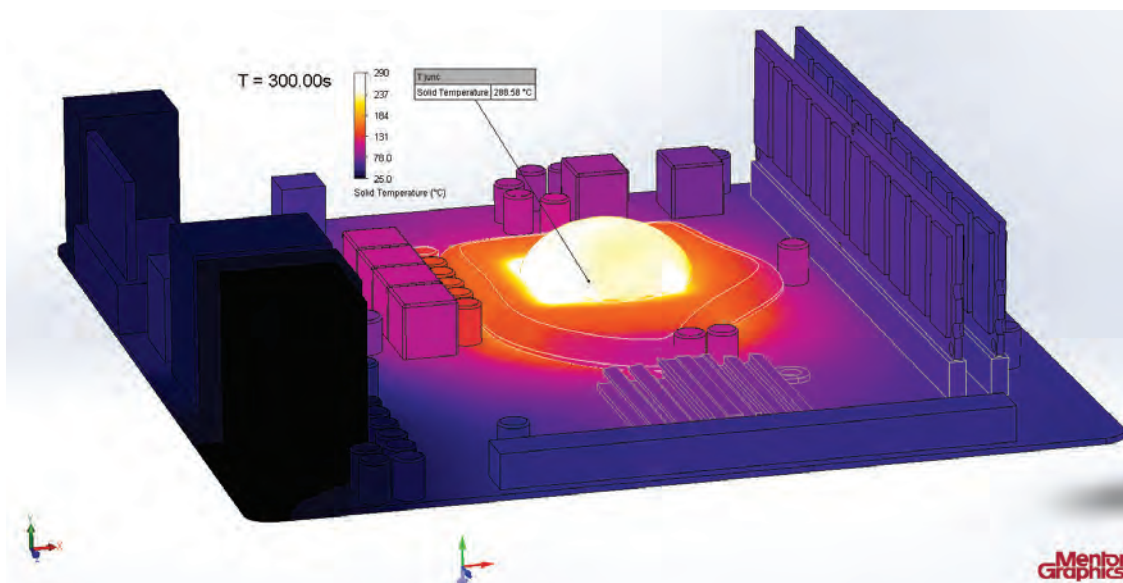
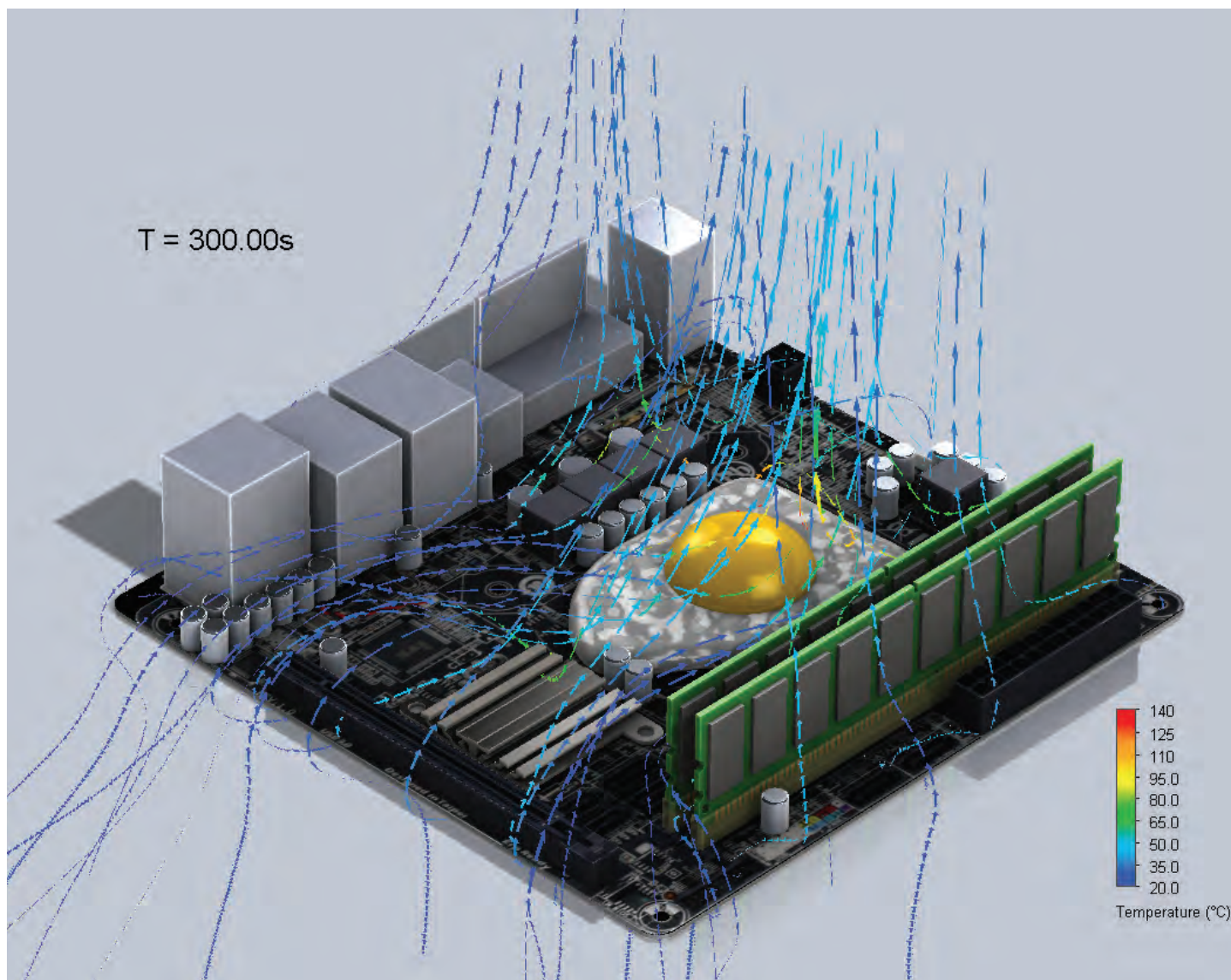


Figure 3. Temperature surface plot of egg after 5 minutes of heating



**Figure 4.** Particle plot, showing air flow around egg and CPU

These two modeling limitations mean that the results are likely to be a slight overestimation of the temperatures while the egg is still cooking, giving a worst-case scenario. This can often be beneficial; if the worst-case scenario is within thermal design constraints, the actual performance should be superior.

Above 65°C, the white begins to coagulate and above 70°C the yolk solidifies. Once solid and cooked, the egg is a much poorer heatsink; it is less thermally conductive and convection within the egg no longer occurs, it is less dense due to water loss, and air/steam gaps are formed underneath the egg, insulating the CPU causing more heat to accumulate. Modeling the egg as always liquid gives a best-case scenario above 70°C.

## Results

Unfortunately, the CPU junction temperature exceeds 90°C within six seconds, at which point the CPU clock would throttle down to reduce the thermal power and prevent

damage to the system – less than ideal for a cooling solution. The egg would also burn and catch fire.

The central location of the CPU on the board and the large obstacles to air flow in

the neighboring memory DIMMS and I/O ports mean limited cold air can passively flow over the hot egg by natural convection. Even adjusting the results for the modeling limitations described earlier, there is simply insufficient cooling.

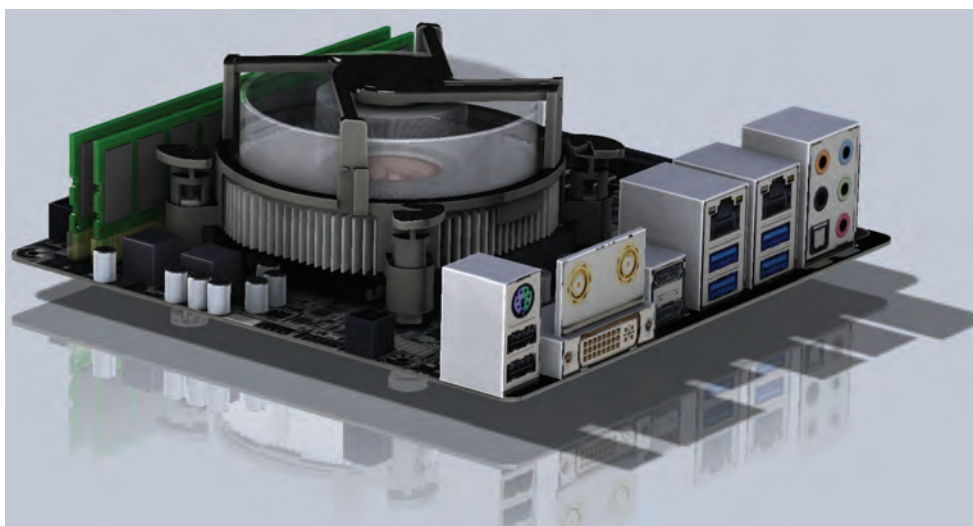


**Figure 5.** Board with egg replaced with stock CPU cooler



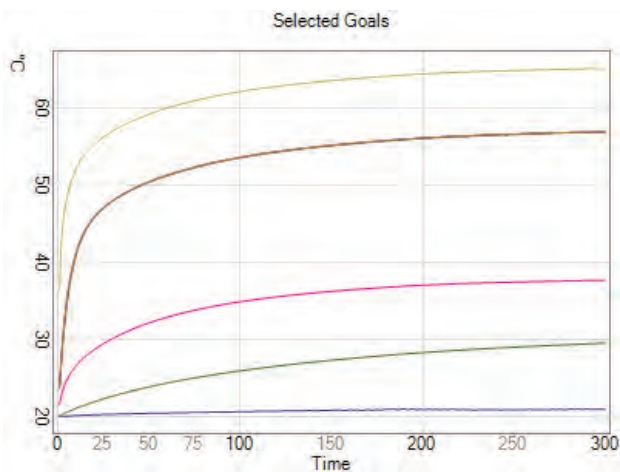


**Figure 6.** Temperature against time for stock cooled CPU

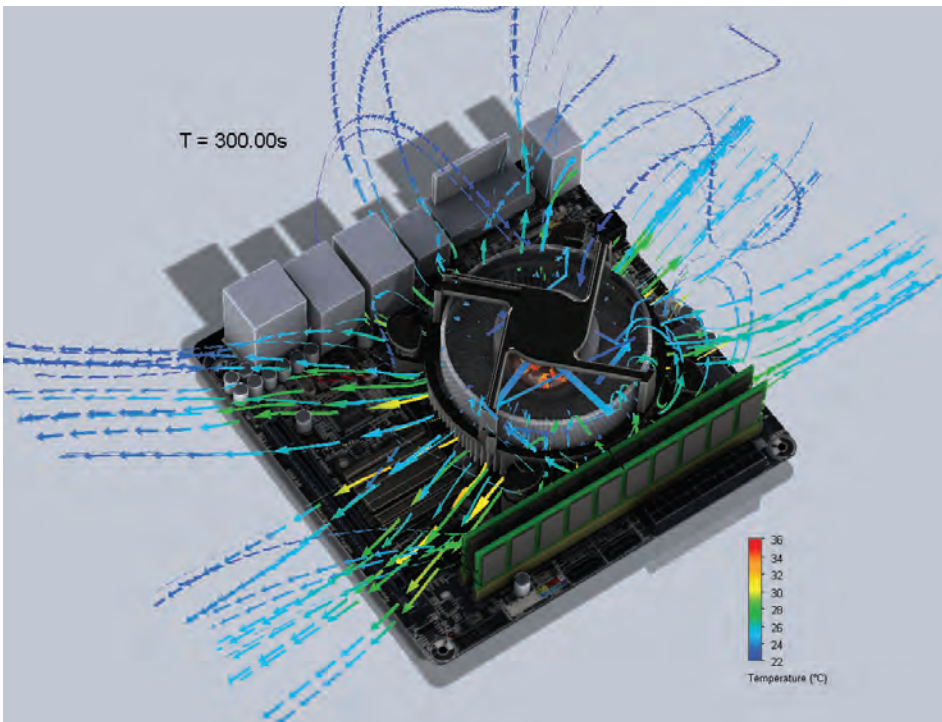


**Figure 7.** Particle plot showing air flow through stock cooler

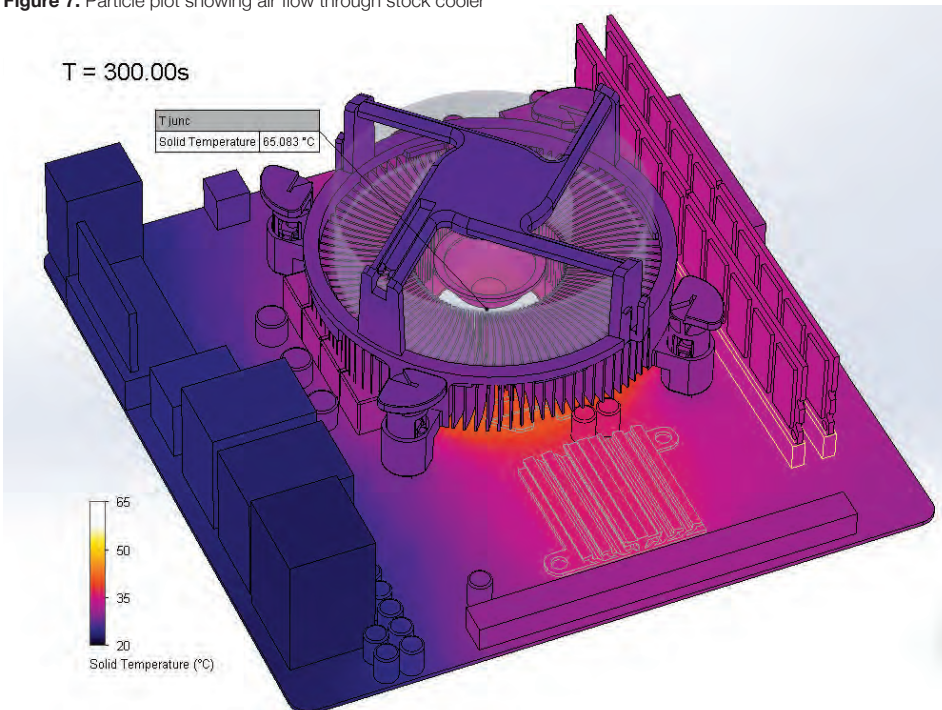


**Figure 8.** Surface plot of stock cooled CPU



For comparison, a new project configuration was created with the egg substituted for a standard Intel® stock CPU cooler radial heatsink and fan. Once solved, this gave a junction temperature of 65.1°C after five minutes of the CPU being under full load at 54W with the system approaching equilibrium.

## Conclusion

The passive cooling of the egg cannot match the forced convection of the stock cooler. An egg-based cooling solution could only keep the CPU below the maximum 90°C  $T_{junc}$  if the CPU performance were throttled down to 10W TDP, so there are only possible applications in lower power environments with plenty of ventilation. With the requirement of frequently swapping out the egg, I can't see this catching on. If the aim is to cook eggs though, CPU's certainly produce enough heat to do so; with thermal throttling, the processor acts as a thermostatically controlled surface at around 90°C, sufficient to cook on. If you value your computer, maybe consider buy a frying pan instead.

## References

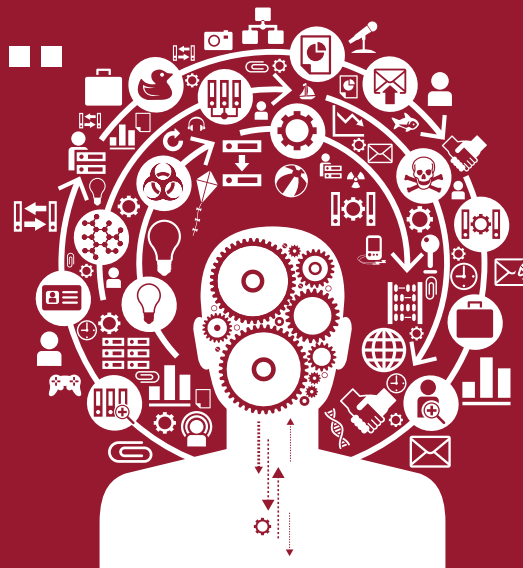
- [1] Intel Corporation, 2014. ARK | Intel® Core™ i3-4130 Processor (3M Cache, 3.40 GHz) [online]. [http://ark.intel.com/products/77480/Intel-Core-i3-4130-Processor-3M-Cache-3\\_40-GHz](http://ark.intel.com/products/77480/Intel-Core-i3-4130-Processor-3M-Cache-3_40-GHz) [accessed April 2015]
- [2] J. McClements, University of Massachusetts, 2001. Thermal Analysis of Foods [online]. <http://people.umass.edu/~mcclemen/581Thermal.html> [accessed April 2015]
- [3] C. Németh, K. Horváth, Á. Drobecz, L. Friedrich, K. Pásztor-Huszár, C. Balla. Calorimetric study of changes induced by preservatives in liquid egg products. Polish Journal of Food and Nutrition Sciences, 2010, Vol.60(4)
- [4] A. Laca, B. Paredes, M. Díaz. Thermal behaviour of lyophilized egg yolk and egg yolk fraction. Journal Of Food Engineering, 2011 Jan, Vol.102(1)
- [5] J. Coimbra, A. Gabas, L. Minim, E. Garcia-Rojas, V. Telis, J. Telis-Romero. Density, heat capacity and thermal conductivity of liquid egg products. Journal of Food Engineering, 2006, Vol.74(2)

# Brownian Motion...

The random musings of a  
Fluid Dynamicist

A set of small, light-blue navigation icons typically found in Beamer presentations, including symbols for back, forward, search, and other slide navigation functions.

**Brownian Motion** or **Pedesis** (from Greek: πήδησις Πεδε:σις 'leaping') is the presumably random moving of particles suspended in a fluid (a liquid or a gas) resulting from their bombardment by the fast-moving atoms or molecules in the gas or liquid. The term 'Brownian Motion' can also refer to the mathematical model used to describe such random movements, which is often called a particle theory.



# This Article Wouldn't Have Happened in My Day!

t's snuck up on me. I didn't realise it had happened until I found myself getting annoyed at the man walking down the high street in my town, stripped to the waist. The temperature had barely touched 15°C, but that seemed more than enough to make the concept of wearing anything above the belt line an exercise in lunacy. I may even have delivered a disapproving 'tsk'.

Reader, I'm getting old.

Things that previously would have at worst bemused me now actively make me angry. Once the penny dropped, it became obvious: I genuinely believe standards are dropping, that people are getting soft and that this (whatever 'this' is) wouldn't have happened in my day. I met a youth the other week who happened to tell me they were off to see a band I saw 18 years ago, and who were obviously far better back then. I now understand why I got a slightly patronising look of pity upon informing them of this.

The thing is, I think I'm alright with my new status. I still like going to gigs, it's just that now most of the audience (who will catch their deaths dressed like that in this weather) will assume I'm there to pick up my children.

I'm now also largely cured of the disease that consumed my 20s: FOMO. A debilitating



condition which renders its sufferers unable to say 'no' to any social event or night out, no matter how unappealing or expensive. All simply because of the Fear Of Missing Out. I can't tell you how much this alone has changed my life, the number of awful venues I no longer feel obliged to go to are legion.

I suspect that I probably was always an old duffer at heart, so that might be why this hasn't been a disappointing revelation. The

other reason is that I'm hoping to be more NASA Voyager (still sending back data after almost 40 years) than MiniDisc (obsolete within a decade). In the words of the anthropologist Ashley Montagu, the trick is to die young as late as possible. Oh, and not become creepy.

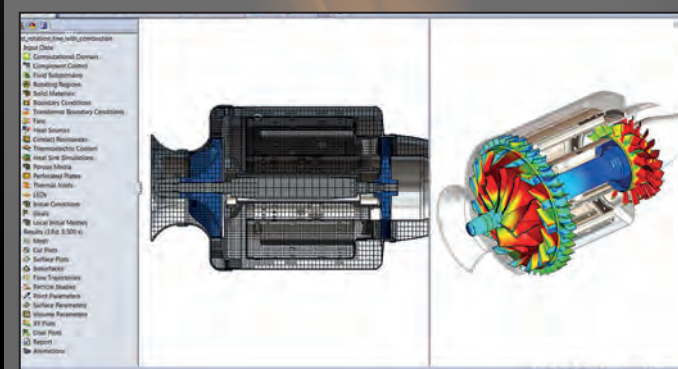
Well, enough rambling. It's about time I wrote a strongly worded letter to my local newspaper about something.

## Turbulent Eddy



# Virtual Labs

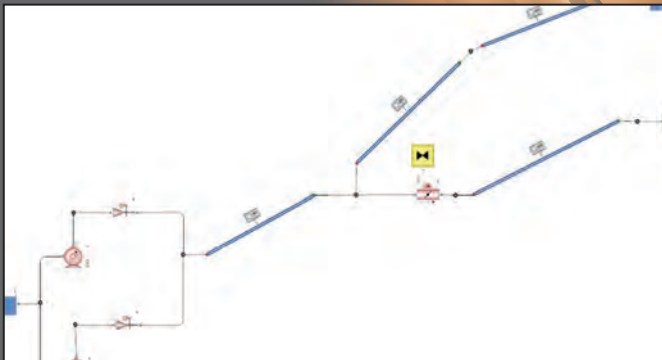
[www.mentor.com/mechanical](http://www.mentor.com/mechanical)



## FloEFD™ for PTC Creo

Test-drive 20 Powerful CFD Models including LED Thermal Characterization, CPU Cooling, Hydraulic Loss Determination, and more

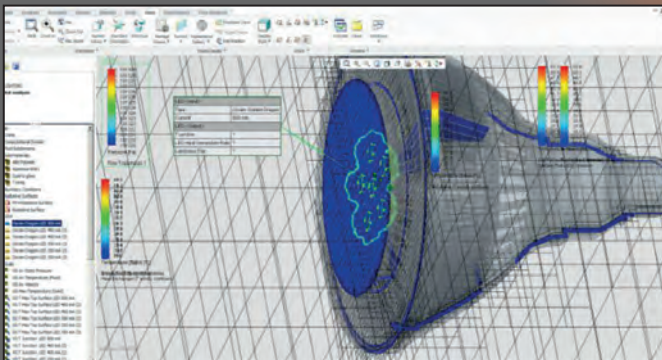
[go.mentor.com/floefd-vl](http://go.mentor.com/floefd-vl)



## Flowmaster®

Build & Analyze a Rising Main Network in Flowmaster

[go.mentor.com/flowmaster-vl](http://go.mentor.com/flowmaster-vl)



## LED Analysis with FloEFD for PTC Creo

Analyze LED Components & Determine Thermal Characteristics

[go.mentor.com/floefd-led-vl](http://go.mentor.com/floefd-led-vl)

- 30 Day Instant Free Access to Full Software
- No License Set-up Required
- Each VLab contains Full Support Material
- 4 Hour Sessions\*
- Save Work between Sessions

\*These sessions can be extended

**REGISTER NOW**  
for your instant 30 Day  
Free Trial

[www.mentor.com/mechanical](http://www.mentor.com/mechanical)



### Enhance

Flowmaster enables designers to embed their intellectual property with ease to create custom components

**Flowmaster®**  
1D Thermo-Fluid  
Simulation  
Software

### Enterprise

Customize your analysis to suit your process with real-time dashboards, Microsoft Excel, or even web applications

### Extend

Take Flowmaster results mobile with response surface modeling for custom applications

**Want to know more? Try Flowmaster online now!**

30 day Instant Free Access  
Full Software  
No Licence Set Up  
Full Support Material

**Virtual Labs**